

Woods Hole Oceanographic Institution



Northwest Tropical Atlantic Station (NTAS): Velocity Data Report for Deployments 1 to 5

by

C. M. Duncombe Rae and A. J. Plueddemann

Woods Hole Oceanographic Institution
Woods Hole, MA 02543

September 2012

Technical Report

Funding was provided by the National Oceanic and Atmospheric Administration
under Grant No. NA09OAR4320129

Approved for public release; distribution unlimited.



Upper Ocean Processes Group
Woods Hole Oceanographic Institution
Woods Hole, MA 02543
UOP Technical Report 2012-03

WHOI-2012-05

**Northwest Tropical Atlantic Station (NTAS):
Velocity Data Report for Deployments 1 to 5**

by

C. M. Duncombe Rae and A. J. Plueddemann

Woods Hole Oceanographic Institution
Woods Hole, Massachusetts 02543

September 2012

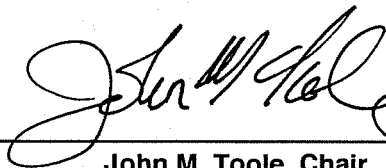
Technical Report

Funding was provided by the National Oceanic and Atmospheric Administration
under Grant No. NA09OAR4320129

Reproduction in whole or in part is permitted for any purpose of the United States
Government. This report should be cited as Woods Hole Oceanographic Institution Tech.
Report., WHOI-2012-05.

Approved for public release; distribution unlimited.

Approved for Distribution:



A handwritten signature in black ink, appearing to read "John M. Toole", is written over a solid horizontal line.

John M. Toole, Chair

Department of Physical Oceanography

Abstract

This report presents velocity data from the Northwest Tropical Atlantic Station (NTAS) deployments 1 through 5, from March 30, 2001, to February 28, 2006. The NTAS project has maintained a series of moorings near $14^{\circ}50'N$, $51^{\circ}00'W$ in the northwest tropical Atlantic for air-sea flux measurement. The moorings include a surface buoy outfitted with Air-Sea Interaction Meteorology (ASIMET) systems for determination of bulk air-sea fluxes and oceanographic sensors along the upper 120 m of the mooring line. This report describes and presents the velocity data recovered from current meters and Acoustic Doppler Current Profilers (ADCPs) during the first five years of the NTAS project.

Contents

| | |
|--|------------|
| Abstract | iii |
| Table of Contents | v |
| List of Figures | vii |
| List of Tables | ix |
| 1 Introduction | 1 |
| 2 Deployment Cruises | 6 |
| 2.1 NTAS-1 Deployment Cruise | 6 |
| 2.2 NTAS-2 Deployment Cruise | 6 |
| 2.3 NTAS-3 Deployment Cruise | 6 |
| 2.4 NTAS-4 Deployment Cruise | 6 |
| 2.5 NTAS-5 Deployment Cruise | 7 |
| 3 Moored Arrays and Instrumentation | 8 |
| 3.1 Mooring Design | 8 |
| 3.2 Aquadopp | 10 |
| 3.3 Acoustic Doppler current profilers | 10 |
| 3.4 Vector Measuring Current Meters | 11 |
| 3.5 Mooring Diagrams | 12 |
| 4 Data Processing Summary | 12 |
| 4.1 Aquadopp | 12 |
| 4.2 VMCM | 13 |
| 4.3 ADCP | 14 |
| 5 Data Presentation | 18 |
| 5.1 Introduction | 18 |
| 5.1.1 Outlier Detection | 18 |
| 5.1.2 Spectral Analysis | 18 |
| 5.2 NTAS-1 Velocity Data | 22 |
| 5.2.1 Aquadopp | 22 |
| 5.2.2 RDI ADCP | 22 |
| 5.3 NTAS-2 Velocity Data | 32 |
| 5.3.1 Aquadopp | 32 |
| 5.3.2 RDI Workhorse | 32 |
| 5.3.3 Vector Measuring Current Meter | 32 |
| 5.4 NTAS-3 Velocity Data | 45 |
| 5.4.1 Aquadopp | 45 |
| 5.4.2 RDI Workhorse | 45 |
| 5.5 NTAS-4 Velocity Data | 54 |

| | | |
|----------|--|------------|
| 5.5.1 | Aquadopp | 54 |
| 5.5.2 | RDI Workhorse ADCP | 54 |
| 5.6 | NTAS-5 Velocity Data | 64 |
| 5.6.1 | Aquadopp | 64 |
| 5.6.2 | RDI Workhorse ADCP | 64 |
| 6 | Comparisons of Data | 74 |
| 6.1 | Intra-Deployment Comparisons | 76 |
| 6.1.1 | Comparison of Current Meters on NTAS-1 | 76 |
| 6.1.2 | Comparison of Current Meters on NTAS-2 | 76 |
| 6.1.3 | Comparison of Current Meters on NTAS-3 | 78 |
| 6.1.4 | Comparison of Current Meters on NTAS-4 | 78 |
| 6.1.5 | Comparison of Current Meters on NTAS-5 | 81 |
| 6.2 | Inter-Deployment Comparisons | 91 |
| | Acknowledgements | 100 |
| | References | 100 |
| | Appendices | 102 |
| A | NTAS Velocity Statistics | 102 |

List of Figures

| | | |
|----|---|----|
| 1 | Site map for NTAS. | 3 |
| 2 | Sea-Beam bathymetry at the NTAS site. | 4 |
| 3 | Buoy position relative to the anchor position. | 5 |
| 4 | Nortek Aquadopp | 8 |
| 5 | RDI NarrowBand and Workhorse ADCPs | 9 |
| 6 | Vector Measuring Current Meter | 9 |
| 7 | NTAS-1 mooring diagram. | 13 |
| 8 | NTAS-2 mooring diagram. | 14 |
| 9 | NTAS-3 mooring diagram. | 15 |
| 10 | NTAS-4 mooring diagram. | 16 |
| 11 | NTAS-5 mooring diagram. | 17 |
| 12 | Plot showing outlier distribution. | 19 |
| 13 | ARGOS sampling rates of buoy position. | 21 |
| 14 | Rotary spectra from NTAS-1. | 22 |
| 15 | Unfiltered current speed time series measured by NTAS-1 Aquadopp. | 23 |
| 16 | Progressive vector diagram of the NTAS-1 Aquadopp current meter. | 25 |
| 17 | Spectrum of NTAS-1 Aquadopp current speed. | 26 |
| 18 | Time series waterfall plots from the NTAS-1 RDI NarrowBand ADCP. | 27 |
| 19 | NTAS-1 RDI NarrowBand spectra from 86 to 22 meters. | 29 |
| 20 | Progressive vector diagram of currents from the NTAS-1 RDI NarrowBand ADCP. | 31 |
| 21 | Rotary spectra from NTAS-2. | 32 |
| 22 | Unfiltered currents from NTAS-2 Aquadopp. | 33 |
| 23 | Progressive vector diagram of currents from the NTAS-2 Aquadopp. | 36 |
| 24 | Spectrum of NTAS-2 Aquadopp current speed. | 37 |
| 25 | Time series waterfall plots from the NTAS-2 RDI Workhorse ADCP. | 38 |
| 26 | NTAS-2 RDI Workhorse spectra from 86 to 22 meters. | 40 |
| 27 | Progressive vector diagram of currents from the NTAS-2 RDI Workhorse. | 41 |
| 28 | Currents from VMCM NTAS-2. | 42 |
| 29 | Progressive vector diagram from the VMCM NTAS-2. | 43 |
| 30 | Spectrum of VMCM on NTAS-2. | 44 |
| 31 | Rotary spectra from NTAS-3. | 45 |
| 32 | Unfiltered currents from NTAS-3 Aquadopp. | 46 |
| 33 | Progressive vector diagram of currents from the NTAS-3 Aquadopp. | 47 |
| 34 | Spectrum of NTAS-3 Aquadopp current speed. | 48 |
| 35 | Time series waterfall plots from the NTAS-3 RDI Workhorse ADCP. | 49 |
| 36 | NTAS-3 RDI Workhorse spectra from 86 to 22 meters. | 52 |
| 37 | Progressive vector diagram of currents from the NTAS-3 RDI Workhorse. | 53 |
| 38 | Rotary spectra from NTAS-4. | 54 |
| 39 | Unfiltered currents from NTAS-4 Aquadopp. | 55 |
| 40 | Progressive vector diagram of currents from the NTAS-4 Aquadopp. | 57 |
| 41 | Spectrum of NTAS-4 Aquadopp current speed. | 58 |
| 42 | Time series waterfall plots from the NTAS-4 RDI Workhorse. | 59 |
| 43 | NTAS-4 RDI Workhorse spectra from 18 to 74 m. | 61 |

| | | |
|----|---|----|
| 44 | Progressive vector diagram of currents from the NTAS-4 RDI Workhorse. | 63 |
| 45 | Rotary spectra from NTAS-5. | 64 |
| 46 | Unfiltered currents from NTAS-5 Aquadopp. | 65 |
| 47 | Progressive vector diagram of currents from the NTAS-5 Aquadopp. | 67 |
| 48 | Spectrum of NTAS-5 Aquadopp current speed. | 68 |
| 49 | Time series waterfall plots from the NTAS-5 RDI Workhorse. | 69 |
| 50 | NTAS-5 RDI Workhorse spectra from 18 to 74 meters. | 71 |
| 51 | Progressive vector diagram of currents from the NTAS-5 RDI Workhorse. | 73 |
| 52 | Data return for NTAS-1 to 5 current meters. | 75 |
| 53 | Vertical profile of all velocity data on NTAS-1. | 76 |
| 54 | Progressive vectors of all velocity data on NTAS-1. | 77 |
| 55 | Spectra for the NTAS-1 current meters. | 78 |
| 56 | Vertical profile of all velocity data on NTAS-2. | 79 |
| 57 | Progressive vectors of all velocity data on NTAS-2. | 80 |
| 58 | Spectra for the NTAS-2 current meters. | 81 |
| 59 | Vertical profile of all velocity data on NTAS-3. | 82 |
| 60 | Progressive vectors of all velocity data on NTAS-3. | 83 |
| 61 | Spectra for the NTAS-3 velocities. | 84 |
| 62 | Vertical profile of all velocity data on NTAS-4. | 85 |
| 63 | Progressive vectors of all velocity data on NTAS-4. | 86 |
| 64 | Spectra for the NTAS-4 current meters. | 87 |
| 65 | Vertical profile of all velocity data on NTAS-5. | 88 |
| 66 | Progressive vectors of all velocity data on NTAS-5. | 89 |
| 67 | Spectra for the NTAS-5 current meters. | 90 |
| 68 | Northward current speeds on NTAS-1 to -5 | 92 |
| 69 | Eastward current speeds on NTAS-1 to -5 | 93 |
| 70 | Vertical profile of all velocity data on NTAS-1 to -5. | 94 |
| 71 | Current magnitude spectra. | 95 |
| 72 | Northward current speed spectra. | 96 |
| 73 | Eastward current speed spectra. | 97 |
| 74 | Rotary spectra from NTAS-1 to -5. | 98 |
| 75 | Progressive vectors of RDI ADCP velocity data on all NTAS 1 to 5. | 99 |

List of Tables

| | | |
|----|---|-----|
| 1 | Site statistics extracted from Cruise Reports and Mooring Logs. | 2 |
| 2 | NTAS velocity instrument information. | 10 |
| 3 | Aquadopp instrument configurations for the NTAS deployments. | 11 |
| 4 | RDI instrument configurations for the NTAS deployments. | 11 |
| 5 | Outlier points discarded from NTAS velocity data | 20 |
| 6 | Spectral peak heights for NTAS-1 Aquadopp. | 24 |
| 7 | Spectral peak heights for NTAS-1 RDI NarrowBand, 90 m bin. | 24 |
| 8 | Spectral peak heights for NTAS-1 RDI NarrowBand, 22 m bin. | 30 |
| 9 | Spectral peak heights for NTAS-2 Aquadopp. | 34 |
| 10 | Spectral peak heights for NTAS-2 RDI Workhorse, 90 m bin. | 34 |
| 11 | Spectral peak heights for NTAS-2 RDI Workhorse, 46 m bin. | 35 |
| 12 | Spectral peak heights from the VMCM on NTAS-2. | 35 |
| 13 | Spectral peak heights for NTAS-3 Aquadopp. | 48 |
| 14 | Spectral peak heights for NTAS-3 RDI Workhorse, 90 m bin. | 51 |
| 15 | Spectral peak heights for NTAS-3 RDI Workhorse, 26 m bin. | 51 |
| 16 | Spectral peak heights for NTAS-4 Aquadopp. | 56 |
| 17 | Spectral peak heights for NTAS-4 RDI Workhorse, 78 m bin. | 56 |
| 18 | Spectral peak heights for NTAS-4 RDI Workhorse, 22 m bin. | 62 |
| 19 | Spectral peak heights for NTAS-5 Aquadopp. | 66 |
| 20 | Spectral peak heights for NTAS-5 RDI Workhorse, 78 m bin. | 66 |
| 21 | Spectral peak heights for NTAS-5 RDI Workhorse, 14 m bin. | 72 |
| A1 | Gross statistical description of the various NTAS velocity time series. | 102 |

1 Introduction

The Northwest Tropical Atlantic Station (NTAS) project for air-sea flux measurement was conceived in order to investigate surface forcing and oceanographic response in a region of the tropical Atlantic with strong sea surface temperature (SST) anomalies and the likelihood of significant local air-sea interaction on interannual to decadal timescales. The site, near 15°N , 51°W , was intended to be maintained through successive mooring turn-arounds, and is complementary to other long-term surface moorings in the tropical Atlantic.

The primary scientific objectives of the NTAS project are to determine the in-situ fluxes of heat, moisture and momentum, to use these in-situ fluxes to make a regional assessment of flux components from numerical weather prediction models and satellites, and to determine the degree to which the oceanic budgets of heat and momentum are locally balanced.

To accomplish these objectives, a surface mooring with sensors suitable for the determination of air-sea fluxes and upper ocean properties was deployed. The surface buoy was outfitted with two Air-Sea Interaction Meteorology (ASIMET) systems. Each system measures, records, and transmits via Argos satellite the surface meteorological variables necessary to compute air-sea fluxes of heat, moisture and momentum. The upper 120 m of the mooring line was outfitted with oceanographic sensors for the measurement of temperature and velocity.

This report presents velocity data recovered from current meters and Acoustic Doppler Current Profilers (ADCPs) from the first five NTAS deployments (March 2001 to February 2006). Cruise reports for the first four deployments (NTAS-1 through -4) have been published [Plueddemann *et al.*, 2001, 2002, 2003, 2006], and the fifth is in preparation [Plueddemann *et al.*, 2012].

A location map for the NTAS site is shown in Figure 1a. A Sea-Beam survey undertaken on deployment of NTAS-3 mooring shows the detailed topography of the bottom around the site (Fig. 2).

On each cruise (with the exception of the first!) the replacement mooring was deployed nearby (Fig. 1b) before the extant mooring was recovered. This was done to provide an overlap in the data series from the two buoys. Consistent prevailing currents and winds at the sites ensured that for the majority of the time each buoy was located in the quarter circle directly to the west of its anchor position (Fig. 3).

This report is arranged in sections as follows:

1. The moored arrays and instrumentation are described (Sections 2 and 3). Peculiarities and unique characteristics of the particular deployments are presented here.
2. Methods and processing common to all deployments are discussed (Section 4).
3. The data are presented in the form of tables and figures (Sections 5 and 6). Here are shown:
 - the time-series of northward and eastward velocities for each instrument;
 - progressive vector diagrams of the currents;
 - tabulations of spectral peaks and summary statistics of each instrument;
 - comparisons of the spectra from two or more current meters from each deployment; and
 - vertical profiles of the currents.

The sites were occupied as shown in Table 1.

Table 1: Site statistics extracted from Cruise Reports and Mooring Logs. Deployment is recorded as the anchor drop time, and recovery as the trigger release time. Note that, since the NTAS-3 buoy was adrift when recovered, the surface meteorological and subsurface instruments were recovered earlier, beginning on 2004-02-19 at 16:49Z. The position was 14°53.7'N, 51°22.817'W, 21.2 n.m. from the anchor position.

| | Anchor position | | Depth (m) | Deployment (UTC) | Recovery (UTC) | Duration (d:h:m) |
|--------|-----------------|--------------|--------------|---------------------|-------------------|---------------------|
| NTAS-1 | 14°49.97'N | 51°00.30'W | 4982 | 2001-03-30 23:17 | 2002-03-06 10:08 | 340:10:51 |
| NTAS-2 | 14°44.301'N | 50°56.823'W | 5043 | 2002-03-04 22:18 | 2003-02-16 12:06 | 348:13:48 |
| NTAS-3 | 14°49.50'N | 51°01.30'W | 4977 | 2003-02-15 05:47 | 2004-02-23 23:10* | 373:17:23* |
| NTAS-4 | 14°44.430'N | 50°56.034'W | 5048 | 2004-02-21 03:16 | 2005-03-13 14:20 | 386:11:04 |
| NTAS-5 | 14°41.0736'N | 51°02.5408'W | 5107 | 2005-03-11 19:35 | 2006-02-28 12:39 | 353:17:04 |

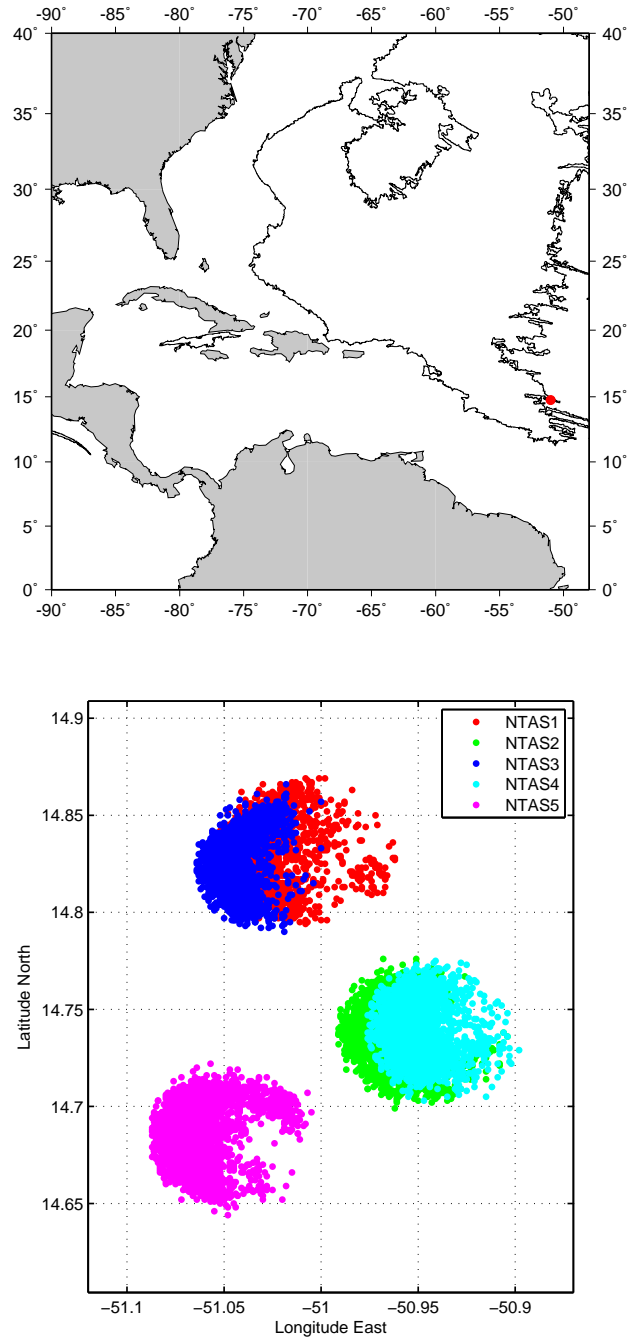


Figure 1: Site map for NTAS. (a) Location. The 5000 m contour is drawn (bathymetry from ETOPO1 [Amante and Eakins, 2008]). (b) The relationship among the NTAS sites are shown by plotting the hourly telemetered position during the deployments. Site positions of consecutive buoys are offset because the replacement buoy was deployed before the currently deployed buoy was recovered, to provide an overlap in time of the data collection.

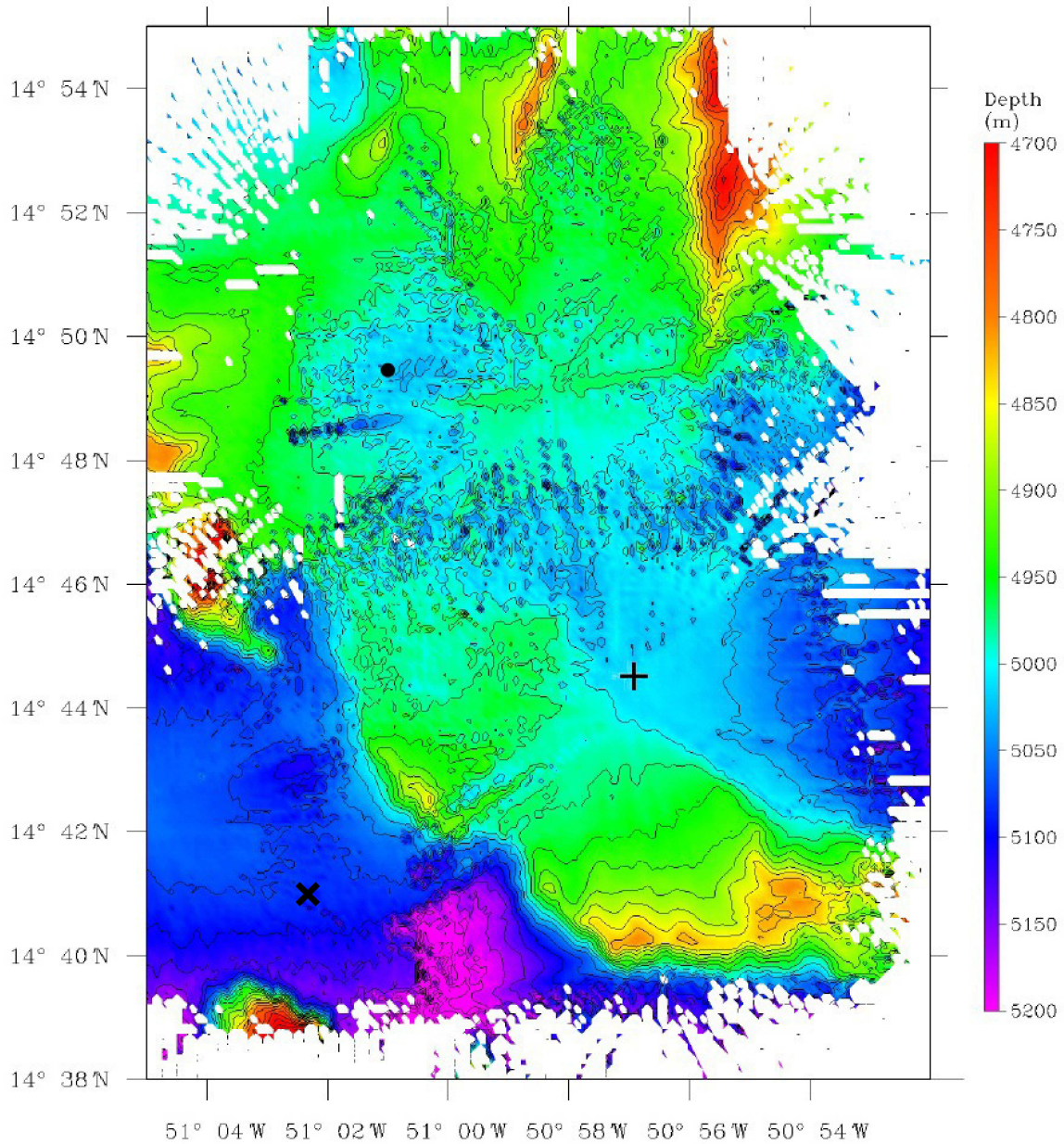


Figure 2: Sea-Beam bathymetry at the NTAS site is shown as determined on the NTAS-3 deployment cruise. The approximate positions of the NTAS-1 and -3 (●), NTAS-2 and -4 (+), and NTAS-5 (×) buoy anchor positions are indicated. Anchor positions of consecutive buoys were offset to allow deployment of the next buoy before recovery of the current one, in order to provide an overlap in time of the data series.

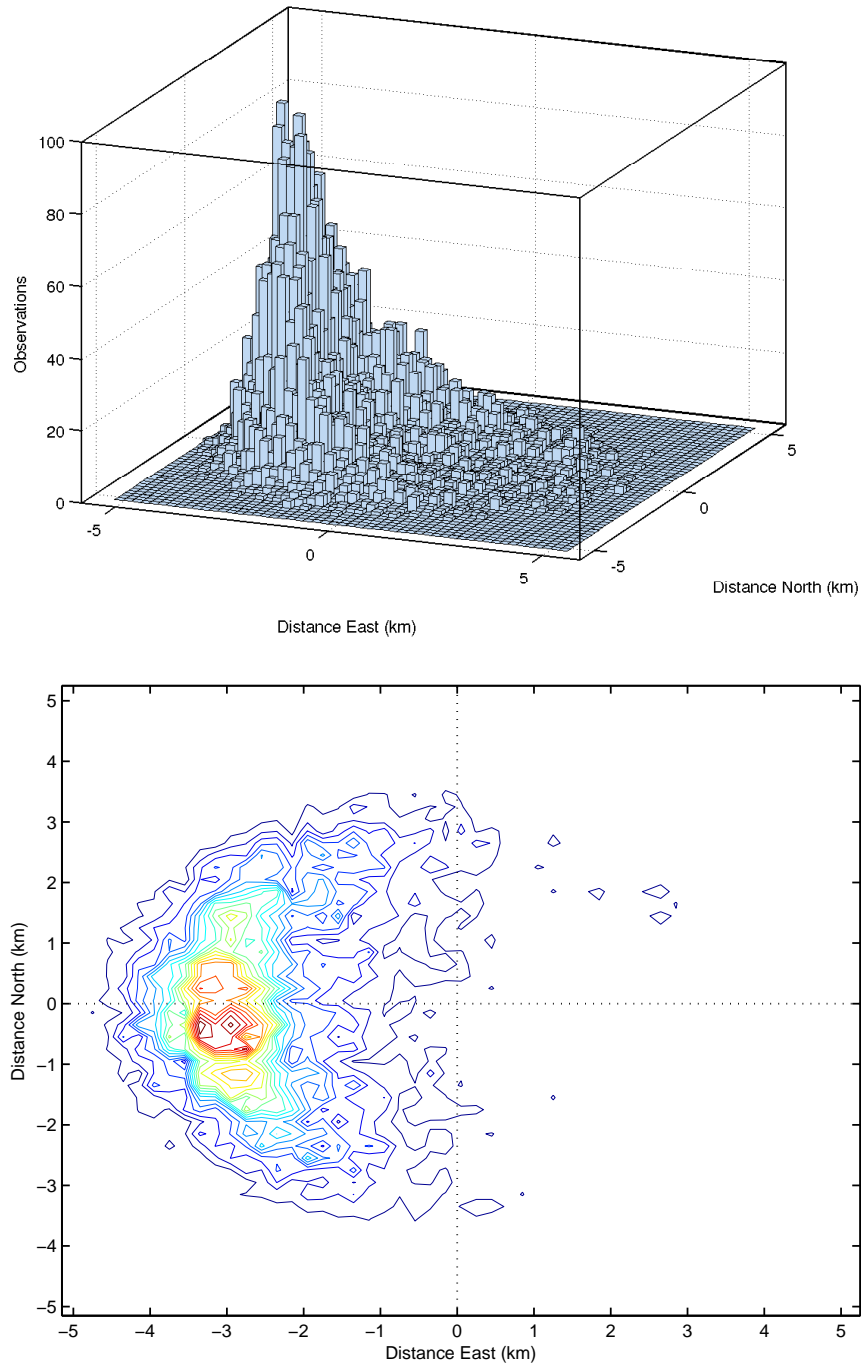


Figure 3: Buoy position relative to the anchor position for all buoy deployments. Position data from each deployment was calculated relative to its anchor positions. The relative position data were binned into a 2-dimensional histogram (`hist3`, *The Mathworks*, 2008). (a) Histogram of the buoy position relative to the anchor position. (b) Contour plot of the histogram data. Anchor position is at (0,0).

2 Deployment Cruises

2.1 NTAS-1 Deployment Cruise

The deployment of NTAS-1 [Plueddemann *et al.*, 2001] was done on R/V *Oceanus*, Cruise 365, Leg 5 (OC365-V). The cruise was completed in 12 days, between 28 March and 8 April 2001. The cruise leg originated from and terminated in Bridgetown, Barbados, West Indies. The NTAS-1 mooring was deployed at $14^{\circ}49.97'N$, $51^{\circ}00.03'W$ on 30 March 2001. The NTAS-1 deployment was followed by a 12-hour data intercomparison period, during which meteorological measurements from the NTAS-1 buoy and *Oceanus* were obtained and shipboard CTD casts were completed.

2.2 NTAS-2 Deployment Cruise

The mooring turnaround of NTAS-1/2 [Plueddemann *et al.*, 2002] was done on the NOAA Ship *Ronald H. Brown*, Cruise RB-02-02. The cruise was completed in 7 days, between 2 and 8 March 2002. The cruise leg originated from and terminated in Bridgetown, Barbados. A Sea-Beam bathymetric survey was done over an area of approximately 140 n.m.^2 (470 km^2), which encompassed the NTAS-1 and NTAS-2 anchor locations. The NTAS-2 mooring was deployed at $14^{\circ}44.30'N$, $50^{\circ}56.82'W$ on 4 March 2002. The NTAS-2 deployment was followed by a 24-hour data intercomparison period, during which meteorological measurements from both buoys and the ship were obtained, and shipboard CTD casts were completed. The NTAS-1 mooring was recovered on 6 March 2002.

2.3 NTAS-3 Deployment Cruise

The NTAS-2/3 mooring turnaround [Plueddemann *et al.*, 2003] was done on the WHOI R/V *Oceanus*, Cruise OC-385-5. The cruise was completed in 12 days, between 12 and 23 February 2003. The cruise originated from Bridgetown, Barbados and terminated in Woods Hole. The NTAS-3 mooring was deployed at $14^{\circ}49.50'N$, $51^{\circ}01.3'W$ on 15 February 2003. The NTAS-3 deployment was followed by a 24-hour data intercomparison period, during which meteorological measurements from both buoys and the ship were obtained, and shipboard CTD casts were made. The NTAS-2 mooring was recovered on 16 February 2003.

2.4 NTAS-4 Deployment Cruise

The NTAS-3/4 mooring turnaround [Plueddemann *et al.*, 2003] was done on the NOAA Ship *Ronald H. Brown*, Cruise RB-04-01. The cruise was completed in 14 days, between 12 and 25 February 2004. The cruise originated from Charleston, SC, and terminated in Bridgetown, Barbados, West Indies. The NTAS-3 buoy, which went adrift on 16 February 2004 due to a mooring component failure, was located and recovered on 19 February 2004. The NTAS-4 mooring was deployed at $14^{\circ}44.43'N$, $50^{\circ}56.03'W$ on 21 February 2004. The NTAS-4 deployment was followed by a 30-hour data intercomparison period, during which meteorological measurements from the NTAS-4 buoy and the ship were obtained. Dragging operations were conducted in an unsuccessful attempt to retrieve the remainder of the NTAS-3 mooring.

2.5 NTAS-5 Deployment Cruise

The NTAS-4/5 mooring turnaround [Plueddemann *et al.*, 2012] was done on the NOAA Ship *Ronald H. Brown*, Cruise RB-05-02. The cruise was completed in 14 days, between 9 and 22 March 2005. The cruise originated from Bridgetown, Barbados, and terminated in Charleston, SC. A bathymetric survey of the NTAS-5 deployment region, a 250 n.m.² area (approximate) centered near 14°44'N, 51°00'W, was completed. The NTAS-5 mooring was deployed at 14°41.07'N, 51°02.64'W on 11 March 2005. The NTAS-5 deployment was followed by a 34-hour data inter-comparison period, during which meteorological measurements from both buoys and the ship were obtained, and shipboard CTD casts were made. The NTAS-4 mooring was recovered on 13 March 2005. Dragging operations were conducted, resulting in successful retrieval of the mooring line from the NTAS-3 mooring.



Figure 4: Nortek Aquadopp mounted on titanium load bar. No anti-fouling paint or transducer coating has been applied.

3 Moored Arrays and Instrumentation

The general configuration common to all deployments is outlined in the following sections. The general mooring design is described, and the current meter configurations tabulated. Thereafter, unique aspects of the individual deployments are explained.

3.1 Mooring Design

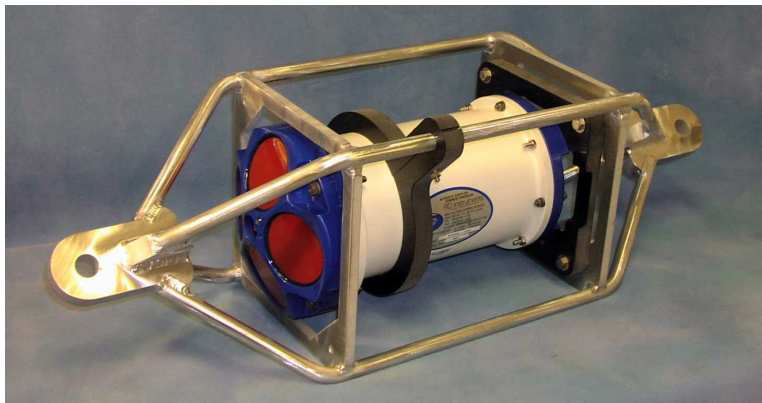
The basic NTAS mooring is an inverse-catenary design of compound construction, utilizing chain, wire rope, nylon and polypropylene. The mooring scope (ratio of total mooring length to water depth) is about 1.25. For NTAS-1 through -4, the surface buoy was 3-meter “discus” design with a foam-filled aluminum hull and a watertight center well housing electronics and batteries. Starting with NTAS-5 a new hull design was used—the Modular Ocean Buoy System (MOBS). The MOBS surface element is a 2.7-meter diameter Surlyn foam buoy with a watertight electronics well and aluminum instrument tower. The ASIMET sensor modules [Hosom *et al.*, 1995] are bolted to the buoy tower at approximately 3 m above the sea surface. Sea surface temperature and salinity are measured by sensors bolted to the bridle legs and cabled to the loggers through a bottom access plate in the buoy well. Further details of the surface instrumentation can be found in the cruise reports [Plueddemann *et al.*, 2001, 2002, 2003, 2006, 2012].

Current meters, current profilers and temperature sensors were attached along the mooring line using load bars or cages (attached in-line between chain or wire sections) and specially designed brackets (clamped along wire rope sections). All instrumentation was in the upper 150 m. Nortek Aquadopp current meters were deployed near the surface on load bars (Fig. 4). RD Instruments ADCPs were deployed in load cages (Fig. 5) at 85 m to 100 m depth with beams pointing upwards. For NTAS-2, a Vector Measuring Current Meter (VMCM) in a load cage (Fig. 6) was deployed near the Aquadopp. Sample intervals ranged from 7.5 minutes (VMCM) to 1 hour (ADCPs).

A summary of the current meter instrument locations, serial numbers, and sample rates is given in Table 2.



(a)



(b)

Figure 5: (a) RD Instruments 300 kHz NarrowBand ADCP mounted in stainless steel load cage. Antifouling paint (blue) has been applied to the upper portion of the cage. (b) RD Instruments 300 kHz Workhorse (BroadBand) ADCP in aluminum load cage. The cage has not been painted and no anti-fouling treatment has been applied to the ADCP.



Figure 6: Vector Measuring Current Meter (VMCM) in mounted in stainless steel load cage. The cage, VMCM sting and VMCM pressure housing have been painted with a white anti-fouling coating.

Table 2: NTAS velocity instrument information. Aquadopp indicates the Aquadopp current meter by Nortek, ADCP indicates an acoustic doppler current profiler by RDI, VMCM is the vector measuring current meter and SN is the instrument serial number. Variables measured were velocity (V), temperature (T), and pressure (P).

| Deployment | Depth (m) | Sensor | SN | Variable(s) Measured | Sample Rate |
|------------|-----------|----------|------|----------------------|-------------|
| NTAS-1 | 8 | Aquadopp | 174 | V, T, P | 30 min |
| NTAS-1 | 100 | ADCP | 593 | V | 15 min |
| NTAS-2 | 6 | Aquadopp | 432 | T, V, P | 60 min |
| NTAS-2 | 7.5 | VMCM | 1 | T, V | 7.5 min |
| NTAS-2 | 100 | ADCP | 2125 | T, V | 60 min |
| NTAS-3 | 6 | Aquadopp | 174 | T, V, P | 60 min |
| NTAS-3 | 100 | ADCP | 2601 | T, V | 60 min |
| NTAS-4 | 6 | Aquadopp | 432 | T, V, P | 60 min |
| NTAS-4 | 85 | ADCP | 2125 | T, V | 60 min |
| NTAS-5 | 6 | Aquadopp | 1226 | T, V, P | 60 min |
| NTAS-5 | 85 | ADCP | 2601 | T, V | 60 min |

3.2 Aquadopp

The Nortek Aquadopp current meter uses the Doppler technique to obtain velocity estimates within a single range bin along three beams. Two beams point horizontally, separated by 90 degrees in azimuth. A third beam points upwards at 45 degrees at an azimuth between the two horizontal beams. The sample volume is about 1 m away from the instrument. A compass and two axes of tilt are used to convert velocities from instrument coordinates to geographic (earth) coordinates. The Aquadopp also measures temperature and pressure. The plastic instrument housing and pressure sensor are rated to 200 m depth. Aquadopp current meters were deployed at 8 m depth (NTAS-1) and 6 m depth (NTAS-2 through -5). A titanium load bar and bolt-on cage originally designed for use with SeaBird SBE-16 SeaCATs was used to attach the Aquadopp in-line between chain sections of the mooring. Because the cage was not designed specifically for the instrument, the transducers protruded slightly beyond the cage bars (Fig. 4).

The Aquadopp instruments were configured as shown in Table 3.

3.3 Acoustic Doppler current profilers

Acoustic Doppler current profilers (ADCPs) apply Doppler processing to the range-gated return from each acoustic transmission (ping). By utilizing four beams in a “Janus” configuration (separated by 90 degrees in azimuth and inclined at 20 or 30 degrees from the vertical), the along-beam velocities can be converted into horizontal velocities. Combining horizontal velocities with tilt and heading information allows transformation to geographic (earth) coordinates on a ping-by-ping basis. In this manner the instrument produces vertical profiles of horizontal velocity. Vertical resolution is set by the ping duration and temporal resolution is set by the ensemble-averaging interval.

A 300 kHz RD Instruments NarrowBand ADCP was deployed on NTAS-1 at 100 m depth. For NTAS-2 through -5, 300 kHz WorkHorse (broadband) ADCPs were deployed at depths of 85 or

Table 3: Aquadopp instrument configurations for the NTAS deployments.

| | NTAS-1 | NTAS-2 | NTAS-3 | NTAS-4 | NTAS-5 |
|-----------------------------|--------|--------|--------|--------|--------|
| Aquadopp SN | 174 | 432 | 174 | 432 | 1226 |
| Deployment depth (m) | 8 | 6 | 6 | 6 | 6 |
| Transmission interval (sec) | 1 | 1 | 1 | 1 | 1 |
| Average interval (sec) | 60 | 180 | 180 | 180 | 180 |
| Sample interval (min) | 30 | 60 | 60 | 60 | 60 |
| Blanking distance (m) | 0.35 | 1.0 | 1.0 | 1.0 | 1.0 |
| Diagnostics interval (min) | 1440 | 1440 | 1440 | 1440 | 1440 |
| Diagnostics samples | 20 | 20 | 20 | 20 | 20 |
| Measurement load (%) | 4 | 22 | 22 | 17 | 17 |
| Power level | HIGH- | HIGH- | HIGH- | HIGH- | HIGH- |
| Compass update rate (sec) | 1 | 1 | 1 | 1 | 1 |
| Coordinate system | earth | ENU | ENU | ENU | ENU |
| Recorder size (MB) | 2 | 5 | 2 | 5 | 9 |

Table 4: RDI instrument configurations for the NTAS deployments. (NB—NarrowBand, WH—Work-Horse.)

| | NTAS-1 | NTAS-2 | NTAS-3 | NTAS-4 | NTAS-5 |
|--------------------------|--------|--------|--------|--------|--------|
| RDI SN | 593 | 2125 | 2601 | 2125 | 2601 |
| ADCP Type | NB | WH | WH | WH | WH |
| Deployment depth (m) | 100 | 100 | 100 | 85 | 85 |
| Time between pings (sec) | 1 | 1.25 | 1 | 1 | 1 |
| Pings per ensemble | 120 | 120 | 120 | 120 | 120 |
| Ensemble interval (min) | 15 | 60 | 60 | 60 | 60 |
| Number of depth bins | 28 | 28 | 28 | 25 | 25 |
| Depth bin length (m) | 4 | 4 | 4 | 4 | 4 |
| Pulse length (m) | 8 | 4 | 4 | 4 | 4 |
| Blank after transmit (m) | 4 | 6 | 6 | 3 | 3 |
| Transducer orientation | up | up | up | up | up |
| Coordinate system | earth | earth | earth | earth | earth |
| Recorder size (MB) | 18 | 40 | 40 | 48 | 48 |

100 m. The ADCP instrument was housed in a welded aluminum load cage, and placed in-line between wire sections of the mooring.

The RDI ADCP instruments were set up in the configurations shown in Table 4.

3.4 Vector Measuring Current Meters

Vector Measuring Current Meters (VMCMs) consist of an electronics housing with a “sting” extending from the upper end cap. Two pairs of cosine-response propeller sensors are attached to the sting, oriented in orthogonal horizontal directions. East and North components of velocity are determined from the orthogonal propeller counts (updated every $\frac{1}{4}$ revolution) and the direction from

a flux-gate compass (updated once per second). The cosine response and continuous accumulation of propeller counts enables the VMCM to measure mean flows accurately in the presence of strong oscillatory flows (e.g., surface wave orbital velocities).

A VMCM was deployed on the NTAS-2 mooring, with the center of the sting at 7.5 m depth. The intent was to allow a comparison of the VMCM velocity to that of the Aquadopp just above it. The VMCM was housed in a stainless steel load cage, and placed in-line between chain sections of the mooring. VMCM velocity accuracy is about $1 \text{ cm}\cdot\text{s}^{-1}$. The record interval was 7.5 min for the NTAS-2 deployment.

3.5 Mooring Diagrams

Sketches showing the detail of near-surface sensors deployed on NTAS-1 through -5 are shown in Figures 7 to 11 (see also Table 2). NTAS-1 used a 300 kHz NarrowBand ADCP with ~ 100 m profiling range, supplemented by an Aquadopp to provide measurements in the “blind spot” created by side-lobe reflections from the surface. NTAS-2 added a VMCM for comparison with the Aquadopp and the NarrowBand ADCP was replaced by a 300 kHz BroadBand Workhorse. The NTAS-3 configuration was analogous to NTAS-2, but without the VMCM. For NTAS-4 and -5 it was recognized that the Workhorse ADCPs were providing only 75–85 m of profiling range, and their deployment depths were moved shallower.

4 Data Processing Summary

4.1 Aquadopp

After instrument recovery and a time check done by placing the instrument (which includes a temperature sensor) in an ice bath for a known interval, binary files are downloaded from the instrument to a laptop computer using the manufacturers “Aquadopp” software. The resulting file is unpacked into multiple ASCII files using the Aquadopp data conversion utility. Three ASCII files are created:

1. Header file, containing instrument metadata, configuration information and a description of the file format for the data and diagnostics files,
2. Data file, containing velocity, amplitude and ancillary data,
3. Diagnostics file, containing the same variables as the data file, but for short, high-frequency bursts defined in the configuration.

The Aquadopp data file is processed as described below to create the data evaluated in this report. The header file is used to populate metadata fields in the processed data file. The diagnostics file is used for evaluation in the event that processed data are suspect.

Aquadopp data are processed by two Matlab scripts. The first script loads the ASCII data file, computes decimal year day from date and time, and assigns a subset of relevant data from the Aquadopp file to Matlab variables. The output of the first script is a Matlab file of unpacked, unprocessed data. These data are evaluated for timing problems (gaps or drift) and adjusted if necessary. A second script reads the time-adjusted data, truncates the record at the start and end of

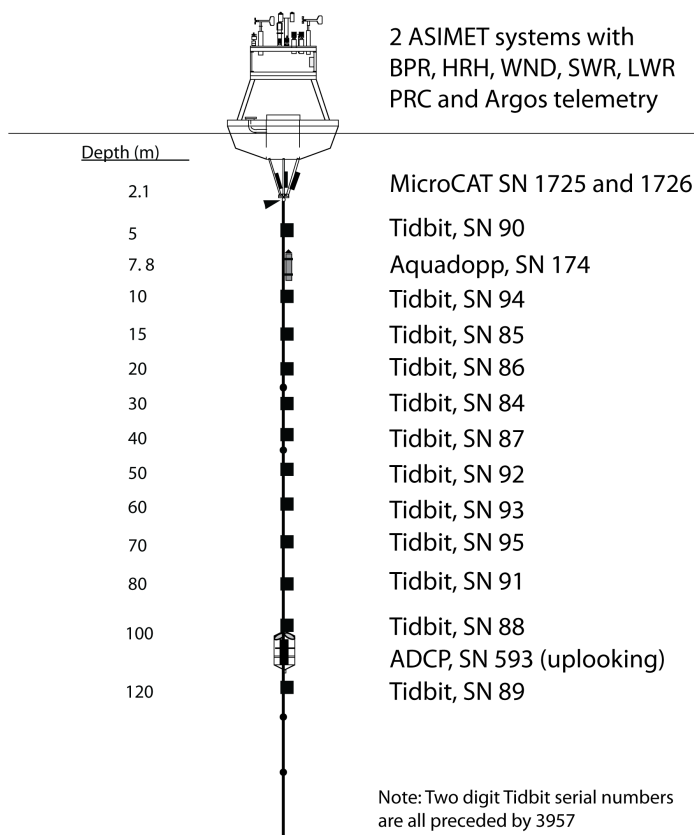


Figure 7: NTAS-1 mooring diagram. Near-surface detail.

deployment, interpolates to a “standard” time base, converts velocities to units of $\text{cm}\cdot\text{s}^{-1}$, applies a sound speed correction, applies a magnetic variation correction, and assigns a depth based on the mooring log. Some basic metadata are also assigned at this stage.

4.2 VMCM

After instrument recovery, and before extracting the card from the instrument, the clock is checked by first securing the props, then releasing and spinning them for up to two minutes, and carefully recording the time of these procedures. VMCM data are stored on Intel type II flash memory cards, in 34-byte little endian binary records. The memory cards are removed from the instruments and copied to a laptop equipped with a PCMCIA/PC card slot using a custom version of Linux that includes support for these devices.

The binary files are processed using a pair of Malab scripts developed by the Upper Ocean

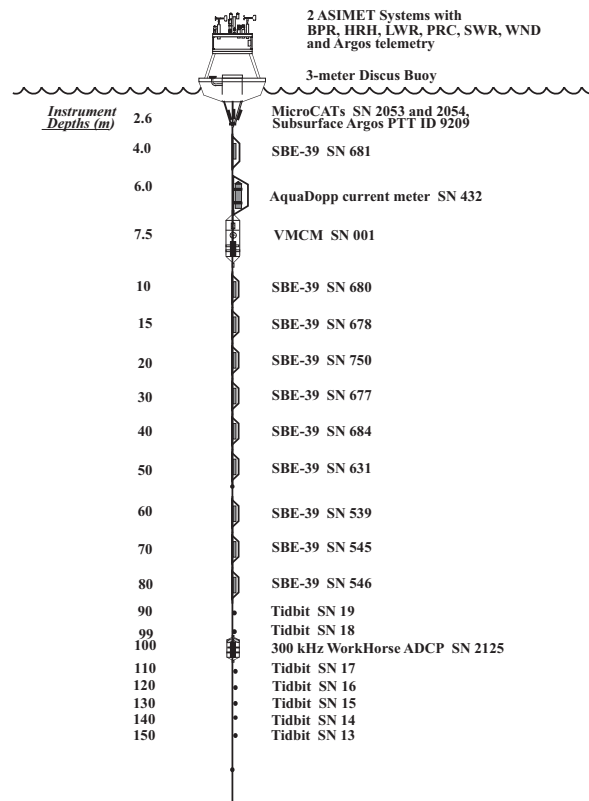


Figure 8: NTAS-2 mooring diagram. Near-surface detail.

Processes Group. The first script unpacks the binary records and generates an ASCII text file containing year, month, day, hour, minute, second, velocity east, velocity north, rotor counts from rotor1 and rotor2, the last compass reading taken during the 1 minute sample period, water temperature, thermistor resistance, tiltx, and tilty. Data are scaled to physical units during this step. In the second Matlab script, which converts the ASCII file to a Matlab data file, the serial date is calculated, and some basic metadata are added. A correction for the magnetic variation is applied.

4.3 ADCP

After instrument recovery and a time check, binary files are downloaded from the instrument to a laptop computer using the manufacturers “WinSC” software. The resulting file is unpacked using the Matlab data conversion utility `upkadc.p.m`. This routine originated with E. Terray (WHOI) and was modified for use by the Upper Ocean Processes Group. The routine unpacks the binary ADCP data into eight Matlab structures containing

1. four components of velocity (east, north, up and error),
2. correlation parameter (counts),
3. backscatter intensity parameter (counts),

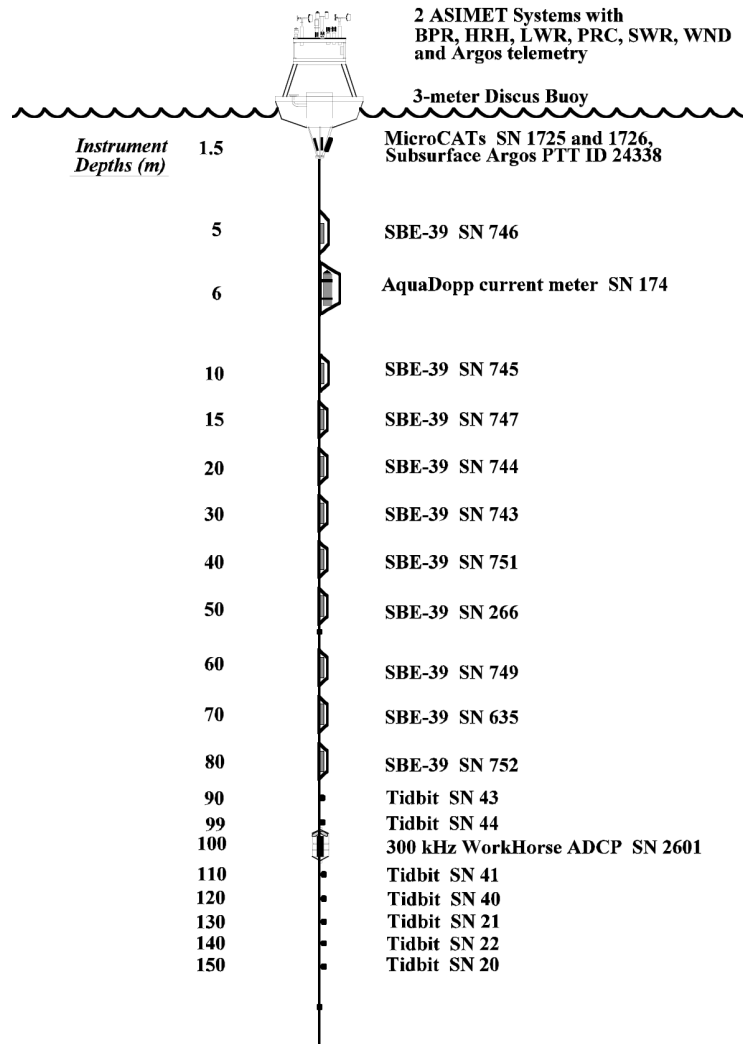


Figure 9: NTAS-3 mooring diagram. Near-surface detail.

4. percent good,
5. environmental data (e.g. time, temperature, heading, pitch, roll),
6. instrument metadata and configuration information,
7. description of the data format, and
8. bin distances from the transducer.

The unpacked data file is processed as described below to create the data evaluated in this report. The instrument metadata and configuration information are used to populate metadata fields in the processed data file.

Unpacked ADCP data are evaluated and processed in Matlab. Unpacked data are evaluated for timing problems (gaps or drift) and adjusted if necessary. Profiles of the mean and standard

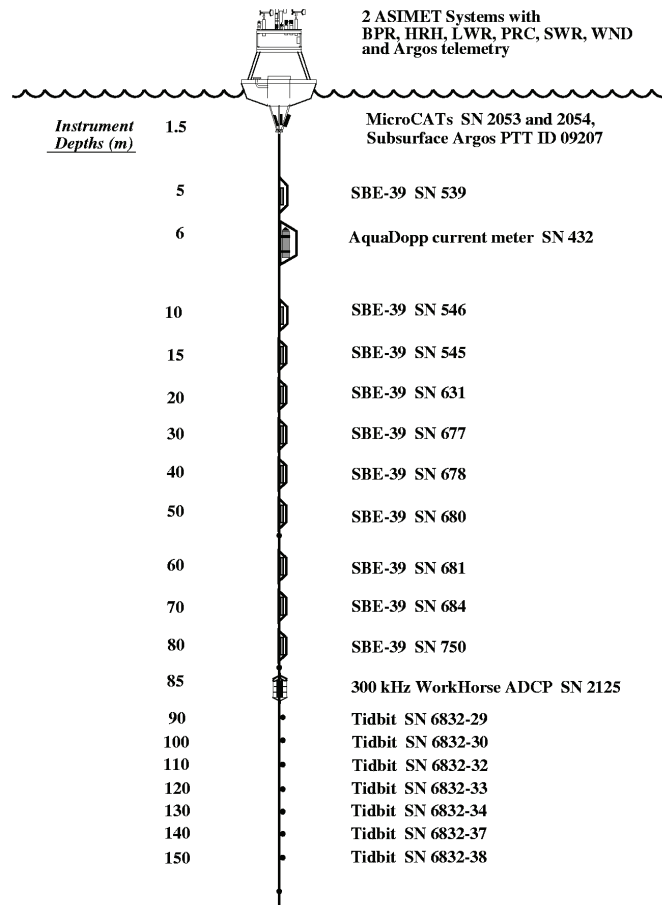


Figure 10: NTAS-4 mooring diagram. Near-surface detail.

deviation of velocity, correlation, intensity and percent good are then evaluated to determine the number of bins with data of sufficient quality to include in further processing. Two principal issues affect data quality for the up-looking ADCPs on NTAS: interference from surface returns and low signal to noise at far range. A combination of quantitative and qualitative criteria is considered in the evaluation.

- Quantitative criteria
 - The mean ADCP correlation parameter should be greater than 60 counts.
 - The mean percent good should be greater than 80%, although values as low as 50% can be tolerated if other criteria are satisfied.
 - The standard deviation of the error velocity should be less than $5 \text{ cm}\cdot\text{s}^{-1}$.
- Qualitative criteria
 - The mean intensity should be decreasing with increasing range and neither intensity nor velocity should show evidence of influence from the surface return.

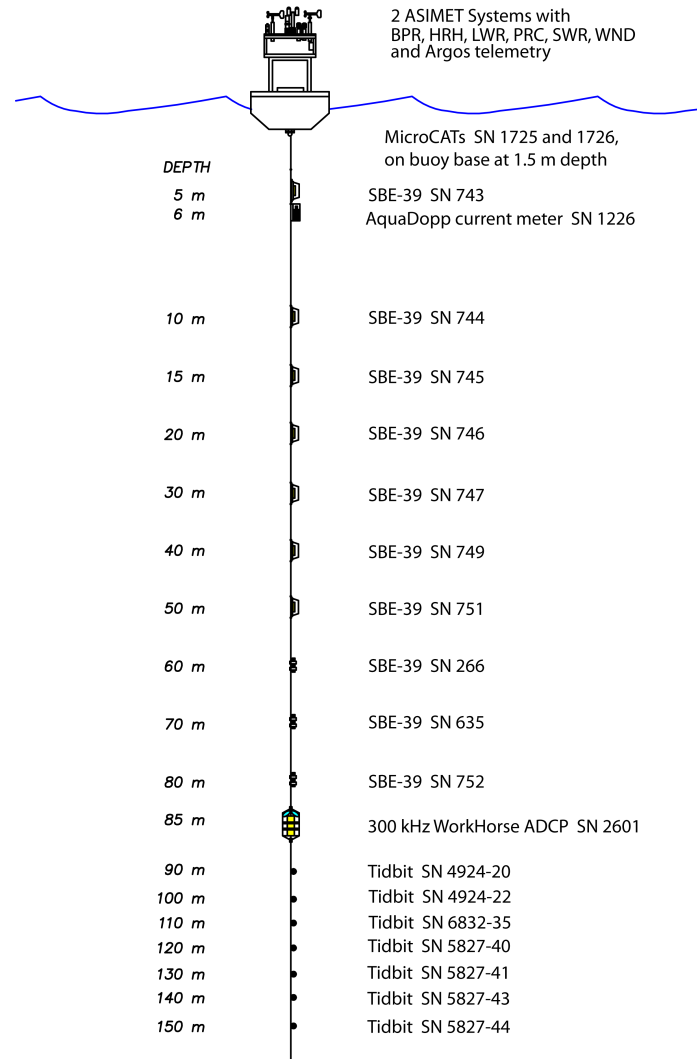


Figure 11: NTAS-5 mooring diagram. Near-surface detail.

- The mean and standard deviation of all four velocity components should vary smoothly with range—“kinks” in the mean profile accompanied by rapid increases in standard deviation are indicative of contamination and/or low signal to noise.

When the number of bins to be included in processing has been determined, a Matlab script is used to compute decimal year day from date and time, assign a subset of data from the unpacked structures to Matlab variables, and truncate the record at the start and end of the deployment. Remaining “bad points” are identified based on an error velocity threshold, and the time series for each bin is interpolated to a “standard” time base. Velocities are converted to units of $\text{cm}\cdot\text{s}^{-1}$, sound speed and magnetic variation corrections are applied and depth bins are assigned based on the mooring log and the distance of each bin from the transducer. Some basic metadata are also assigned at this stage.

5 Data Presentation

5.1 Introduction

The data presentation is briefly described, then each deployment's detail description follows. For each deployment, in addition to the processing outlined in Section 4,

- simple quality control checks on the application of magnetic variation and time base alignment were done, and adjusted where necessary;
- egregious outliers in the velocity data were detected and removed, described in Section 5.1.1.
- The time series of data were plotted.
- A statistical summary of means and variabilities of these time series were tabulated and are presented in an Appendix (Table A1).
- The spectra of the current data were determined and plotted, following the method described in Section 5.1.2. Where several depth bins are sampled by the same instrument (acoustic doppler profilers) the spectra are presented separately and also together in a waterfall plot.
- A table of spectral peaks was extracted from the spectrum for each current meter; and
- a progressive vector plot was prepared for each current meter.

The methods for dealing with outliers and creating spectra are outlined in the following paragraphs.

5.1.1 Outlier Detection

An example of the distribution of the NTAS data before scanning for outliers is shown in Figure 12. It was noted that in comparison to the normal (gaussian) distribution, the NTAS data exhibited long tails. Stripping data further than three standard deviations (3σ) from the mean (as might be reasonable in cleaning strictly normally distributed data) might have eliminated valid geophysical observations. Additionally the shape of the deviations from normal in the near-surface data together with features in the time series suggested that transient phenomena, such as passage of vortices, were being recorded. For this reason, only velocities greater than 5σ from the mean were discarded and replaced by interpolation for the preparation of this report. The number of points discarded for each deployment are listed in Table 5.

5.1.2 Spectral Analysis

The spectra of the data were determined using functions from the Matlab signal processing toolbox [The Mathworks, 2008]. The power spectral density estimate was made using the Welch spectral estimator. The Welch method splits the input signal into overlapping segments, applies a windowing filter and a fast Fourier transform (FFT) to determine the spectrum of each segment, and averages the spectra obtained. In this presentation the current meter record was split into segments $1/8$ as long as the data record, with 50% overlap and a Hann window applied. The confidence

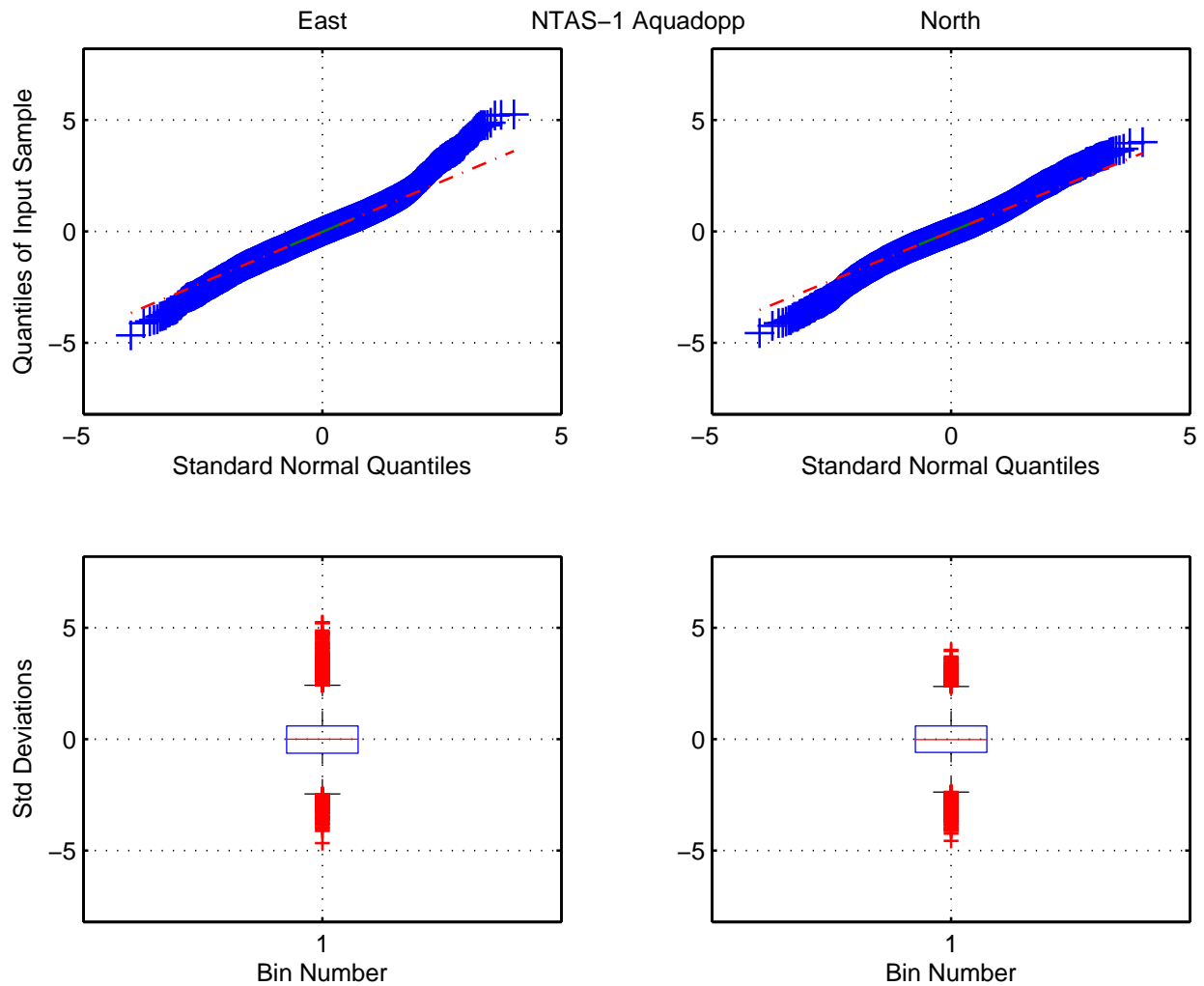


Figure 12: Plot of NTAS-1 Aquadopp velocity data, normalized by subtracting the mean and dividing by the standard deviation of each bin, showing (top) the deviation from the Gaussian distribution and (bottom) the location and variability of (left) East and (right) North current speeds. These plots show the long-tail nature of the current velocity distribution, up to 4 standard deviations from the mean, suggesting that values 4 or 5 standard deviations from the mean should not necessarily be regarded as outliers.

Table 5: The number of outlier points discarded from NTAS velocity data. AQD denotes a Nortek Aquadopp; RDI-N—RDI NarrowBand ADCP; RDI-W—RDI Workhorse ADCP; and VMCM—Vector Measuring Current Meter.

| Deployment | Instrument | Data points discarded | | From Total |
|------------|------------|-----------------------|-------|------------|
| | | East | North | |
| NTAS-1 | AQD | 3 | 0 | 16342 |
| NTAS-1 | RDI-N | 6 | 0 | 588186 |
| NTAS-2 | AQD | 0 | 0 | 8365 |
| NTAS-2 | RDI-W | 24 | 19 | 150570 |
| NTAS-2 | VMCM | 0 | 0 | 66774 |
| NTAS-3 | AQD | 95 | 0 | 8857 |
| NTAS-3 | RDI-W | 1 | 7 | 159588 |
| NTAS-4 | AQD | 0 | 0 | 6534 |
| NTAS-4 | RDI-W | 3 | 3 | 148384 |
| NTAS-5 | AQD | 0 | 0 | 8488 |
| NTAS-5 | RDI-W | 0 | 2 | 135808 |

level was set to 90%. Once the spectrum was obtained, the frequency and power spectral density were transformed by taking the base-10 logarithm of each. The best fit regression line to the transformed spectrum was determined and subtracted to detrend the spectrum, allowing the spectral peak heights to be measured.

The background level of instrumental noise was determined by assuming that this level could be estimated from the highest frequencies. The spectrum was split into 16 segments and the segments compared using the Wilcoxon rank sum test [Wilcoxon, 1945; *The Mathworks*, 2008: ranksum]. Those segments at high frequencies found to have the same median according to the statistical test were then grouped and the background level determined as the median of these grouped values.

To investigate the influence of the movement of the buoy on the current data, the velocity of the surface movement of the buoy was calculated from the Argos position and time stamp and the rotary spectrum was calculated. The data buoy position can only be determined to within ~ 1000 m using the Argos system [Galbraith and Allsup, 2005]. The Argos position is sampled ~ 2 –4 hourly (Fig. 13) and telemetered approximately every six hours [N. Galbraith, WHOI, pers. comm.]. Consequently, this velocity record was noisy, with errors inherently larger than can be expected for direct water velocity measurements, requiring careful attention in discarding outliers.

The approach was to:

1. convert position in terms of latitude and longitude to distances from the median position of the buoy;
2. calculate differences in time (δt) and displacement ($\delta \mathbf{x}$);
3. calculate velocity $\mathbf{v} = \delta \mathbf{x} / \delta t$.
4. Outliers in current speed ($|\mathbf{v}|$) were then discarded, with outliers determined as values lying further from the upper and lower quartiles than 1.5 times the interquartile range.

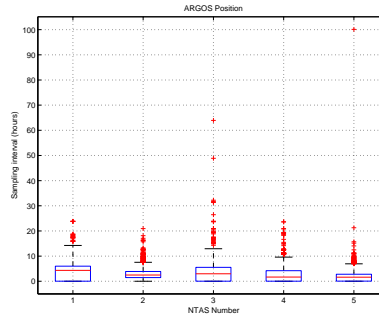


Figure 13: Boxplots of the time between observations of the buoy position using ARGOS satellite

5. The remaining velocity data were interpolated onto a regular timebase with intervals equal to the median of the position time differences ($\Delta t = \tilde{\delta t}$)
6. the spectrum of the regular velocity series was determined in the same manner as for the velocity spectra above (not shown),
7. in addition the rotary spectra of the position were determined from the autospectra, cross spectra, and quadrature spectra of the scalar components calculated using FFT,

The result for NTAS-1 is shown in Figure 14, and is somewhat representative of the rest of the deployments. In essence, the buoy motion is restricted by the diameter of the watch circle and the low frequency response is much less than that of the current meter. At inertial frequencies the buoy motion is more influential, yet still a few orders of magnitude less than the currents. At the higher frequencies the buoy motion is of the same order of magnitude as the currents and could have a strong influence on, e.g., the tidal response in the current record. The details will be discussed for each cruise below.

In the following sections the data from the NTAS deployments are presented.

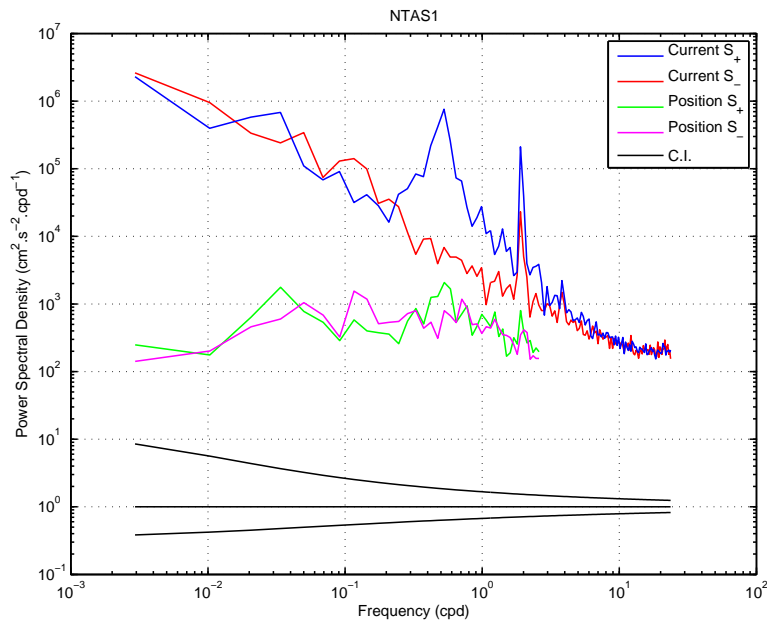


Figure 14: Showing the rotary spectra of velocities determined from the near-surface current meter (Aquadopp at 8 m) and the Argos buoy position from NTAS-1.

5.2 NTAS-1 Velocity Data

Rotary spectra for estimating the influence of the buoy motion on velocity data are shown in Figure 14.

5.2.1 Aquadopp

The time series of the speeds measured with the Aquadopp current meter is shown in Figure 15. The current velocities are shown integrated in a progressive vector diagram in Figure 16. The spectrum is shown in Figure 17. The spectral peaks are tabulated in Table 6.

5.2.2 RDI ADCP

RDI NarrowBand ADCP data were collected on NTAS-1. Time series of the current speed data are shown (Fig. 18).

The spectra for all RDI NarrowBand ADCP bins are shown as a waterfall plot in Figure 19. Tables of the spectral peaks obtained from the RDI Workhorse bins are shown in Tables 7 and 8. Only the deepest (90 m) and shallowest (22 m) bins are tabulated. Progressive vector diagrams for all bins of the NarrowBand ADCP data are shown in Figure 20.

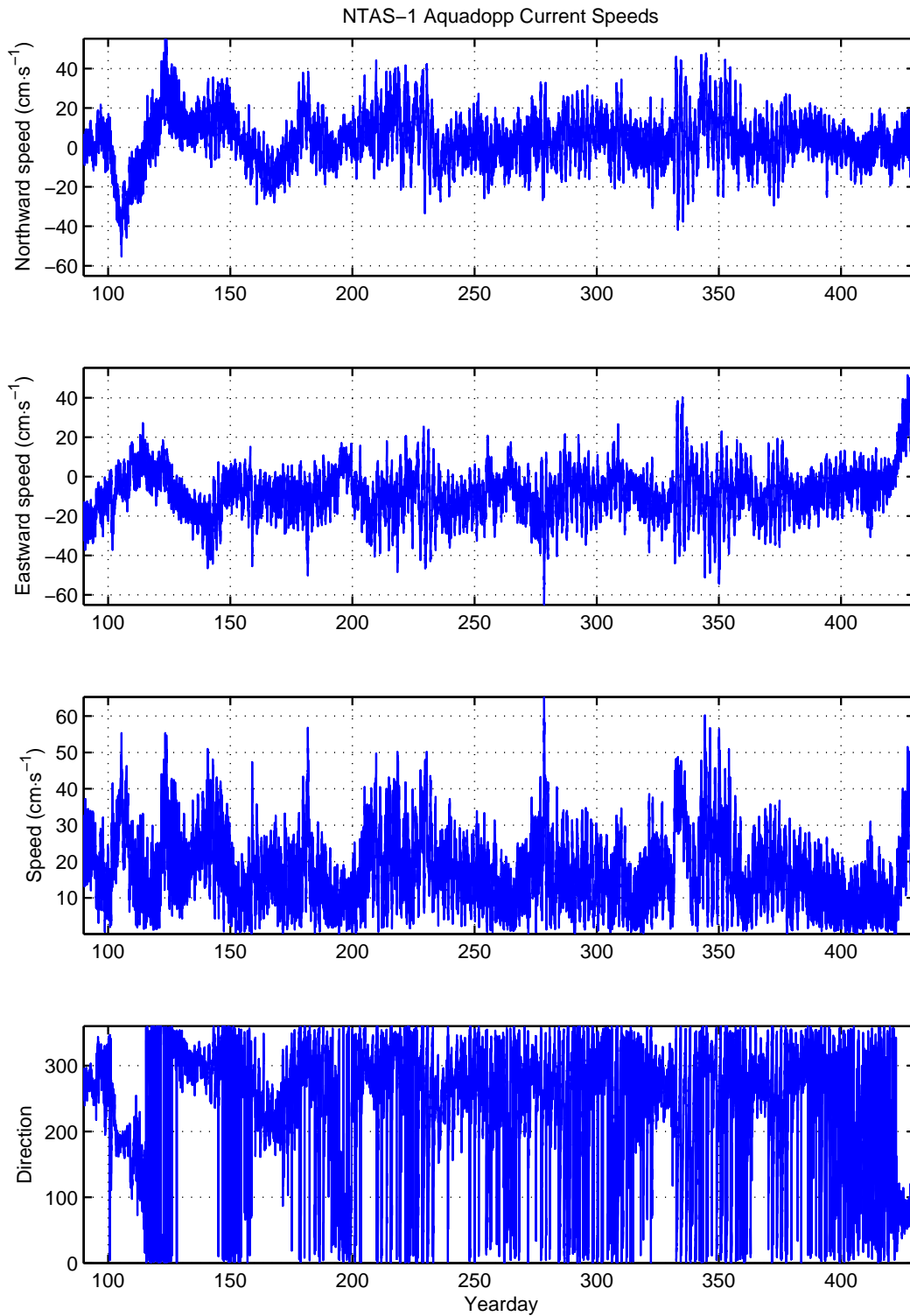


Figure 15: Unfiltered current speed time series measured by NTAS-1 Aquadopp. The abscissa is marked in days since the beginning of the year or deployment of NTAS-1 (2001). (a) Northward speeds in $\text{cm}\cdot\text{s}^{-1}$. (b) Eastward speeds in $\text{cm}\cdot\text{s}^{-1}$. (c) Magnitude in $\text{cm}\cdot\text{s}^{-1}$. (d) Direction in degrees clockwise from North.

Table 6: Spectral peak heights for NTAS-1 Aquadopp. Peaks are ordered relative to the baseline.

| Top 15 Peak Frequencies (NTAS-1 Aquadopp 7.8 m) | | | |
|---|----------|------------|---|
| f (cpd) | T (day) | T (hr) | PeakHgt ($\text{cm}^2 \cdot \text{s}^{-2}$) |
| 1.94531 | 0.51406 | 12.33735 | 114.695 |
| 0.49219 | 2.03175 | 48.76190 | 180.231 |
| 0.02344 | 42.66667 | 1024.00000 | 4348.405 |
| 1.00781 | 0.99225 | 23.81395 | 31.451 |
| 1.40625 | 0.71111 | 17.06667 | 20.847 |
| 1.31250 | 0.76190 | 18.28571 | 12.316 |
| 3.84375 | 0.26016 | 6.24390 | 3.601 |
| 21.77344 | 0.04593 | 1.10226 | 0.418 |
| 23.48437 | 0.04258 | 1.02196 | 0.372 |
| 2.41406 | 0.41424 | 9.94175 | 4.111 |
| 1.21875 | 0.82051 | 19.69231 | 8.415 |
| 22.10156 | 0.04525 | 1.08590 | 0.359 |
| 22.54687 | 0.04435 | 1.06445 | 0.351 |
| 22.92187 | 0.04363 | 1.04703 | 0.342 |
| 22.47656 | 0.04449 | 1.06778 | 0.341 |

Table 7: Spectral peak heights for NTAS-1 RDI NarrowBand, 90 m bin. Peaks are ordered relative to the baseline.

| Top 15 Peak Frequencies (NTAS-1 NarrowBand 90 m) | | | |
|--|----------|------------|---|
| f (cpd) | T (day) | T (hr) | PeakHgt ($\text{cm}^2 \cdot \text{s}^{-2}$) |
| 1.94531 | 0.51406 | 12.33735 | 65.618 |
| 0.02344 | 42.66667 | 1024.00000 | 2744.690 |
| 0.53906 | 1.85507 | 44.52174 | 82.059 |
| 1.40625 | 0.71111 | 17.06667 | 19.147 |
| 2.43750 | 0.41026 | 9.84615 | 7.449 |
| 4.03125 | 0.24806 | 5.95349 | 2.349 |
| 3.86719 | 0.25859 | 6.20606 | 2.350 |
| 47.74219 | 0.02095 | 0.50270 | 0.175 |
| 38.85938 | 0.02573 | 0.61761 | 0.201 |
| 47.97656 | 0.02084 | 0.50024 | 0.148 |
| 47.46094 | 0.02107 | 0.50568 | 0.147 |
| 4.28906 | 0.23315 | 5.59563 | 1.716 |
| 2.67188 | 0.37427 | 8.98246 | 2.739 |
| 47.88281 | 0.02088 | 0.50122 | 0.141 |
| 37.75781 | 0.02648 | 0.63563 | 0.179 |

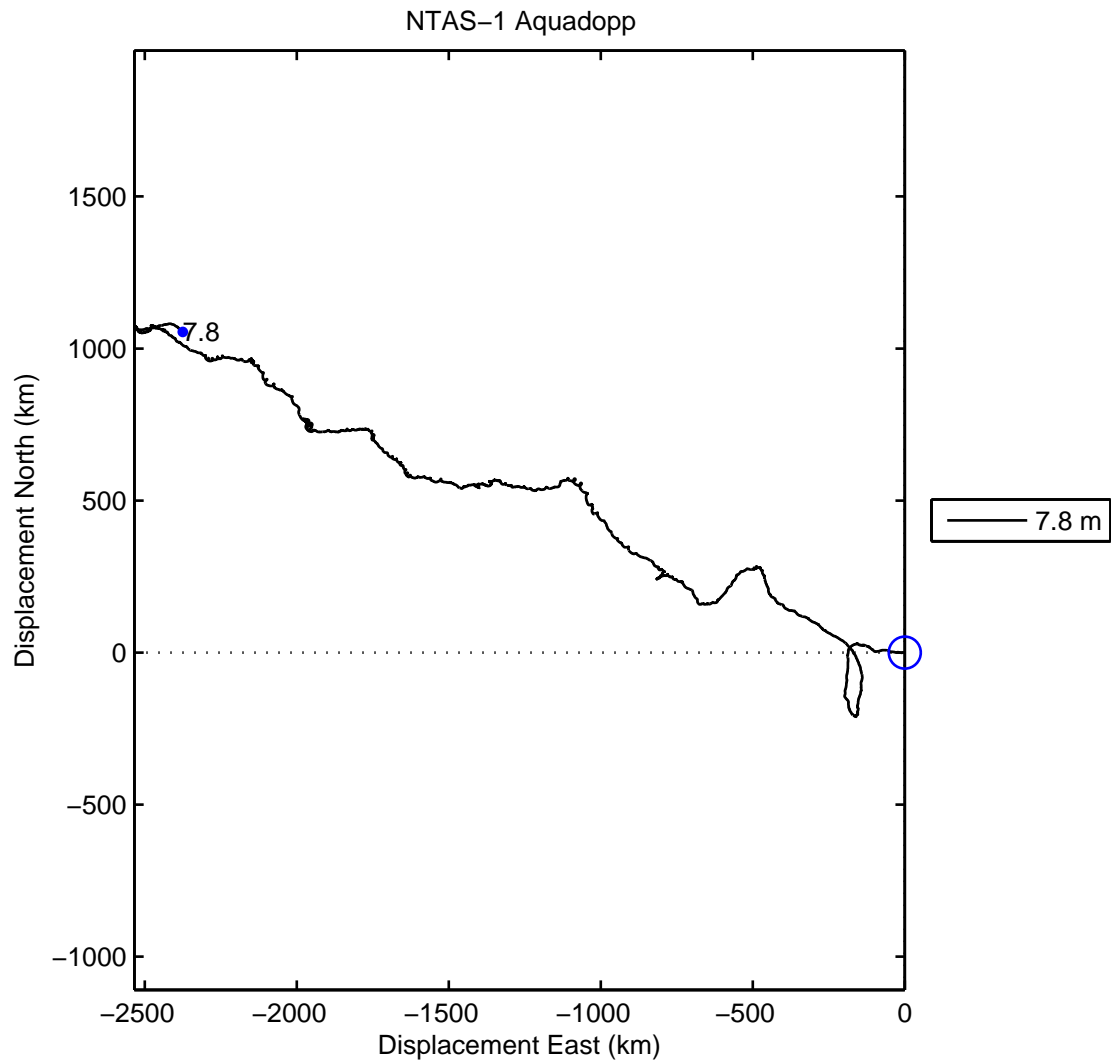


Figure 16: Progressive vector diagram of the NTAS-1 Aquadopp current meter.

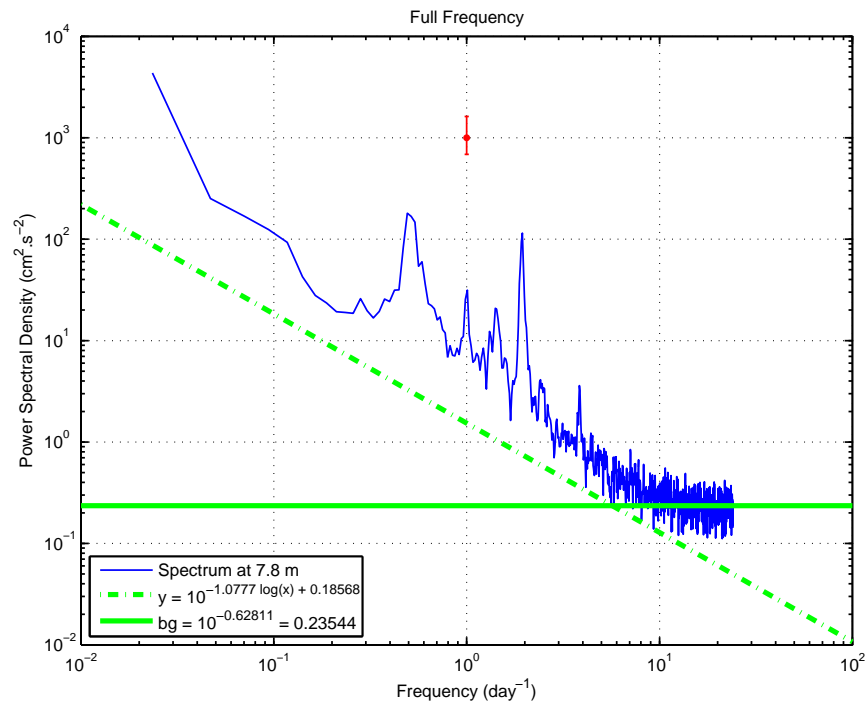


Figure 17: Spectrum of NTAS-1 Aquadopp current speed. Symbol at top center indicates confidence interval for the spectrum. Dashed line has the slope of the least-squares regression line passing through the data, but has been shifted down to pass through the minimum spectral density. The solid line indicates the level of instrumental noise, determined from the leveling off of the tail of the high frequency spectrum. The equation in the legend describes the best fit regression line through the spectral data.

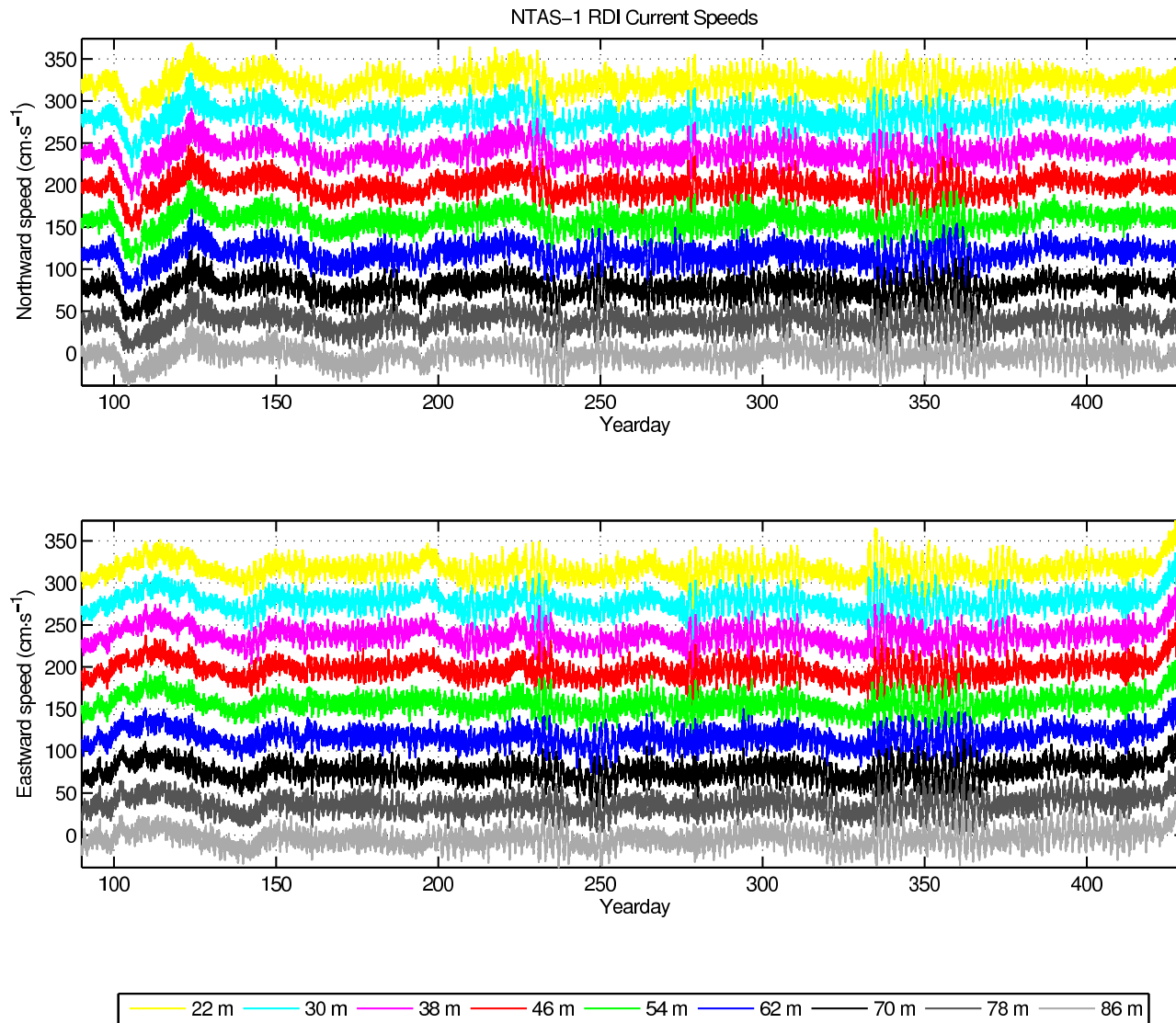


Figure 18: (a) Waterfall plots of the current speed time series from the NTAS-1 RDI NarrowBand. Northerly (top) and easterly (bottom) current speeds for the ADCP bins. Series are offset by $40 \text{ cm}\cdot\text{s}^{-1}$. In each plot the axis values are correct for the lowest series. Each subsequent series is offset upwards. In each plot the series are from every second 4 m bin, i.e., the [86, 78, 70, 62, 54, 46, 38, 30, 22] m bins (reading upwards from the deepest trace in each case).

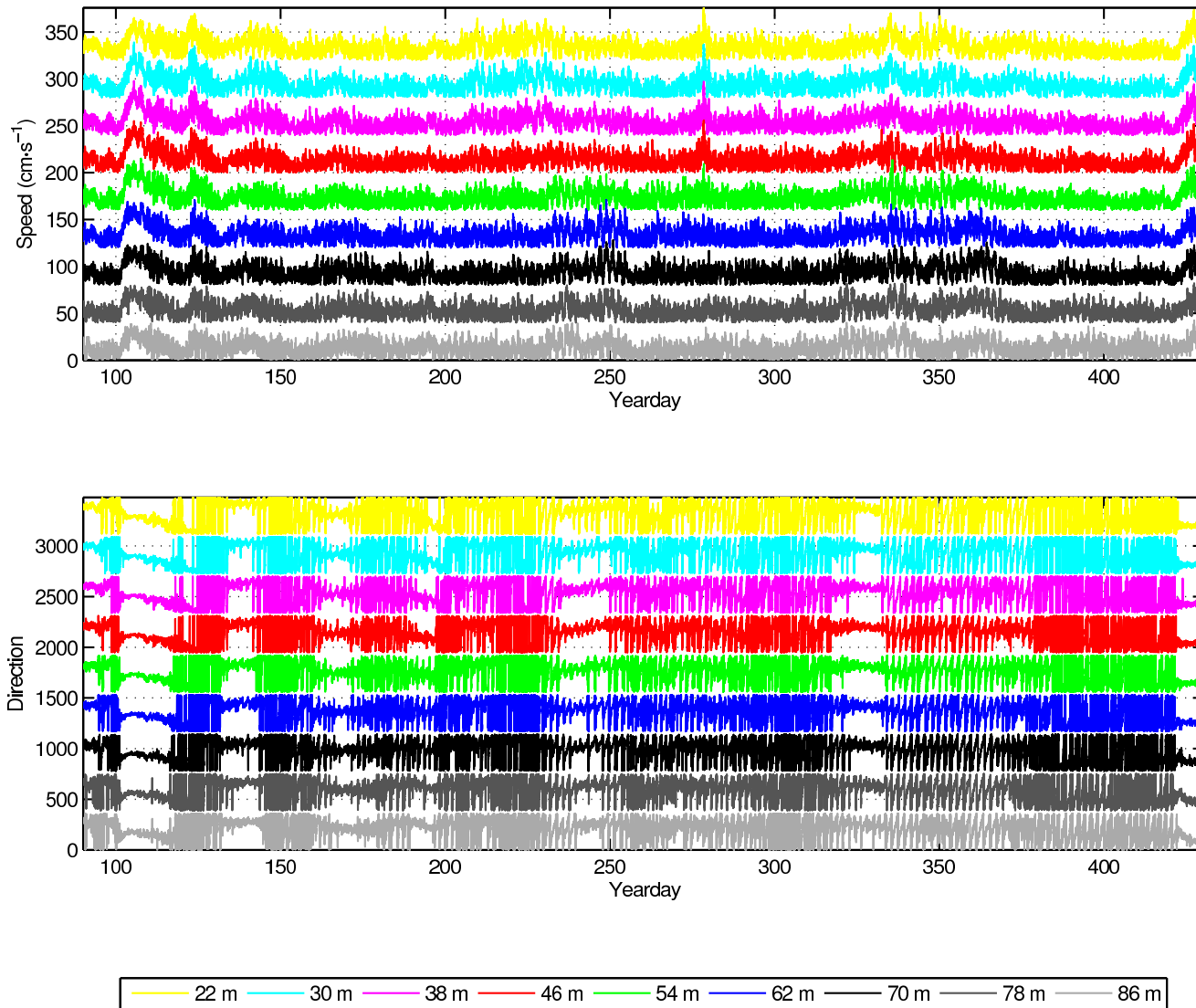


Figure 18: (b) Waterfall plots of the currents time series from the NTAS-1 RDI NarrowBand. Current magnitude (top) and direction (bottom). The magnitude is offset by $40 \text{ cm}\cdot\text{s}^{-1}$. Each direction plot is offset by 390 degrees from the one below. In each plot the axis values are correct for the lowest series. Each subsequent series is offset upwards. In each plot the series are from every second 4 m bin, i.e., the [86, 78, 70, 62, 54, 46, 38, 30, 22] m bins (reading from the lowest trace in each case).

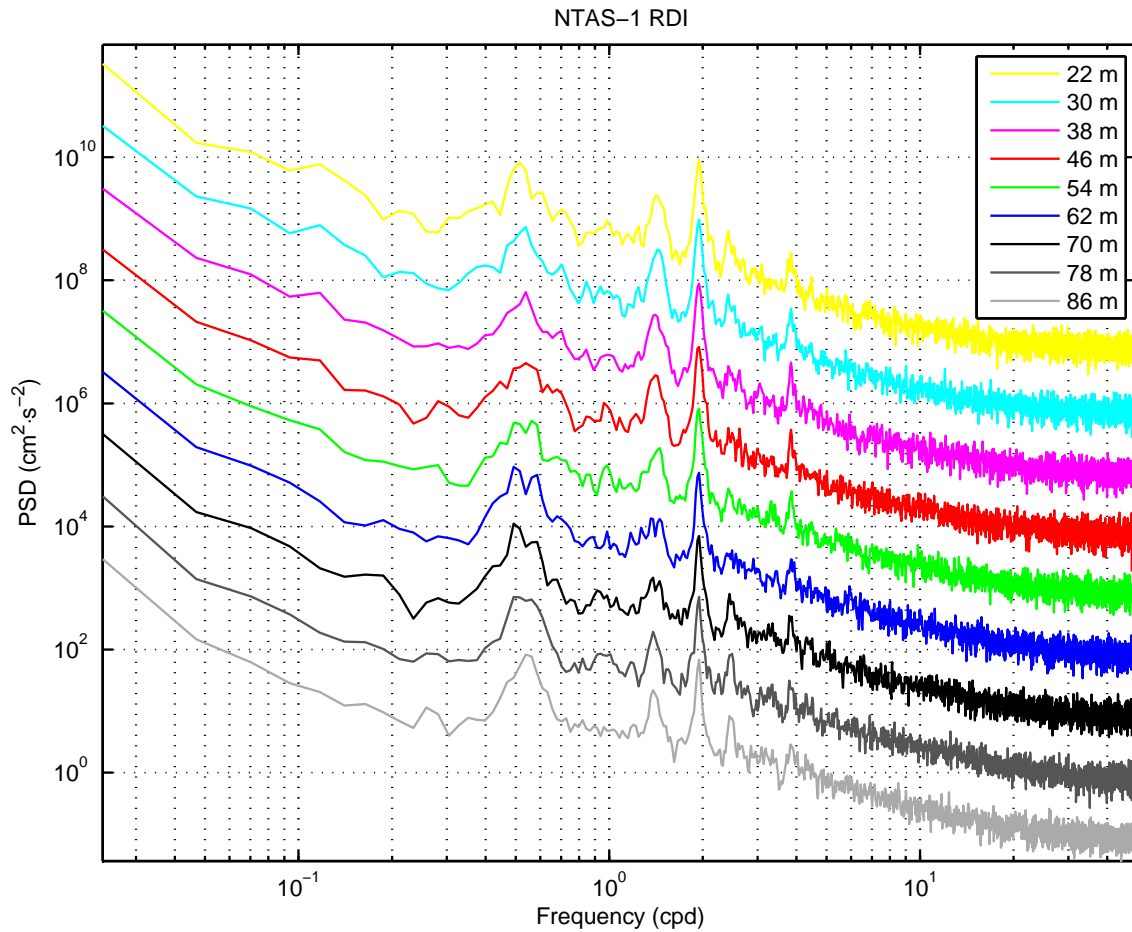


Figure 19: NTAS-1 RDI NarrowBand spectra from 86 to 22 meters (spectra for every second 4 m bin are shown from bottom to top, each spectrum offset by 10× the previous spectrum).

Table 8: Spectral peak heights for NTAS-1 RDI NarrowBand, 22 m bin. Peaks are ordered relative to the baseline.

| Top 15 Peak Frequencies (NTAS-1 NarrowBand 22 m) | | | |
|--|----------|------------|---|
| f (cpd) | T (day) | T (hr) | PeakHgt ($\text{cm}^2 \cdot \text{s}^{-2}$) |
| 1.94531 | 0.51406 | 12.33735 | 91.099 |
| 0.02344 | 42.66667 | 1024.00000 | 3287.050 |
| 0.51563 | 1.93939 | 46.54545 | 81.293 |
| 1.42969 | 0.69945 | 16.78689 | 23.611 |
| 2.41406 | 0.41424 | 9.94175 | 6.354 |
| 0.70313 | 1.42222 | 34.13333 | 14.105 |
| 0.98438 | 1.01587 | 24.38095 | 9.404 |
| 1.24219 | 0.80503 | 19.32075 | 7.600 |
| 3.84375 | 0.26016 | 6.24390 | 2.832 |
| 3.75000 | 0.26667 | 6.40000 | 2.138 |
| 1.14844 | 0.87075 | 20.89796 | 5.698 |
| 2.69531 | 0.37101 | 8.90435 | 2.237 |
| 3.96094 | 0.25247 | 6.05917 | 1.500 |
| 3.09375 | 0.32323 | 7.75758 | 1.815 |
| 46.42969 | 0.02154 | 0.51691 | 0.158 |

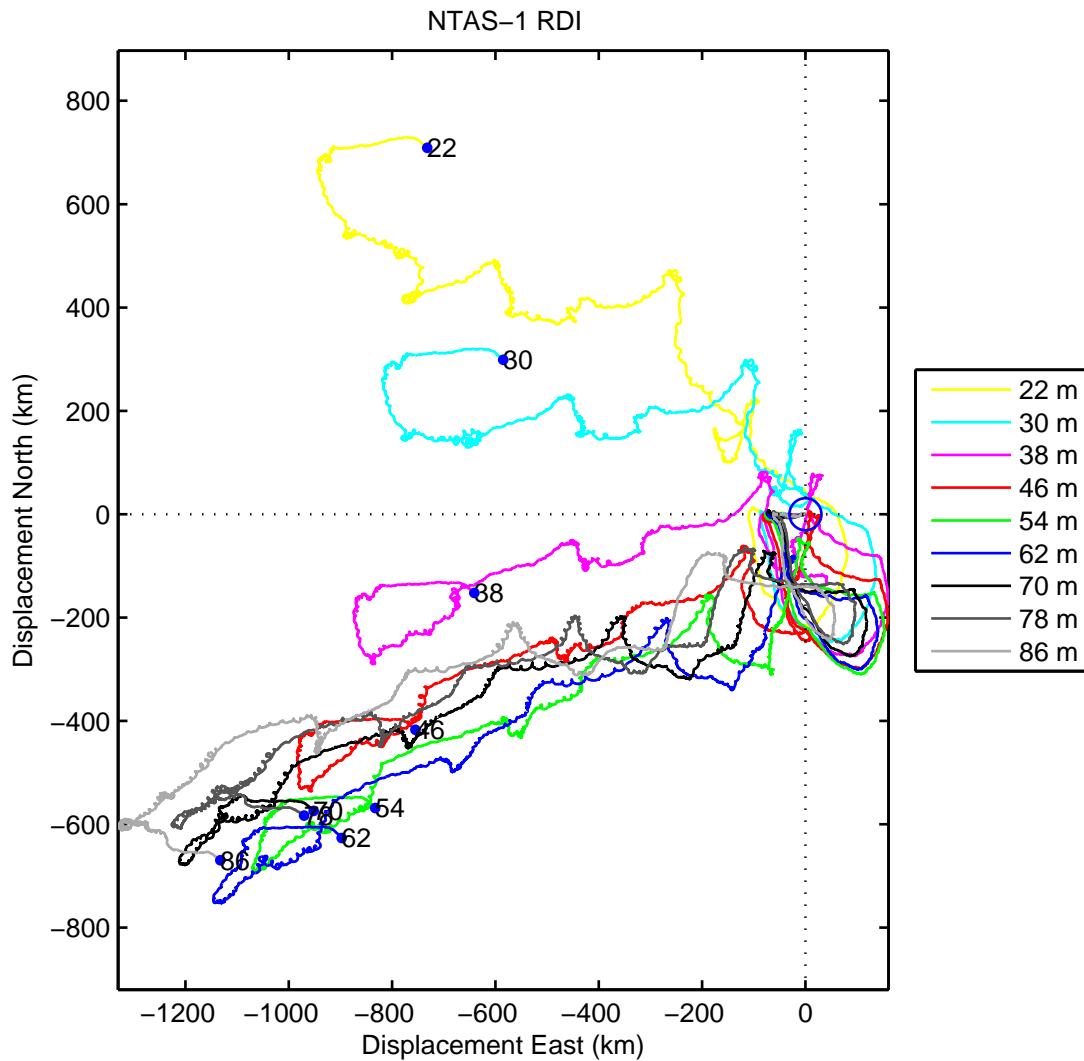


Figure 20: Superimposed progressive vector diagram of currents from the NTAS-1 RDI NarrowBand ADCP. Vectors start at \circ at the origin (0,0) and end at the \bullet . Every second 4 m bin from 22 to 86 m is plotted as listed in the legend on the figure.

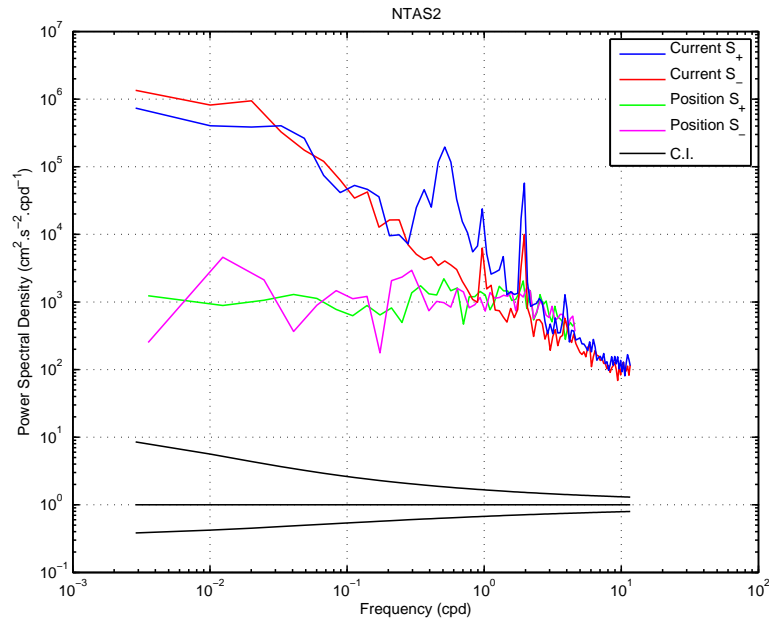


Figure 21: Showing the rotary spectra of velocities determined from the near-surface current meter (Aquadopp at 6 m) and the Argos buoy position from NTAS-2.

5.3 NTAS-2 Velocity Data

Rotary spectra estimating the influence of the buoy motion on velocity data are shown in Figure 21.

5.3.1 Aquadopp

The time series of the speeds measured with the Aquadopp current meter is shown in Figure 22. The current velocities are shown integrated in a progressive vector diagram in Figure 23. The spectrum is shown in Figure 24. The spectral peaks are tabulated in Table 9.

5.3.2 RDI Workhorse

A time series of the current speed data from the RDI workhorse ADCP is shown in Figure 25. The spectra for all RDI Workhorse ADCP bins are shown as a waterfall plot in Figure 26. Tables of the spectral peaks obtained from the RDI Workhorse bins are shown in Tables 10 and 11. Only the deepest (90 m) and shallowest (46 m) bins are tabulated. Progressive vector diagrams for all bins of the Workhorse data are shown in Figure 27.

5.3.3 Vector Measuring Current Meter

During initial processing of the VMCM on NTAS-2, a magnetic variation of -15.55° was applied, instead of the required -17.5° . This was corrected during the analysis.

The time series of speeds measured with the VMCM current meter is shown in Figure 28. The current velocities are shown integrated in a progressive vector diagram in Figure 29. The spectrum is shown in Figure 30. The spectral peaks are tabulated in Table 12.

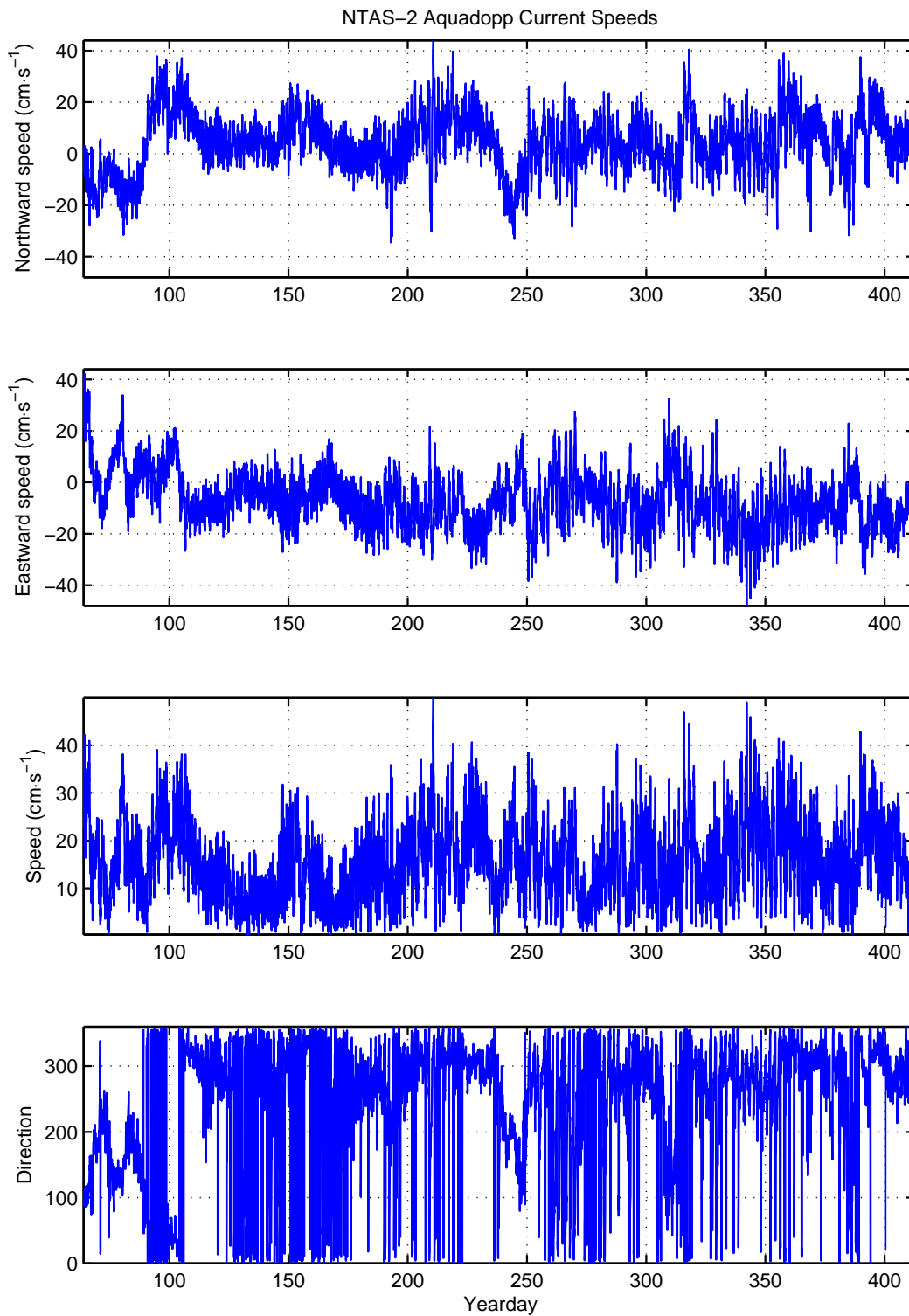


Figure 22: Unfiltered currents from NTAS-2 Aquadopp. (a) Northward current speeds. (b) Eastward current speeds. (c) Magnitude. (d) Direction.

Table 9: Spectral peak heights for NTAS-2 Aquadopp. Peaks are ordered relative to the baseline.

| Top 15 Peak Frequencies (NTAS-2 Aquadopp 6 m) | | | |
|---|----------|------------|---|
| f (cpd) | T (day) | T (hr) | PeakHgt ($\text{cm}^2 \cdot \text{s}^{-2}$) |
| 1.93359 | 0.51717 | 12.41212 | 105.072 |
| 0.51562 | 1.93939 | 46.54545 | 134.692 |
| 1.00781 | 0.99225 | 23.81395 | 50.375 |
| 0.01172 | 85.33333 | 2048.00000 | 10558.943 |
| 0.59766 | 1.67320 | 40.15686 | 43.403 |
| 1.40625 | 0.71111 | 17.06667 | 11.879 |
| 2.43750 | 0.41026 | 9.84615 | 3.909 |
| 1.48828 | 0.67192 | 16.12598 | 7.033 |
| 1.12500 | 0.88889 | 21.33333 | 9.915 |
| 11.47266 | 0.08716 | 2.09193 | 0.419 |
| 9.86719 | 0.10135 | 2.43230 | 0.499 |
| 8.90625 | 0.11228 | 2.69474 | 0.556 |
| 3.86719 | 0.25859 | 6.20606 | 1.663 |
| 11.13281 | 0.08982 | 2.15579 | 0.399 |
| 0.94922 | 1.05350 | 25.28395 | 10.826 |

Table 10: Spectral peak heights for NTAS-2 RDI Workhorse, 90 m bin. Peaks are ordered relative to the baseline.

| Top 15 Peak Frequencies (NTAS-2 Workhorse 90 m) | | | |
|---|----------|------------|---|
| f (cpd) | T (day) | T (hr) | PeakHgt ($\text{cm}^2 \cdot \text{s}^{-2}$) |
| 0.01172 | 85.33333 | 2048.00000 | 6638.381 |
| 1.94531 | 0.51406 | 12.33735 | 41.315 |
| 0.52734 | 1.89630 | 45.51111 | 67.912 |
| 1.39453 | 0.71709 | 17.21008 | 12.900 |
| 11.91797 | 0.08391 | 2.01377 | 1.405 |
| 2.46094 | 0.40635 | 9.75238 | 5.933 |
| 2.08594 | 0.47940 | 11.50562 | 6.580 |
| 2.37891 | 0.42036 | 10.08867 | 5.750 |
| 3.82031 | 0.26176 | 6.28221 | 3.574 |
| 11.21484 | 0.08917 | 2.14002 | 1.263 |
| 3.86719 | 0.25859 | 6.20606 | 3.349 |
| 8.53125 | 0.11722 | 2.81319 | 1.543 |
| 1.33594 | 0.74854 | 17.96491 | 8.341 |
| 0.75000 | 1.33333 | 32.00000 | 13.579 |
| 1.48828 | 0.67192 | 16.12598 | 7.154 |

Table 11: Spectral peak heights for NTAS-2 RDI Workhorse, 46 m bin. Peaks are ordered relative to the baseline.

Top 15 Peak Frequencies (NTAS-2 Workhorse 46 m)

| f (cpd) | T (day) | T (hr) | PeakHgt ($\text{cm}^2 \cdot \text{s}^{-2}$) |
|----------|----------|------------|---|
| 0.01172 | 85.33333 | 2048.00000 | 7375.793 |
| 1.94531 | 0.51406 | 12.33735 | 62.631 |
| 0.53906 | 1.85507 | 44.52174 | 33.399 |
| 1.41797 | 0.70523 | 16.92562 | 10.966 |
| 0.48047 | 2.08130 | 49.95122 | 28.110 |
| 1.34766 | 0.74203 | 17.80870 | 10.235 |
| 11.94141 | 0.08374 | 2.00981 | 1.501 |
| 11.76562 | 0.08499 | 2.03984 | 1.519 |
| 10.60547 | 0.09429 | 2.26298 | 1.463 |
| 1.00781 | 0.99225 | 23.81395 | 11.410 |
| 1.47656 | 0.67725 | 16.25397 | 8.130 |
| 3.91406 | 0.25549 | 6.13174 | 3.390 |
| 9.03516 | 0.11068 | 2.65629 | 1.529 |
| 10.18359 | 0.09820 | 2.35673 | 1.358 |
| 0.69141 | 1.44633 | 34.71186 | 14.109 |

Table 12: Spectral peak heights from the VMCM on NTAS-2. Peaks are ordered relative to the baseline.

Top 15 Peak Frequencies (NTAS-2 VMCM 7.5 m)

| f (cpd) | T (day) | T (hr) | PeakHgt ($\text{cm}^2 \cdot \text{s}^{-2}$) |
|---------|----------|------------|---|
| 1.93232 | 0.51751 | 12.42029 | 82.018 |
| 0.51529 | 1.94067 | 46.57610 | 105.563 |
| 1.00715 | 0.99290 | 23.82963 | 34.988 |
| 1.40532 | 0.71158 | 17.07790 | 12.167 |
| 0.01171 | 85.38951 | 2049.34827 | 7489.546 |
| 2.11970 | 0.47177 | 11.32237 | 4.044 |
| 1.48730 | 0.67236 | 16.13660 | 6.358 |
| 2.49445 | 0.40089 | 9.62135 | 2.774 |
| 2.42419 | 0.41251 | 9.90023 | 2.778 |
| 0.94859 | 1.05419 | 25.30060 | 9.215 |
| 4.00518 | 0.24968 | 5.99225 | 1.249 |
| 1.20624 | 0.82902 | 19.89659 | 6.406 |
| 1.12426 | 0.88947 | 21.34738 | 6.928 |
| 3.86464 | 0.25876 | 6.21015 | 1.235 |
| 2.93947 | 0.34020 | 8.16473 | 1.610 |

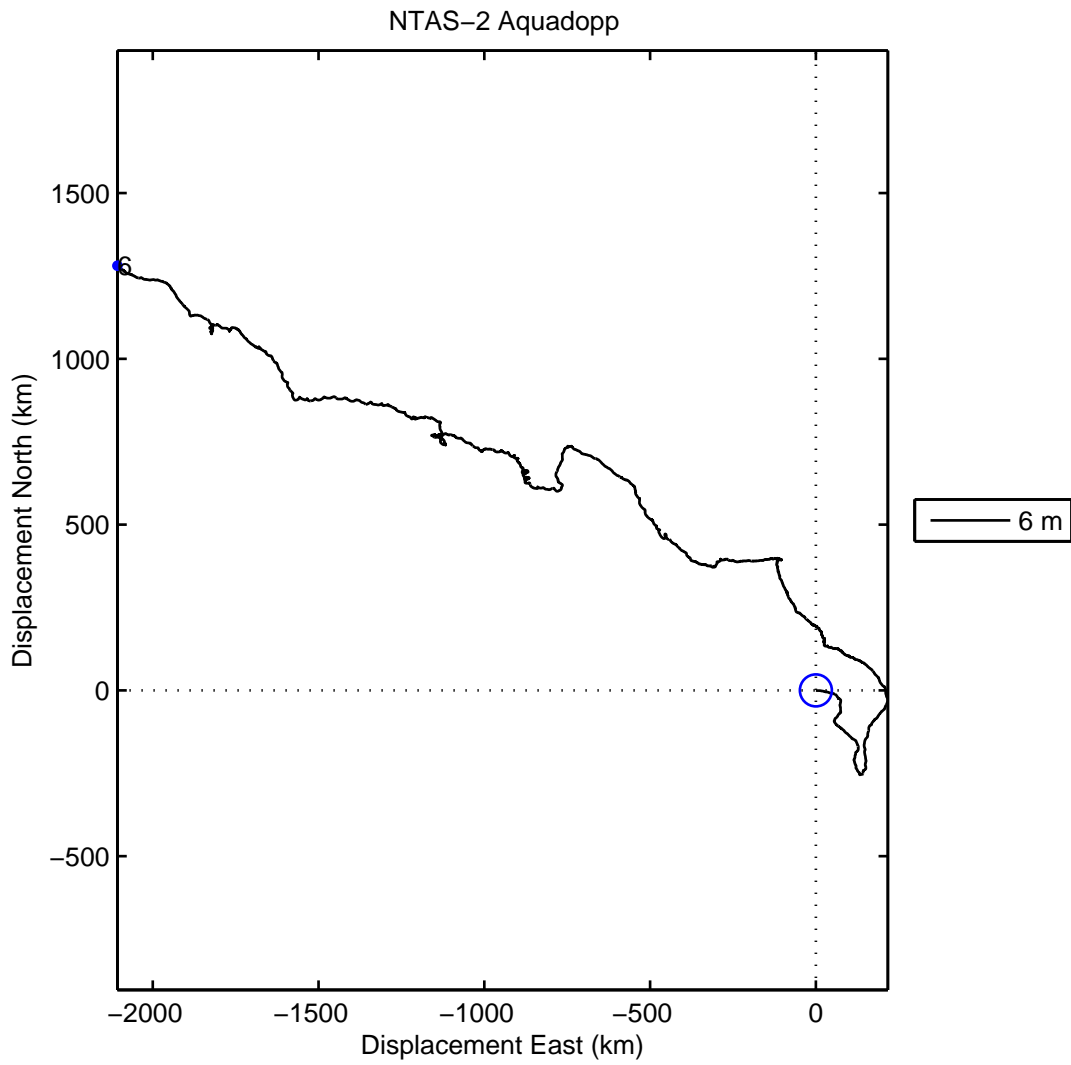


Figure 23: Progressive vector diagram of currents from the NTAS-2 Aquadopp.

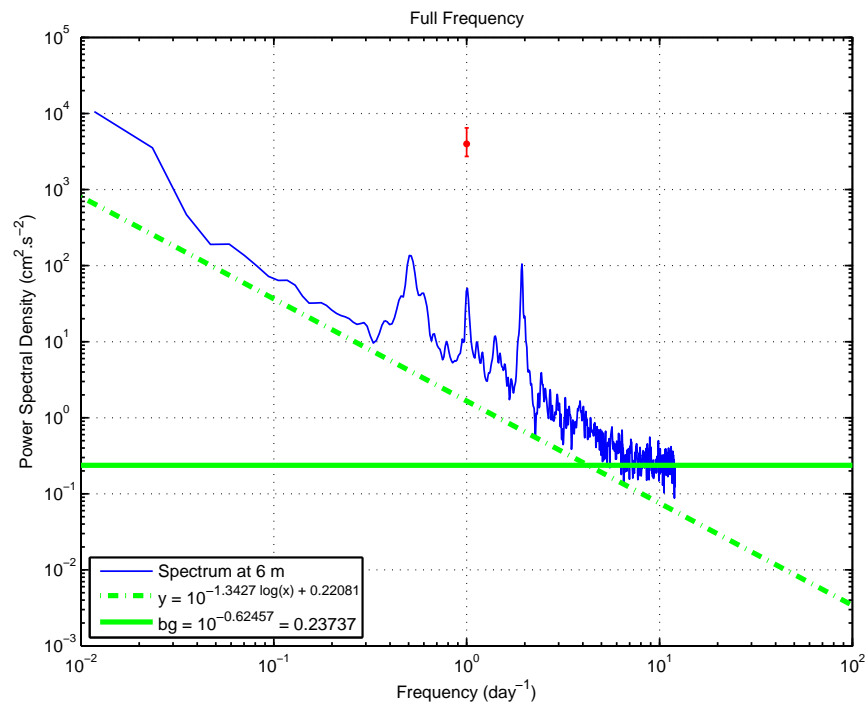


Figure 24: Spectrum of NTAS-2 Aquadopp current speed. Symbol at top center indicates confidence interval for the spectrum. Dashed line has the slope of the least-squares regression line passing through the data, but has been shifted down to pass through the minimum spectral density. The solid line indicates the level of instrumental noise, determined from the leveling off of the tail of the high frequency spectrum.

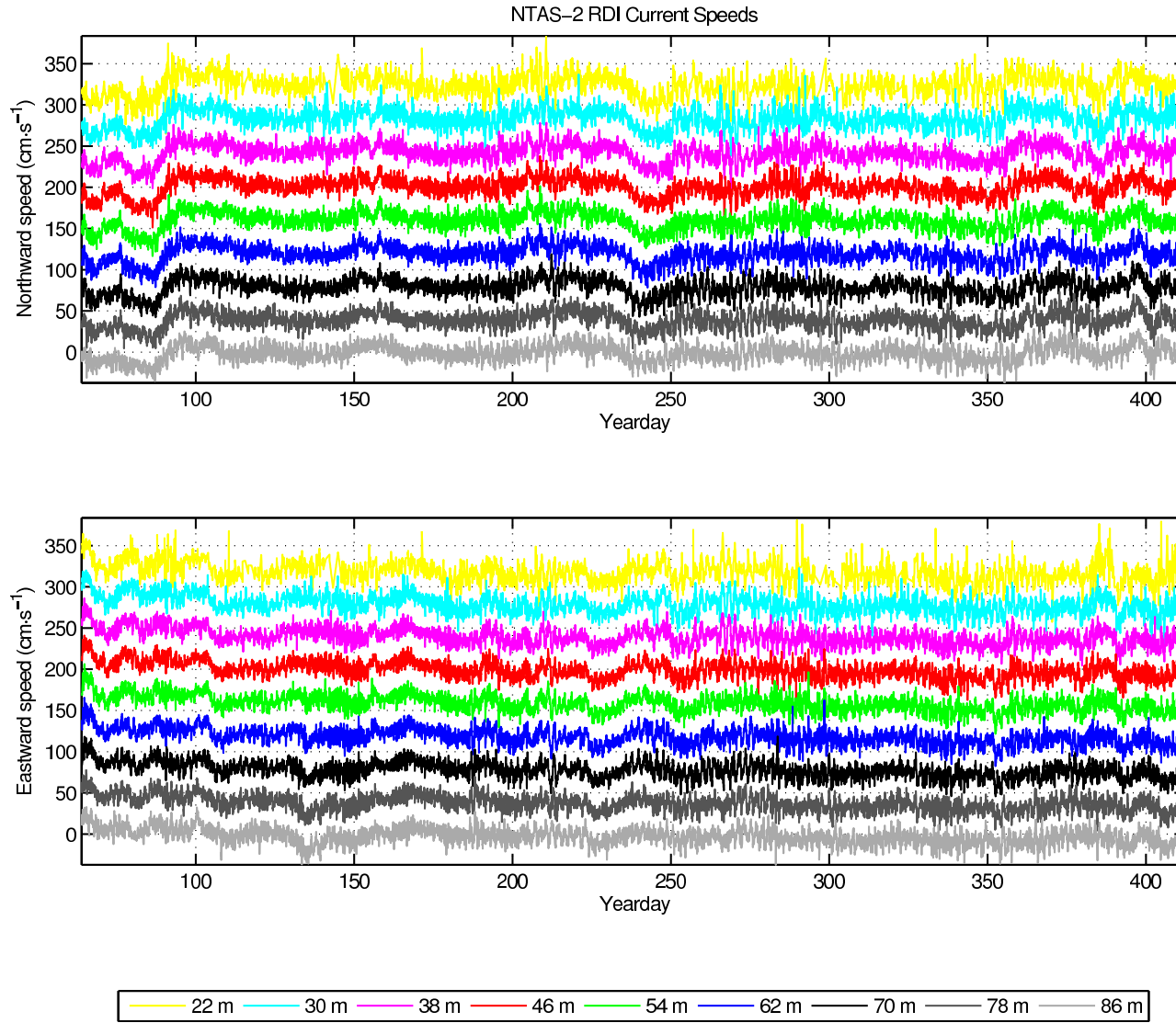


Figure 25: (a) Waterfall plots of the current speed time series from the NTAS-2 RDI Workhorse ADCP. Northerly (top) and easterly (bottom) current speeds for the ADCP bins. Series are offset by $40 \text{ cm}\cdot\text{s}^{-1}$. In each plot the axis values are correct for the lowest series. Each subsequent series is offset upwards. In each plot the series are from every second 4 m bin, i.e., the [86, 78, 70, 62, 54, 50, 46, 38, 30, 22] m bins (reading upwards from the deepest trace in each case).

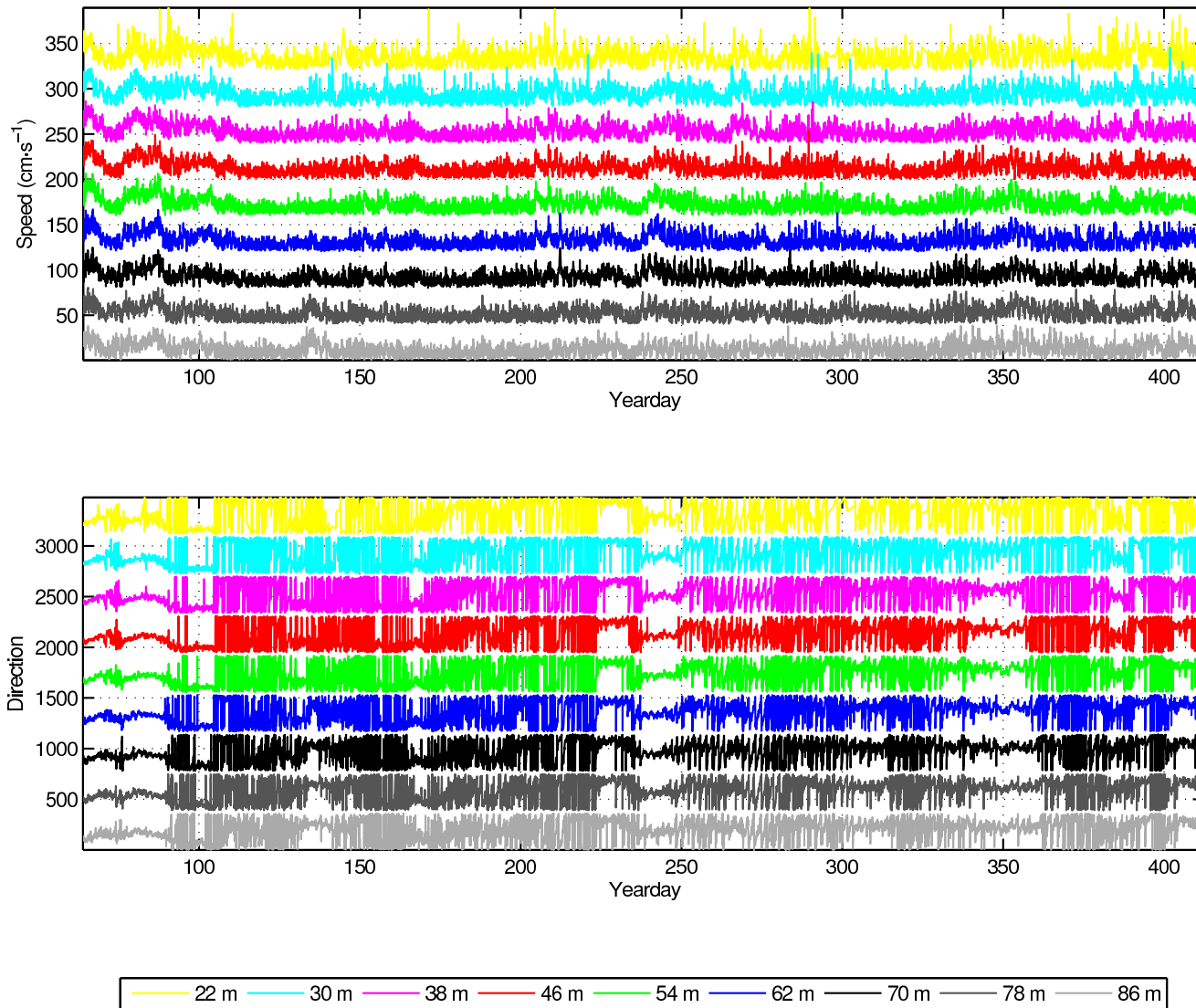


Figure 25: (b) Waterfall plots of the currents time series from the NTAS-2 RDI Workhorse. Current magnitude (top) and direction (bottom). The magnitude is offset by $40 \text{ cm}\cdot\text{s}^{-1}$. Each direction plot is offset by 390 degrees from the one below. In each plot the axis values are correct for the lowest series. Each subsequent series is offset upwards. In each plot the series are from every second 4 m bin, i.e., the [86, 78, 70, 62, 54, 50, 46, 38, 30, 22] m bins (reading from the lowest trace in each case).

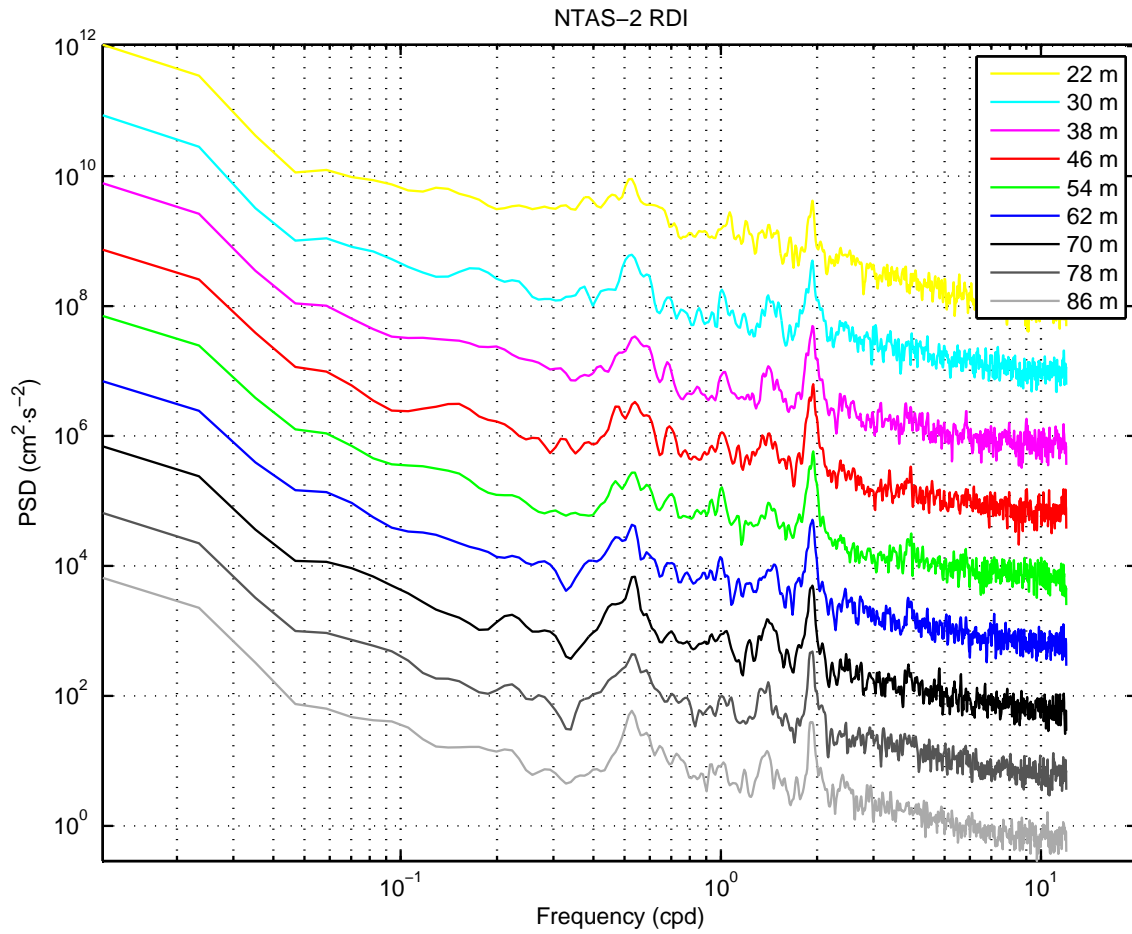


Figure 26: NTAS-2 RDI Workhorse spectra from 86 to 22 meters (spectra for every second 4 m bin are shown from bottom to top, each spectrum offset by $10\times$ the previous spectrum).

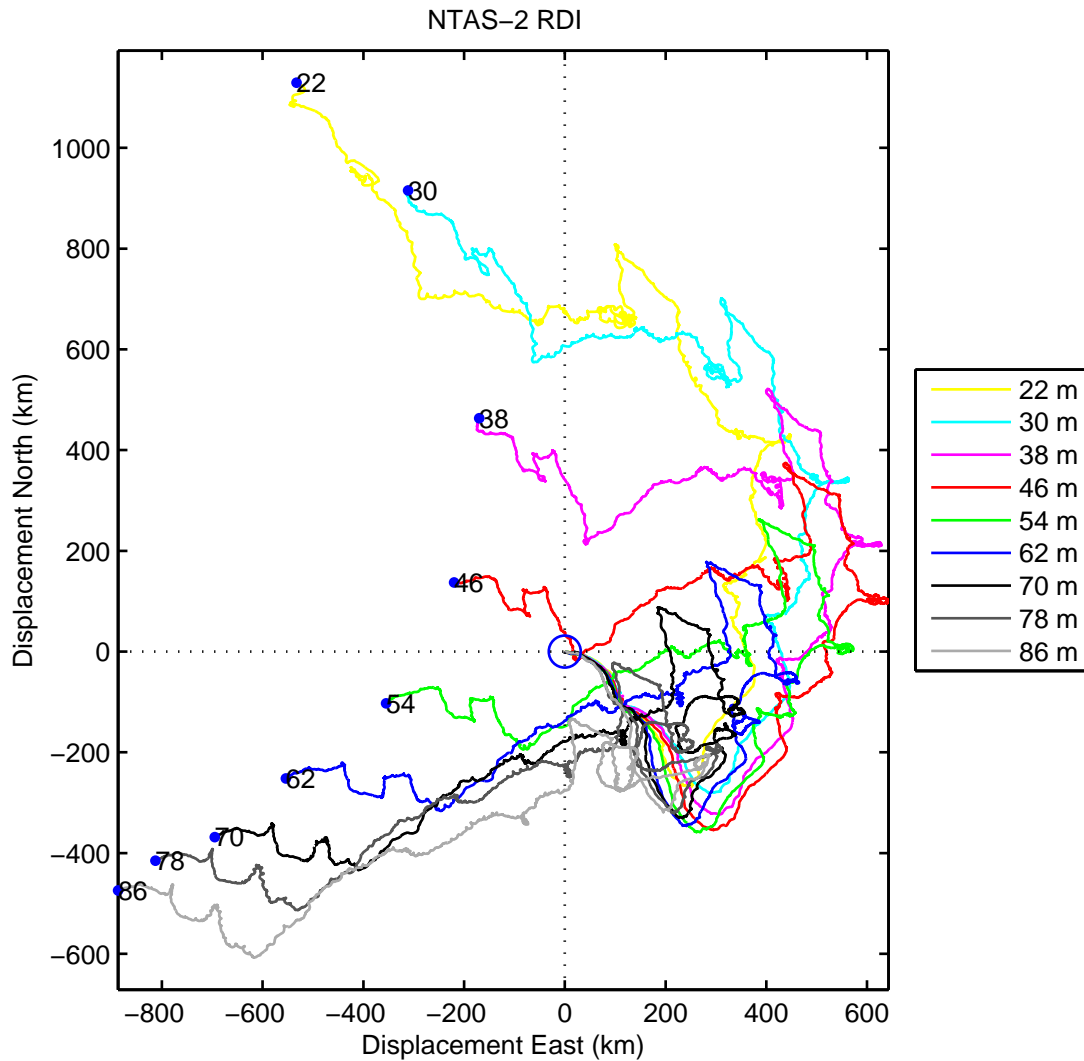


Figure 27: Superimposed progressive vector diagram of currents from the NTAS-2 RDI Workhorse. Vectors start at \circ at the origin (0,0) and end at the \bullet . Every second 4 m bin from 22 to 86 m is plotted as listed in the legend on the figure.

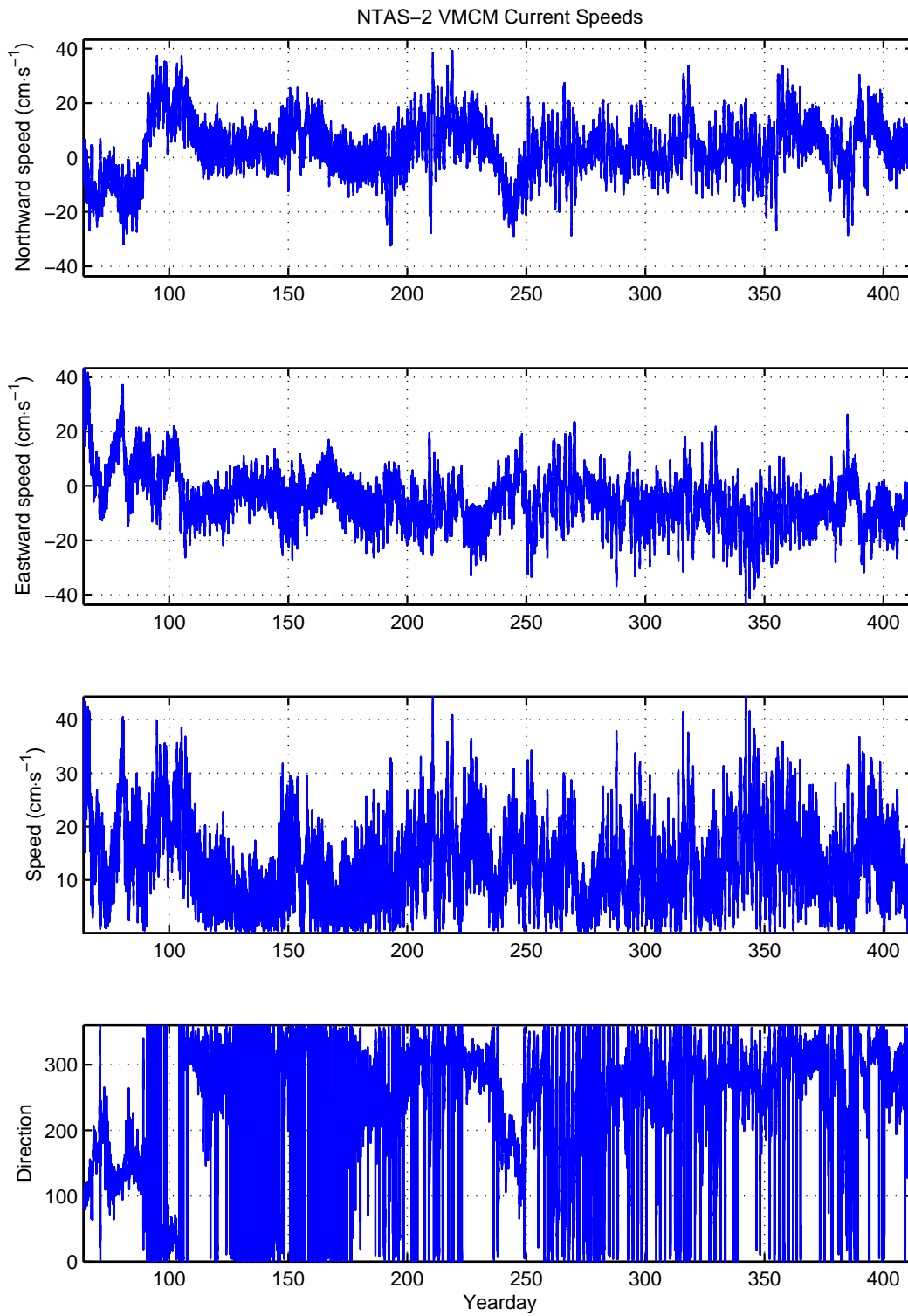


Figure 28: Currents from VMCM NTAS-2. (a) Northward. (b) Eastward. (c) Magnitude. (d) Direction.

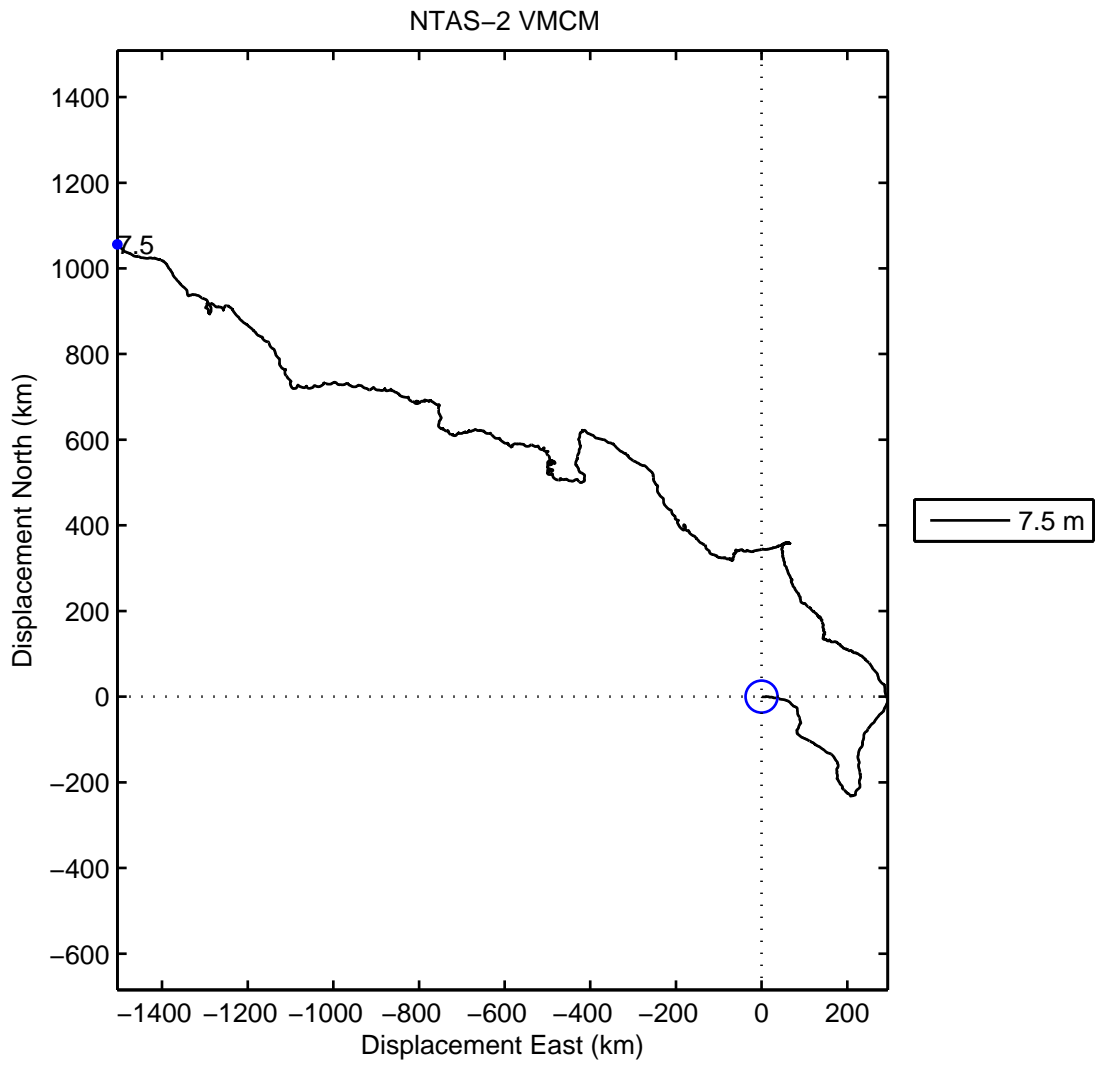


Figure 29: Progressive vector diagram from the VMCM NTAS-2.

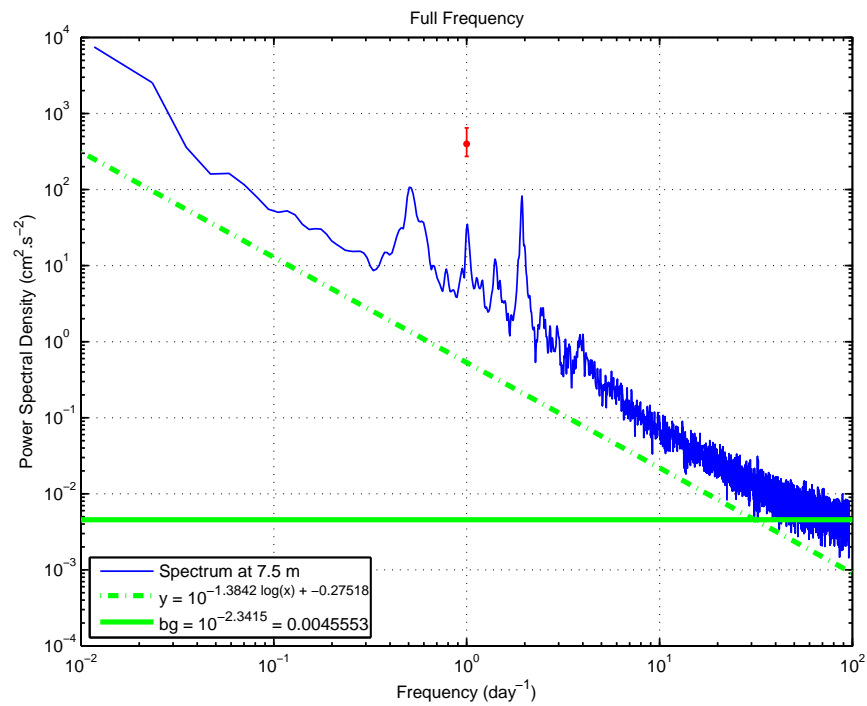


Figure 30: Spectrum from the vector measuring current meter deployed on NTAS-2. Symbol at top center indicates confidence interval for the spectrum. Dashed line has the slope of the least-squares regression line passing through the data, but has been shifted down to pass through the minimum spectral density. The solid line indicates the level of instrumental noise, determined from the leveling off of the tail of the high frequency spectrum.

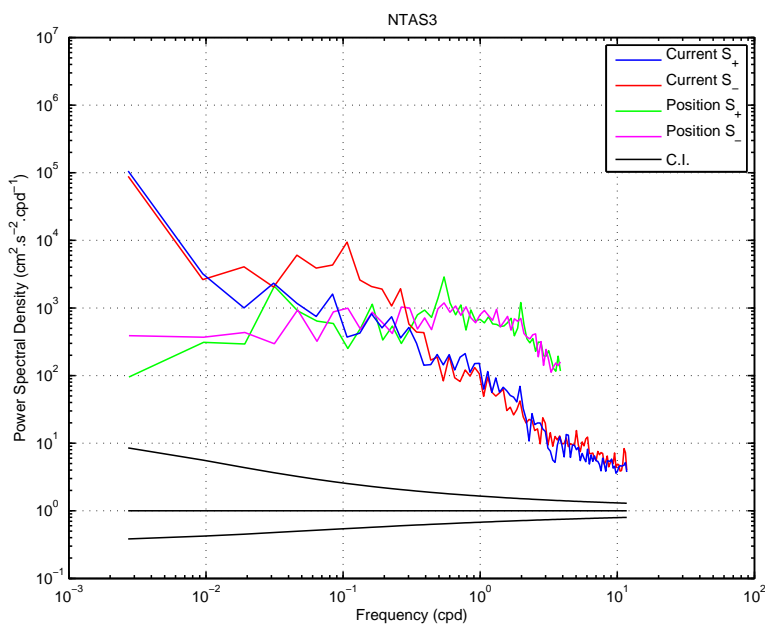


Figure 31: Showing the rotary spectra of velocities determined from the near-surface current meter (Aquadopp at 6 m) and the Argos buoy position from NTAS-3.

5.4 NTAS-3 Velocity Data

The NTAS-3 buoy went adrift on 16 February 2004 due to a mooring component failure. The last position within the watch circle was at 18:10Z on 15 February 2004, after which the buoy showed a persistent drift to the NW at about 0.25 kt. The buoy, with surface meteorological and upper subsurface instruments, was located and recovered on 19 February 2004, beginning at 16:49Z. The position of recovery was 14°53.7'N, 51°22.817'W, about 21.2 n.m. from the anchor position. For the purposes of this report and due to the proximity of the buoy when recovered to its nominal anchor position, the three days of data were not discarded from the analysis.

Rotary spectra for estimating the influence of the buoy motion on velocity data are shown in Figure 31.

5.4.1 Aquadopp

The time series of the speeds measured with the Aquadopp current meter on NTAS-3 is shown in Figure 32. The current velocities are shown integrated in a progressive vector diagram in Figure 33. The spectrum is shown in Figure 34. The spectral peaks are tabulated in Table 13. It is apparent from these data that the Aquadopp instrument deployed on NTAS-3 failed and returned erroneous data. This is especially evident when the data are plotted alongside the RDI data (not shown).

5.4.2 RDI Workhorse

A time series of the current speed data from the RDI workhorse ADCP is shown in Figure 35. The spectra for all RDI Workhorse ADCP bins are shown as a waterfall plot in Figure 36. Tables of

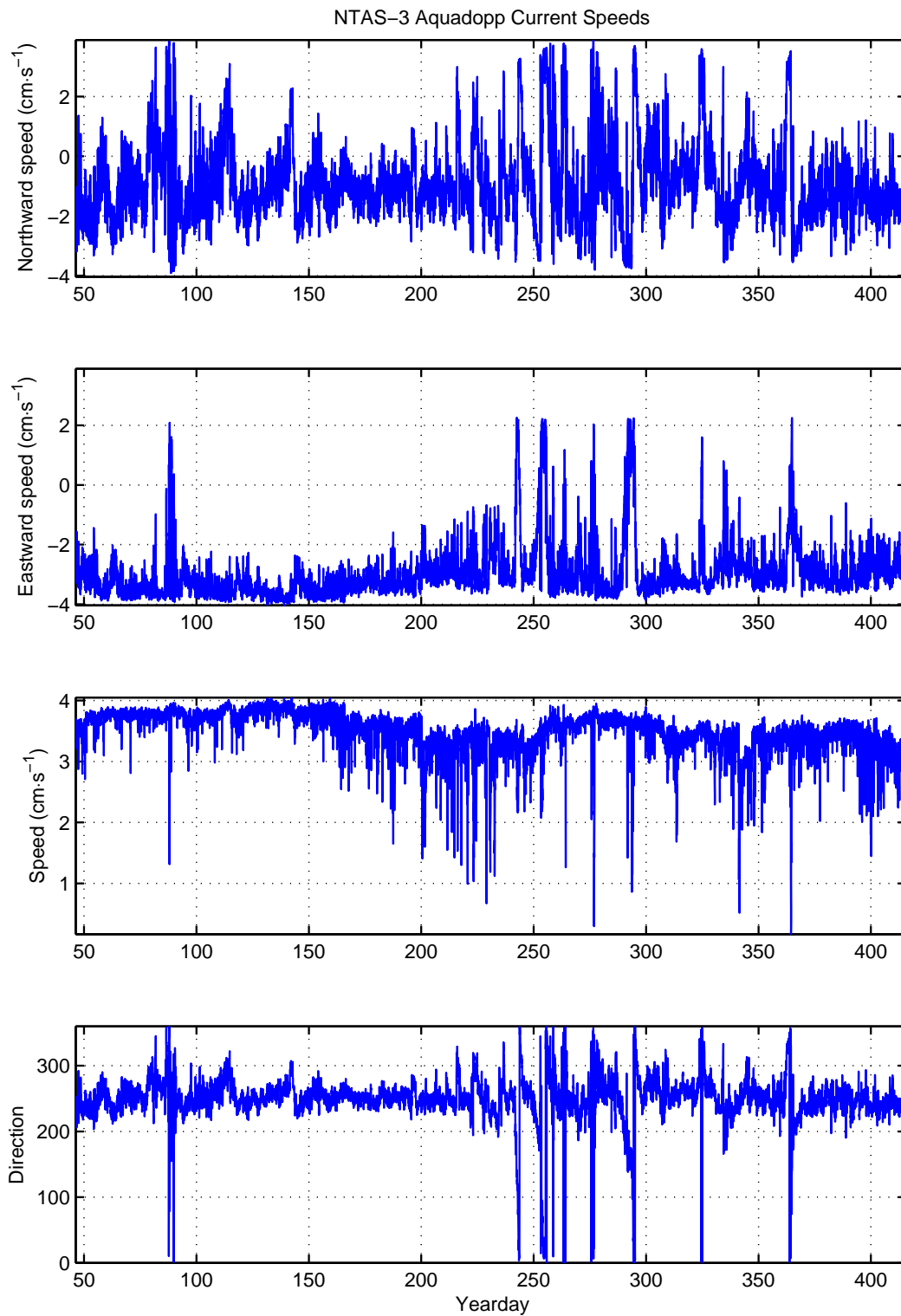


Figure 32: Unfiltered currents from NTAS-3 Aquadopp. (a) Northward current speeds. (b) Eastward current speeds. (c) Magnitude. (d) Direction.

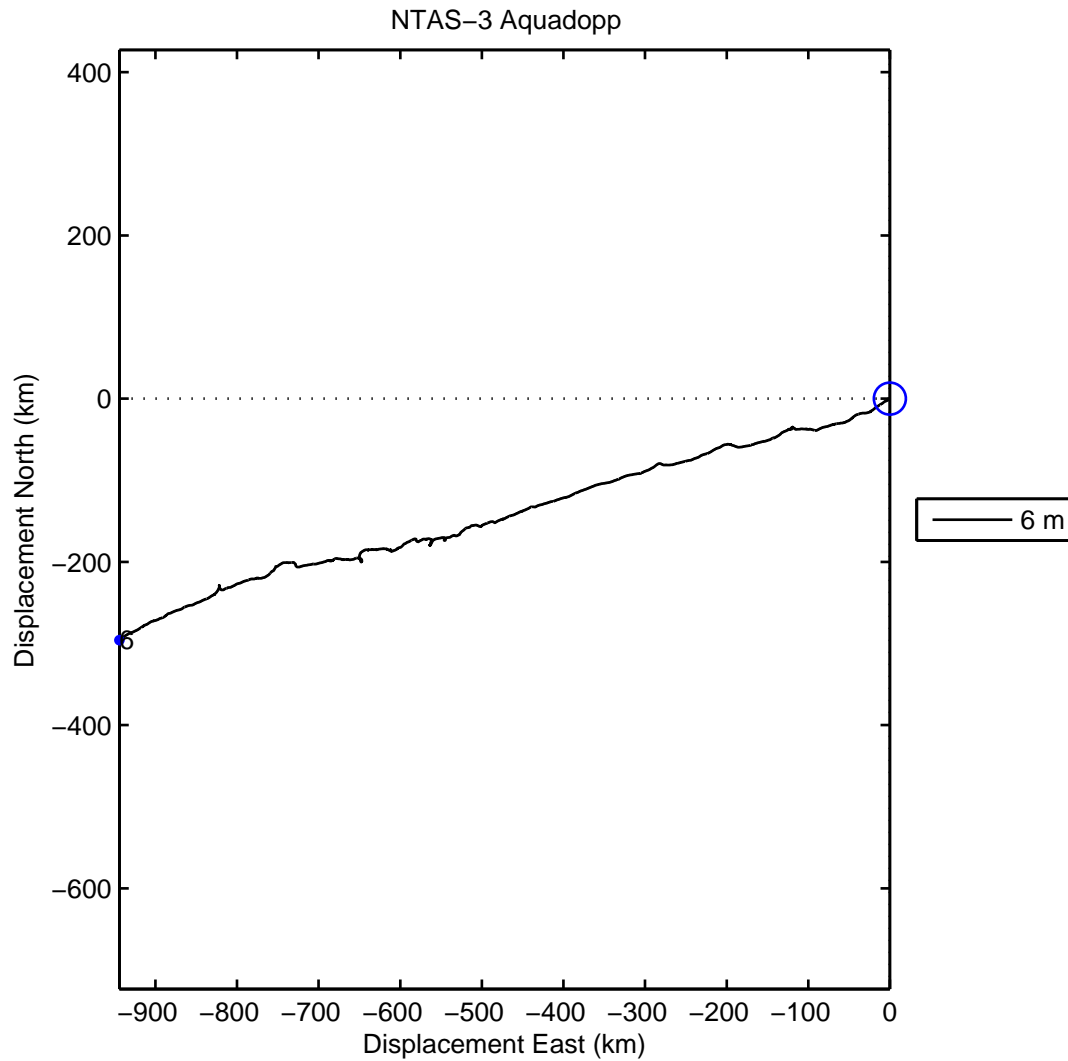


Figure 33: Progressive vector diagram of currents from the NTAS-3 Aquadopp.

the spectral peaks obtained from the RDI Workhorse bins are shown in Tables 14 and 15. Only the deepest (90 m) and shallowest (26 m) bins are tabulated. Progressive vector diagrams for all bins of the Workhorse data are shown in Figure 37.

Table 13: Spectral peak heights for NTAS-3 Aquadopp. Peaks are ordered relative to the baseline.

| Top 15 Peak Frequencies (NTAS-3 Aquadopp 6 m) | | | |
|---|----------|------------|---|
| f (cpd) | T (day) | T (hr) | PeakHgt ($\text{cm}^2 \cdot \text{s}^{-2}$) |
| 0.01172 | 85.33333 | 2048.00000 | 512.470 |
| 0.99609 | 1.00392 | 24.09412 | 0.116 |
| 1.06641 | 0.93773 | 22.50549 | 0.042 |
| 1.96875 | 0.50794 | 12.19048 | 0.022 |
| 0.75000 | 1.33333 | 32.00000 | 0.049 |
| 1.88672 | 0.53002 | 12.72050 | 0.017 |
| 10.85156 | 0.09215 | 2.21166 | 0.003 |
| 11.88281 | 0.08416 | 2.01972 | 0.003 |
| 9.64453 | 0.10369 | 2.48846 | 0.003 |
| 1.82813 | 0.54701 | 13.12821 | 0.016 |
| 11.15625 | 0.08964 | 2.15126 | 0.003 |
| 9.16406 | 0.10912 | 2.61893 | 0.003 |
| 0.87891 | 1.13778 | 27.30667 | 0.032 |
| 11.00391 | 0.09088 | 2.18104 | 0.002 |
| 3.57422 | 0.27978 | 6.71475 | 0.008 |

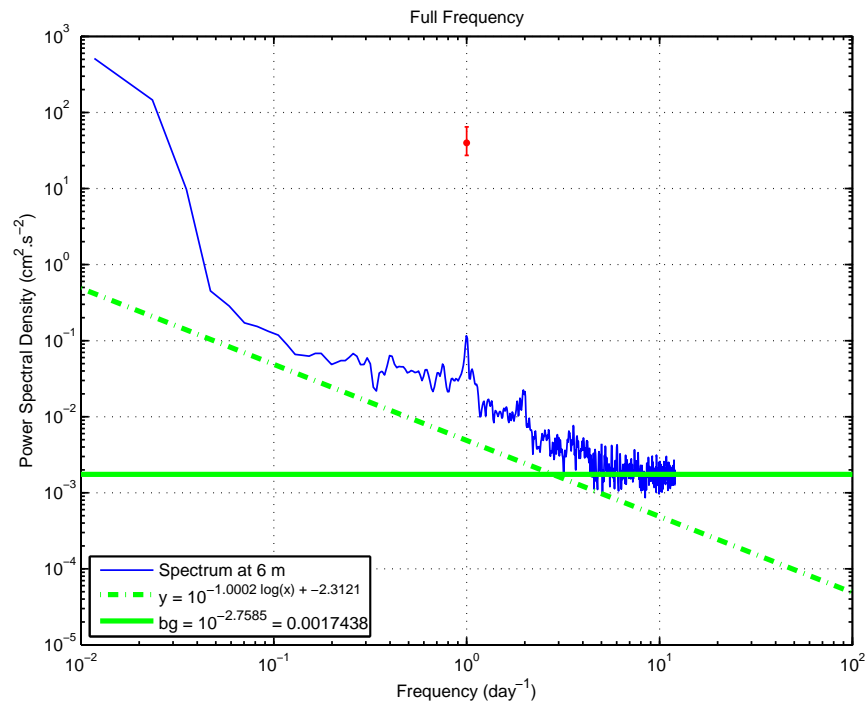


Figure 34: Spectrum of NTAS-3 Aquadopp current speed. Symbol at top center indicates confidence interval for the spectrum. Dashed line has the slope of the least-squares regression line passing through the data, but has been shifted down to pass through the minimum spectral density. The solid line indicates the level of instrumental noise, determined from the leveling off of the tail of the high frequency spectrum.

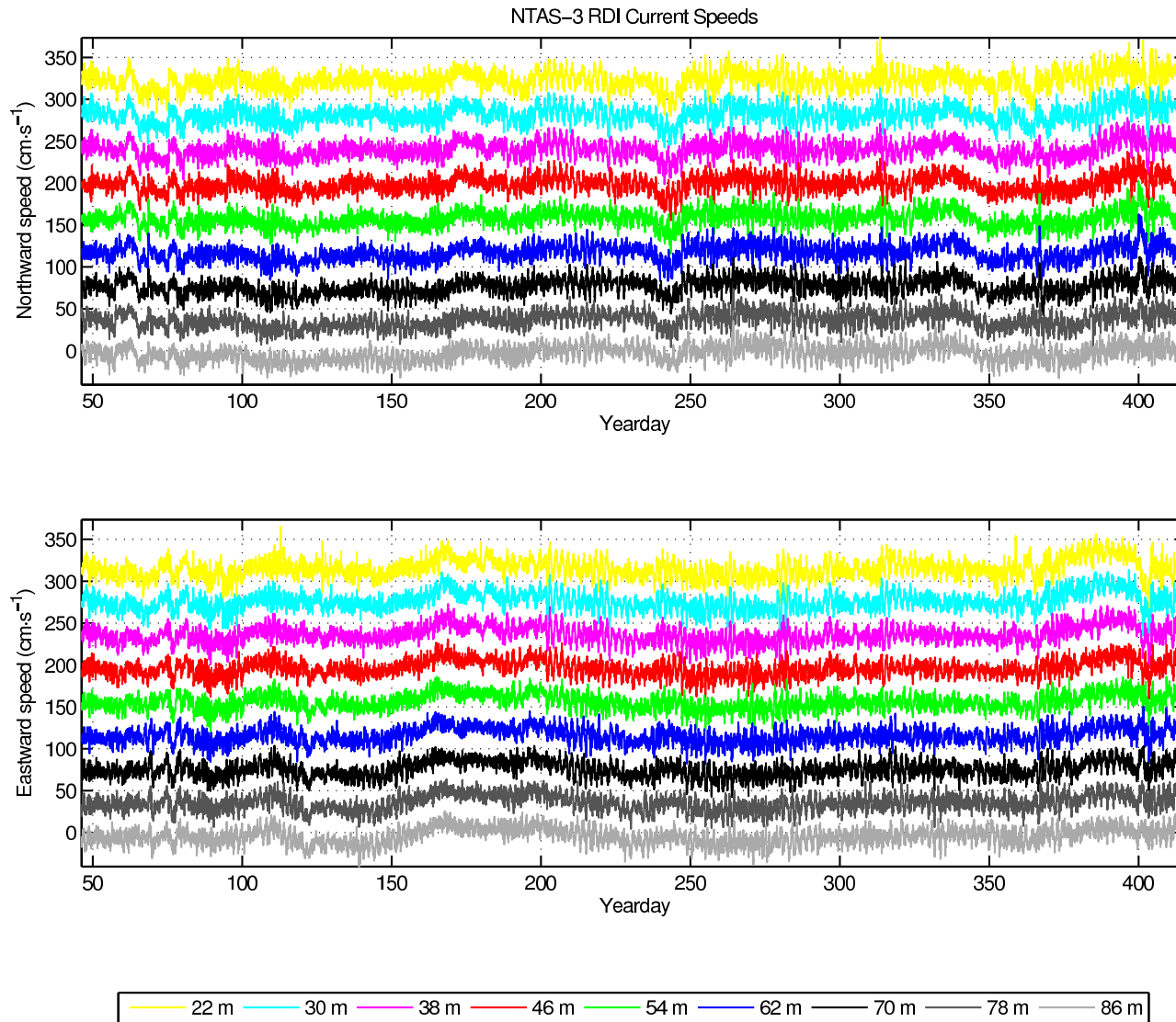


Figure 35: (a) Waterfall plots of the current speed time series from the NTAS-3 RDI Workhorse ADCP. Northerly (top) and easterly (bottom) current speeds for the ADCP bins. Series are offset by $40 \text{ cm}\cdot\text{s}^{-1}$. In each plot the axis values are correct for the lowest series. Each subsequent series is offset upwards. In each plot the series are from every second 4 m bin, i.e., the [86, 78, 70, 62, 54, 46, 38, 30, 22] m bins (reading upwards from the deepest trace in each case).

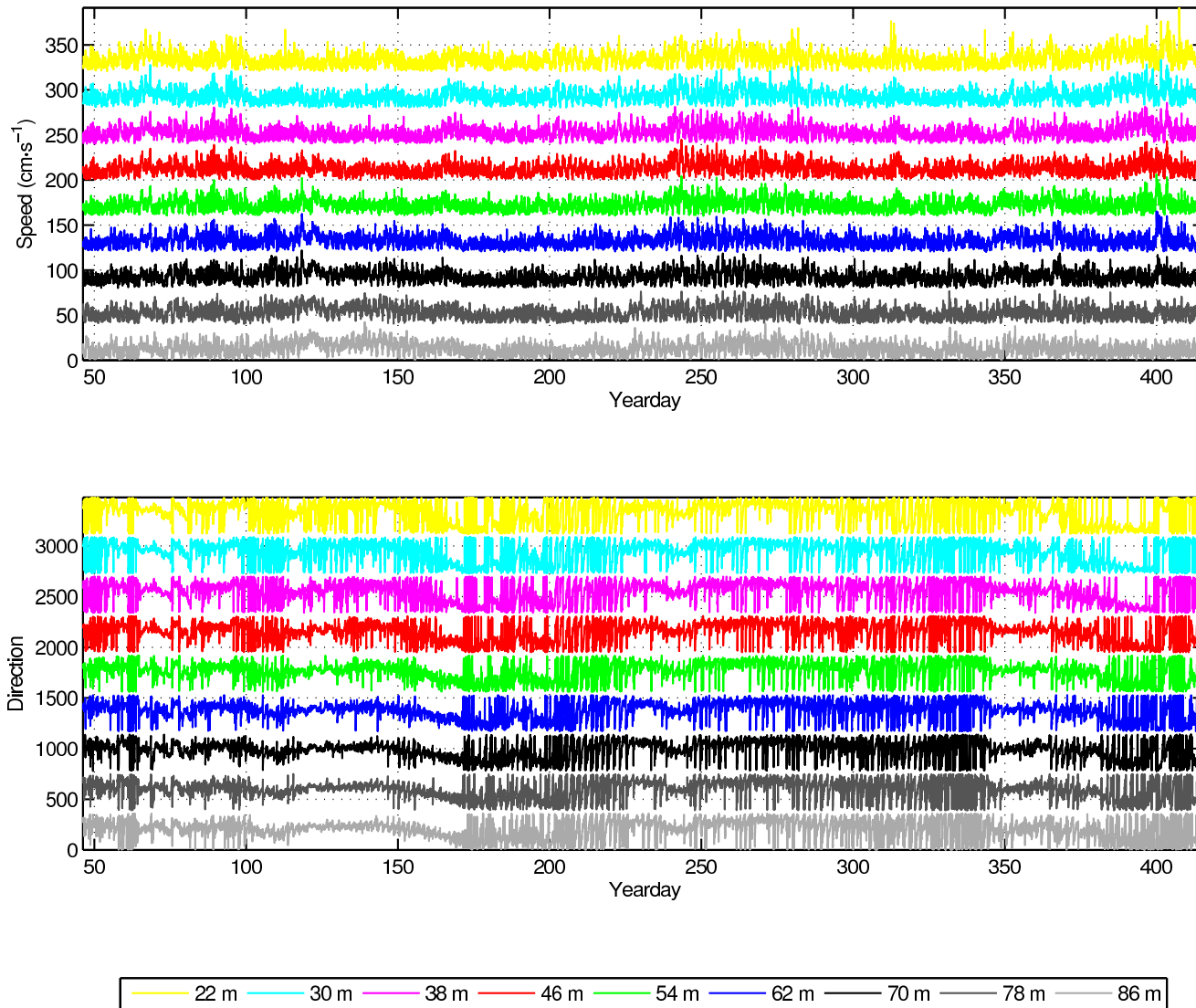


Figure 35: (b) Waterfall plots of the currents time series from the NTAS-3 RDI Workhorse. Current magnitude (top) and direction (bottom). The magnitude is offset by $40 \text{ cm}\cdot\text{s}^{-1}$. Each direction plot is offset by 390 degrees from the one below. In each plot the axis values are correct for the lowest series. Each subsequent series is offset upwards. In each plot the series are from every second 4 m bin, i.e., the [86, 78, 70, 62, 54, 46, 38, 30, 22] m bins (reading from the lowest trace in each case).

Table 14: Spectral peak heights for NTAS-3 RDI Workhorse, 90 m bin. Peaks are ordered relative to the baseline.

| Top 15 Peak Frequencies (NTAS-3 Workhorse 90 m) | | | |
|---|----------|------------|---|
| f (cpd) | T (day) | T (hr) | PeakHgt ($\text{cm}^2 \cdot \text{s}^{-2}$) |
| 0.01172 | 85.33333 | 2048.00000 | 7495.426 |
| 1.93359 | 0.51717 | 12.41212 | 31.387 |
| 0.51562 | 1.93939 | 46.54545 | 83.177 |
| 0.60937 | 1.64103 | 39.38462 | 38.174 |
| 1.40625 | 0.71111 | 17.06667 | 15.114 |
| 0.67969 | 1.47126 | 35.31034 | 27.533 |
| 3.41016 | 0.29324 | 7.03780 | 4.138 |
| 1.80469 | 0.55411 | 13.29870 | 7.405 |
| 3.80859 | 0.26256 | 6.30154 | 3.547 |
| 10.14844 | 0.09854 | 2.36490 | 1.257 |
| 1.32422 | 0.75516 | 18.12389 | 8.909 |
| 2.54297 | 0.39324 | 9.43779 | 4.684 |
| 2.49609 | 0.40063 | 9.61502 | 4.748 |
| 2.58984 | 0.38612 | 9.26697 | 4.411 |
| 0.86719 | 1.15315 | 27.67568 | 12.656 |

Table 15: Spectral peak heights for NTAS-3 RDI Workhorse, 26 m bin. Peaks are ordered relative to the baseline.

| Top 15 Peak Frequencies (NTAS-3 Workhorse 26 m) | | | |
|---|----------|------------|---|
| f (cpd) | T (day) | T (hr) | PeakHgt ($\text{cm}^2 \cdot \text{s}^{-2}$) |
| 0.01172 | 85.33333 | 2048.00000 | 8601.201 |
| 1.93359 | 0.51717 | 12.41212 | 66.268 |
| 0.53906 | 1.85507 | 44.52174 | 77.266 |
| 1.39453 | 0.71709 | 17.21008 | 18.582 |
| 2.07422 | 0.48211 | 11.57062 | 9.771 |
| 2.53125 | 0.39506 | 9.48148 | 5.700 |
| 11.15625 | 0.08964 | 2.15126 | 1.369 |
| 1.48828 | 0.67192 | 16.12598 | 9.160 |
| 0.72656 | 1.37634 | 33.03226 | 17.736 |
| 3.87891 | 0.25780 | 6.18731 | 3.521 |
| 0.94922 | 1.05350 | 25.28395 | 13.073 |
| 1.78125 | 0.56140 | 13.47368 | 7.173 |
| 10.03125 | 0.09969 | 2.39252 | 1.352 |
| 11.95312 | 0.08366 | 2.00784 | 1.100 |
| 2.42578 | 0.41224 | 9.89372 | 4.823 |

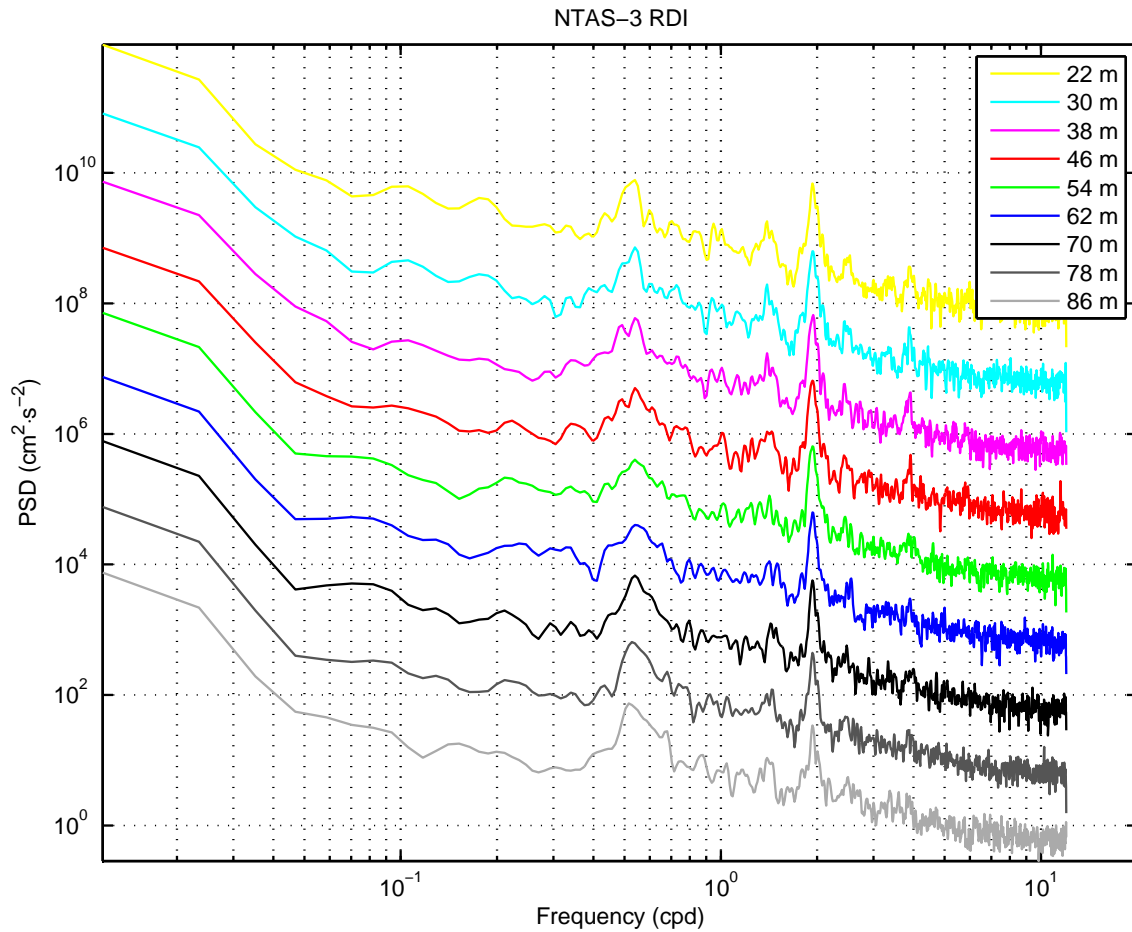


Figure 36: NTAS-3 RDI Workhorse spectra from 86 to 22 meters (spectra for every second 4 m bin are shown from bottom to top, each spectrum offset by $10\times$ the previous spectrum).

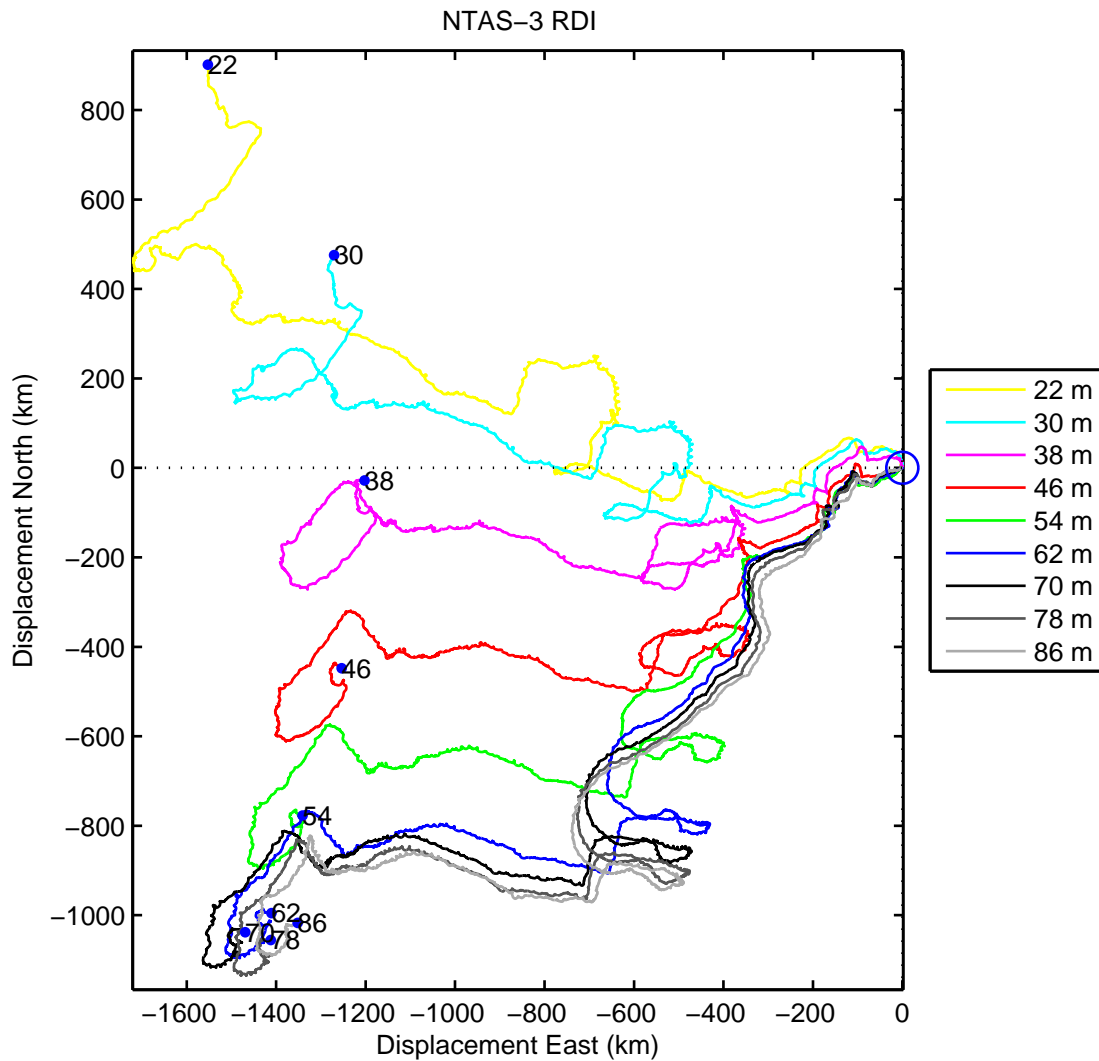


Figure 37: Superimposed progressive vector diagram of currents from the NTAS-3 RDI Workhorse. Vectors start at \circ at the origin (0,0) and end at the \bullet . Every second 4 m bin from 22 to 86 m is plotted as listed in the legend on the figure.

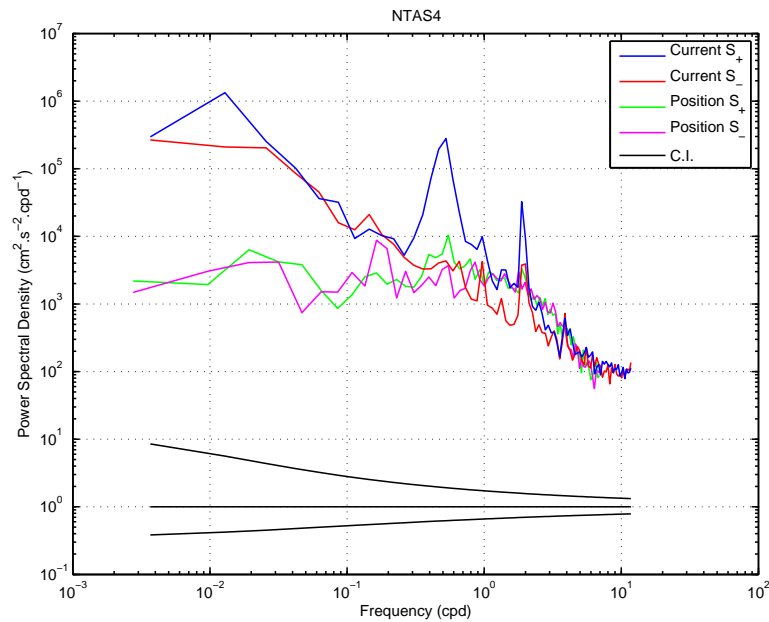


Figure 38: The rotary spectra of velocities determined from the near-surface current meter (Aquadopp at 6 m) and the Argos buoy position from NTAS-4.

5.5 NTAS-4 Velocity Data

Rotary spectra for estimating the influence of the buoy motion on velocity data are shown in Figure 38.

5.5.1 Aquadopp

The time series of the speeds measured with the Aquadopp current meter is shown in Figure 39. The current velocities are shown integrated in a progressive vector diagram in Figure 40. The spectrum is shown in Figure 41. The spectral peaks are tabulated in Table 16.

5.5.2 RDI Workhorse ADCP

A time series of the current speed data from the RDI workhorse ADCP is shown in Figure 42. The spectra for all RDI Workhorse ADCP bins are shown as a waterfall plot in Figure 43. Tables of the spectral peaks obtained from the RDI Workhorse bins are shown in Tables 17 and 18. Only the deepest (78 m) and shallowest (22 m) bins are tabulated. Progressive vector diagrams for all bins of the Workhorse data are shown in Figure 44.

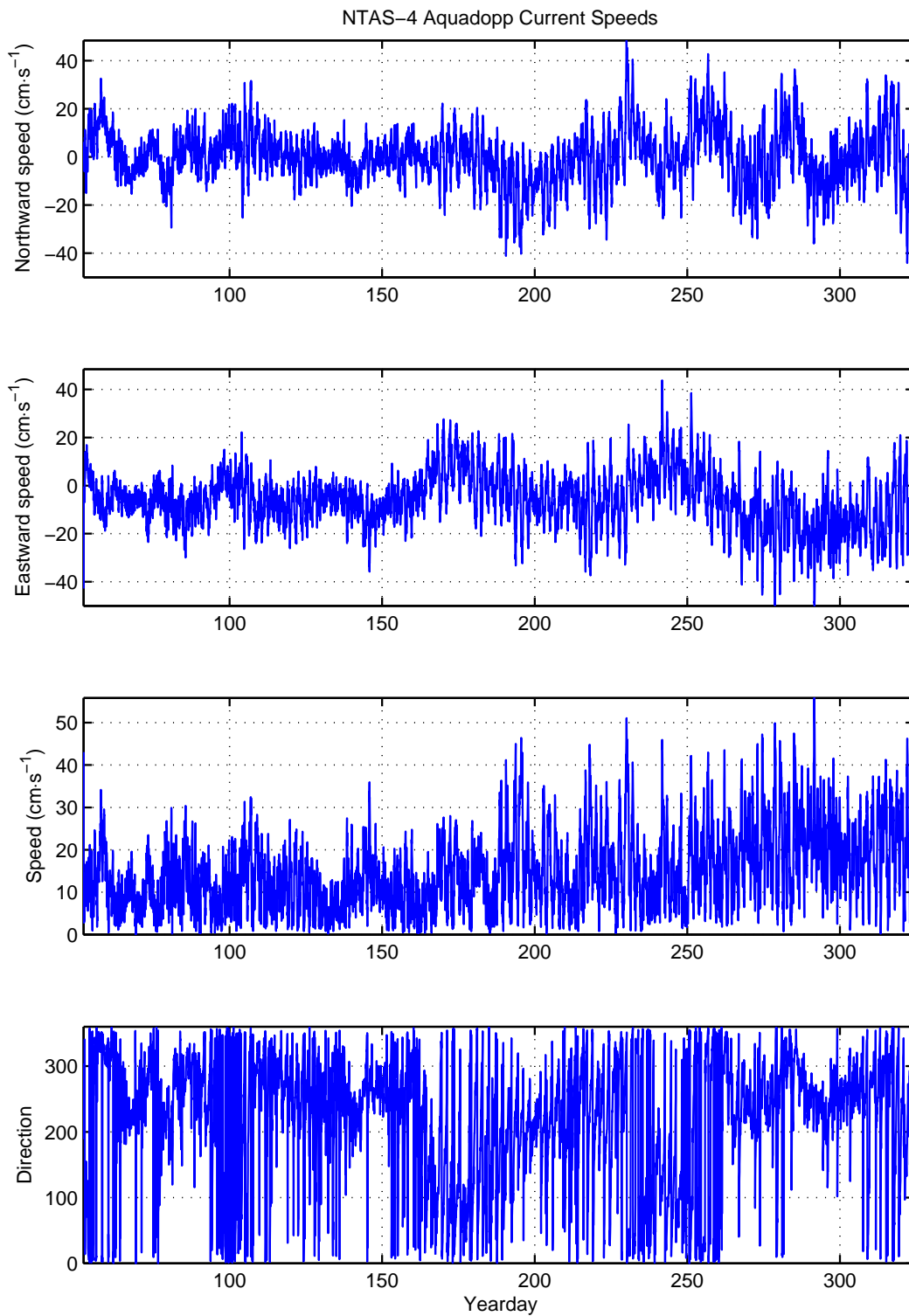


Figure 39: Unfiltered currents from NTAS-4 Aquadopp. (a) Northward current speeds. (b) Eastward current speeds. (c) Magnitude. (d) Direction.

Table 16: Spectral peak heights for NTAS-4 Aquadopp. Peaks are ordered relative to the baseline.

| Top 15 Peak Frequencies (NTAS-4 Aquadopp 6 m) | | | |
|---|---------|----------|---|
| f (cpd) | T (day) | T (hr) | PeakHgt ($\text{cm}^2 \cdot \text{s}^{-2}$) |
| 1.92188 | 0.52033 | 12.48780 | 71.999 |
| 0.53906 | 1.85507 | 44.52174 | 165.286 |
| 1.00781 | 0.99225 | 23.81395 | 27.944 |
| 1.47656 | 0.67725 | 16.25397 | 12.231 |
| 2.53125 | 0.39506 | 9.48148 | 4.667 |
| 10.40625 | 0.09610 | 2.30631 | 0.420 |
| 11.67188 | 0.08568 | 2.05622 | 0.344 |
| 3.82031 | 0.26176 | 6.28221 | 2.018 |
| 8.55469 | 0.11689 | 2.80548 | 0.549 |
| 11.43750 | 0.08743 | 2.09836 | 0.342 |
| 1.38281 | 0.72316 | 17.35593 | 10.160 |
| 11.01563 | 0.09078 | 2.17872 | 0.356 |
| 11.32031 | 0.08834 | 2.12008 | 0.339 |
| 10.75781 | 0.09296 | 2.23094 | 0.355 |
| 10.87500 | 0.09195 | 2.20690 | 0.346 |

Table 17: Spectral peak heights for NTAS-4 RDI Workhorse, 78 m bin. Peaks are ordered relative to the baseline.

| Top 15 Peak Frequencies (NTAS-4 Workhorse 78 m) | | | |
|---|----------|------------|---|
| f (cpd) | T (day) | T (hr) | PeakHgt ($\text{cm}^2 \cdot \text{s}^{-2}$) |
| 0.01172 | 85.33333 | 2048.00000 | 5244.393 |
| 1.93359 | 0.51717 | 12.41212 | 30.560 |
| 0.52734 | 1.89630 | 45.51111 | 60.366 |
| 1.41797 | 0.70523 | 16.92562 | 13.633 |
| 2.00391 | 0.49903 | 11.97661 | 9.721 |
| 2.49609 | 0.40063 | 9.61502 | 6.942 |
| 0.67969 | 1.47126 | 35.31034 | 23.011 |
| 0.99609 | 1.00392 | 24.09412 | 13.200 |
| 2.44922 | 0.40829 | 9.79904 | 5.438 |
| 0.73828 | 1.35450 | 32.50794 | 15.350 |
| 1.08984 | 0.91756 | 22.02151 | 9.256 |
| 11.61328 | 0.08611 | 2.06660 | 1.003 |
| 3.87891 | 0.25780 | 6.18731 | 2.605 |
| 11.68359 | 0.08559 | 2.05416 | 0.899 |
| 1.76953 | 0.56512 | 13.56291 | 5.068 |

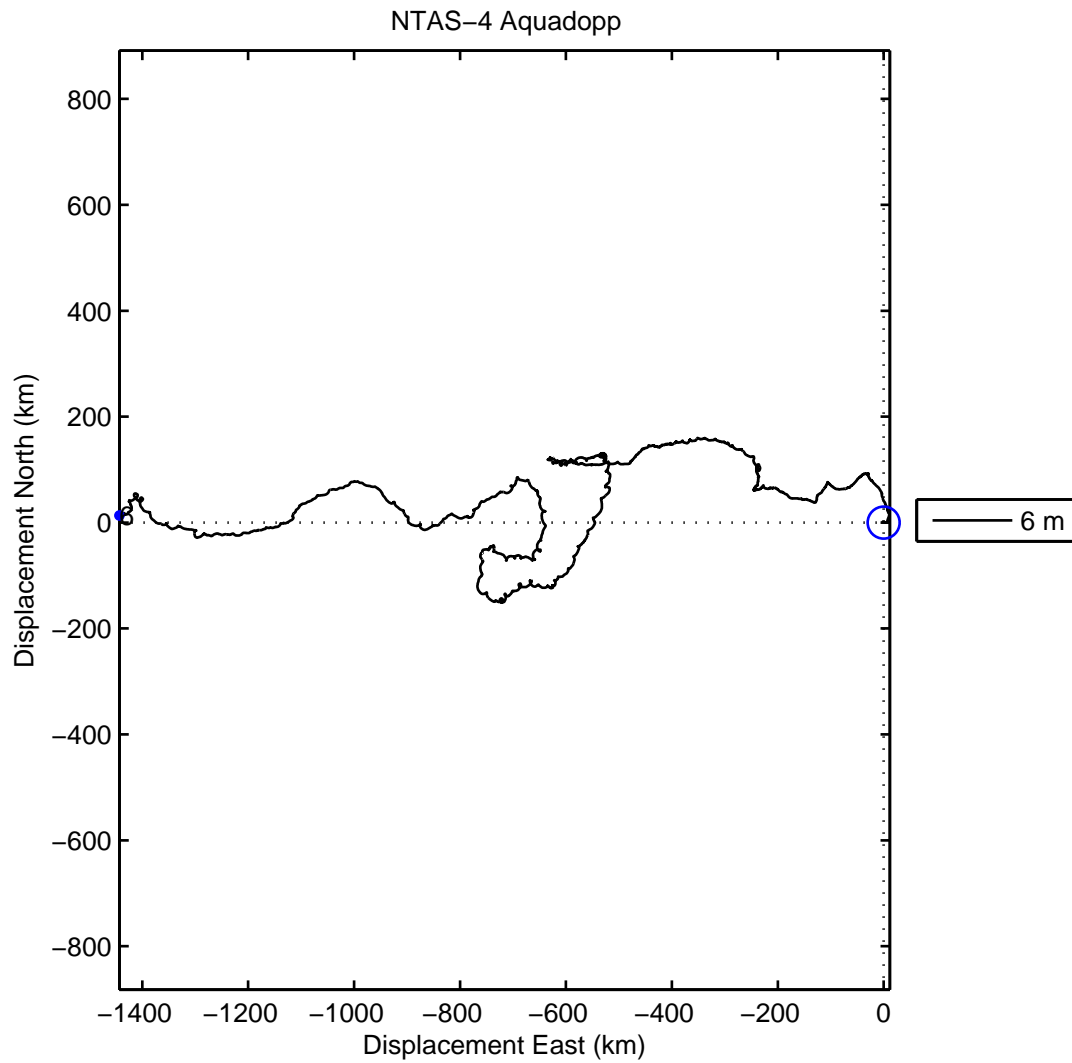


Figure 40: Progressive vector diagram of currents from the NTAS-4 Aquadopp.

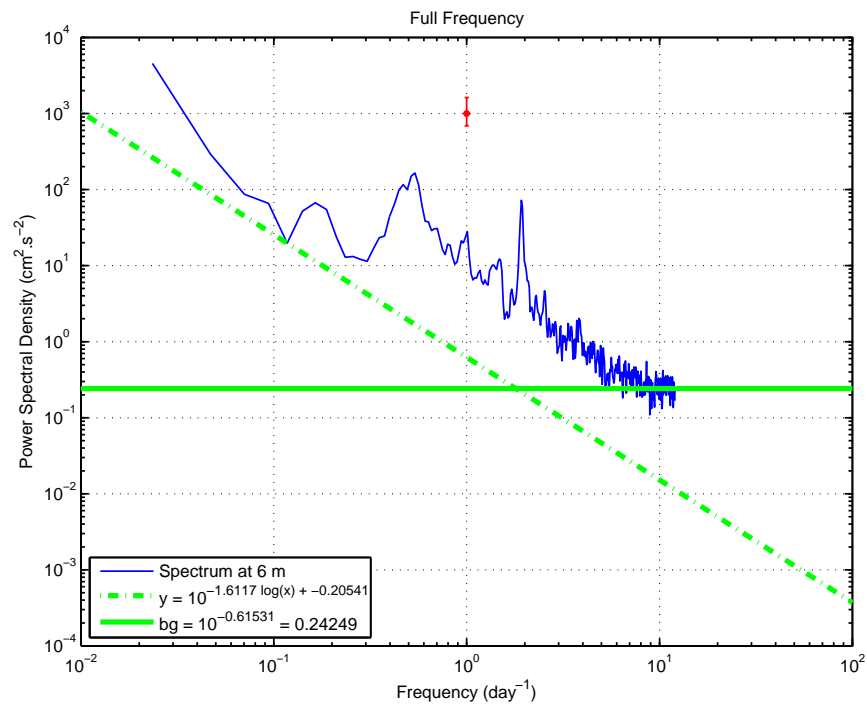


Figure 41: Spectrum of NTAS-4 Aquadopp current speed. Symbol at top center indicates confidence interval for the spectrum. Dashed line has the slope of the least-squares regression line passing through the data, but has been shifted down to pass through the minimum spectral density. The solid line indicates the level of instrumental noise, determined from the leveling off of the tail of the high frequency spectrum.

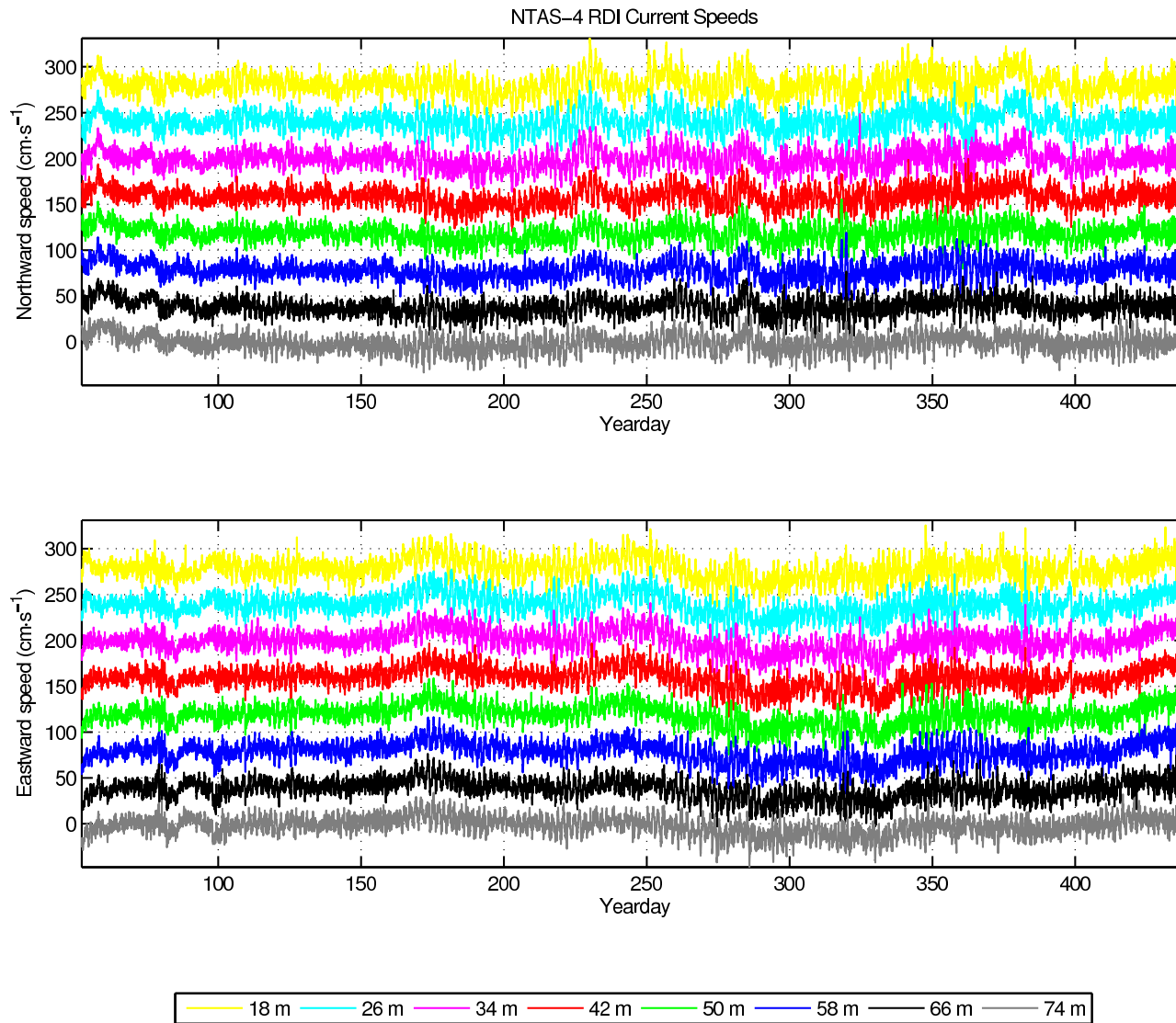


Figure 42: (a) Waterfall plots of the current speed time series from the NTAS-4 RDI Workhorse. Northerly (top) and easterly (bottom) current speeds for the ADCP bins. Series are offset by $40 \text{ cm}\cdot\text{s}^{-1}$. In each plot the axis values are correct for the lowest series. Each subsequent series is offset upwards. In each plot the series are from the [74, 66, 58, 50, 42, 34, 26, 18] m bins (every second data bin reading upwards from the lowest trace in each case).

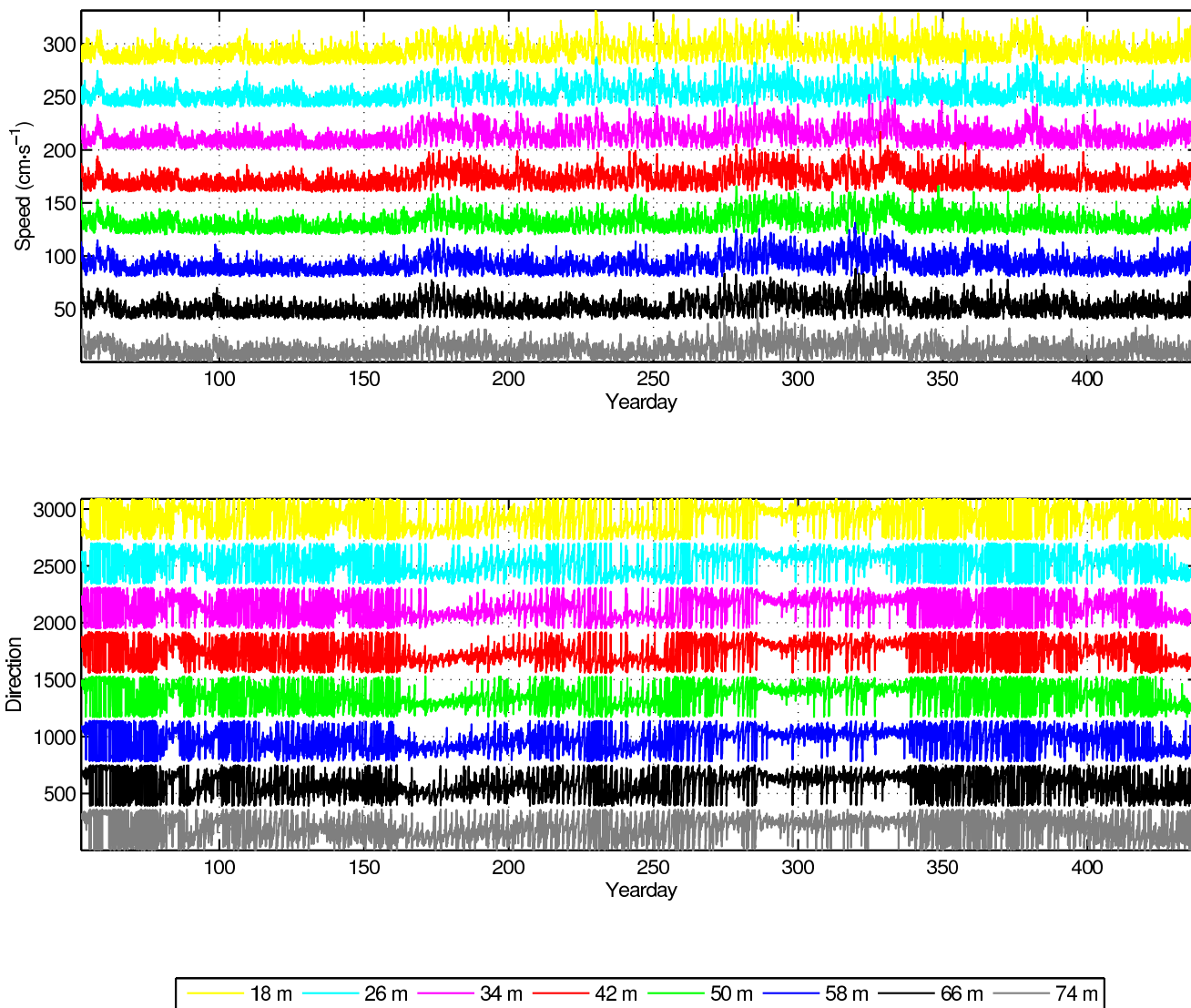


Figure 42: (b) Waterfall plots of the currents time series from the NTAS-4 RDI Workhorse. Current magnitude (top) and direction (bottom). The magnitude is offset by $40 \text{ cm}\cdot\text{s}^{-1}$. Each direction plot is offset by 390 degrees from the one below. In each plot the axis values are correct for the lowest series. Each subsequent series is offset upwards. In each plot the series are from the [74, 66, 58, 50, 42, 34, 26, 18] m bins (every second data bin reading upwards from the lowest trace in each case).

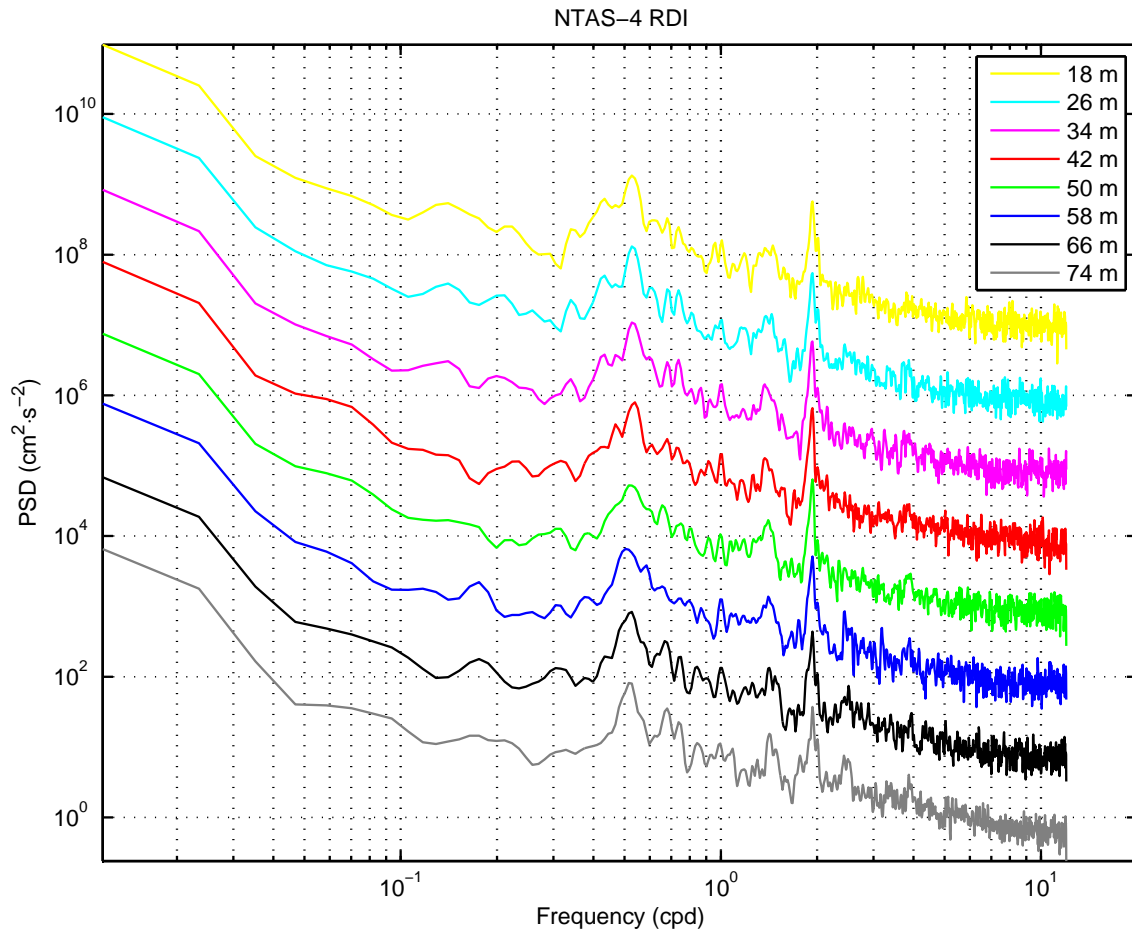


Figure 43: NTAS-4 RDI Workhorse spectra from 18 to 74 meters (every second 4 m bin is plotted from bottom (74 m) to top (18 m), each spectrum offset upwards by $10\times$ the previous spectrum).

Table 18: Spectral peak heights for NTAS-4 RDI Workhorse, 22 m bin. Peaks are ordered relative to the baseline.

| Top 15 Peak Frequencies (NTAS-4 Workhorse 22 m) | | | |
|---|----------|------------|---|
| f (cpd) | T (day) | T (hr) | PeakHgt ($\text{cm}^2 \cdot \text{s}^{-2}$) |
| 0.01172 | 85.33333 | 2048.00000 | 9305.085 |
| 1.93359 | 0.51717 | 12.41212 | 55.888 |
| 0.52734 | 1.89630 | 45.51111 | 130.495 |
| 2.01562 | 0.49612 | 11.90698 | 17.400 |
| 0.43359 | 2.30631 | 55.35135 | 55.712 |
| 0.67969 | 1.47126 | 35.31034 | 34.543 |
| 0.62109 | 1.61006 | 38.64151 | 33.710 |
| 0.73828 | 1.35450 | 32.50794 | 27.132 |
| 1.38281 | 0.72316 | 17.35593 | 12.777 |
| 1.44141 | 0.69377 | 16.65041 | 12.208 |
| 9.98437 | 0.10016 | 2.40376 | 1.996 |
| 11.55469 | 0.08654 | 2.07708 | 1.498 |
| 7.89844 | 0.12661 | 3.03858 | 2.093 |
| 1.00781 | 0.99225 | 23.81395 | 13.667 |
| 11.12109 | 0.08992 | 2.15806 | 1.416 |

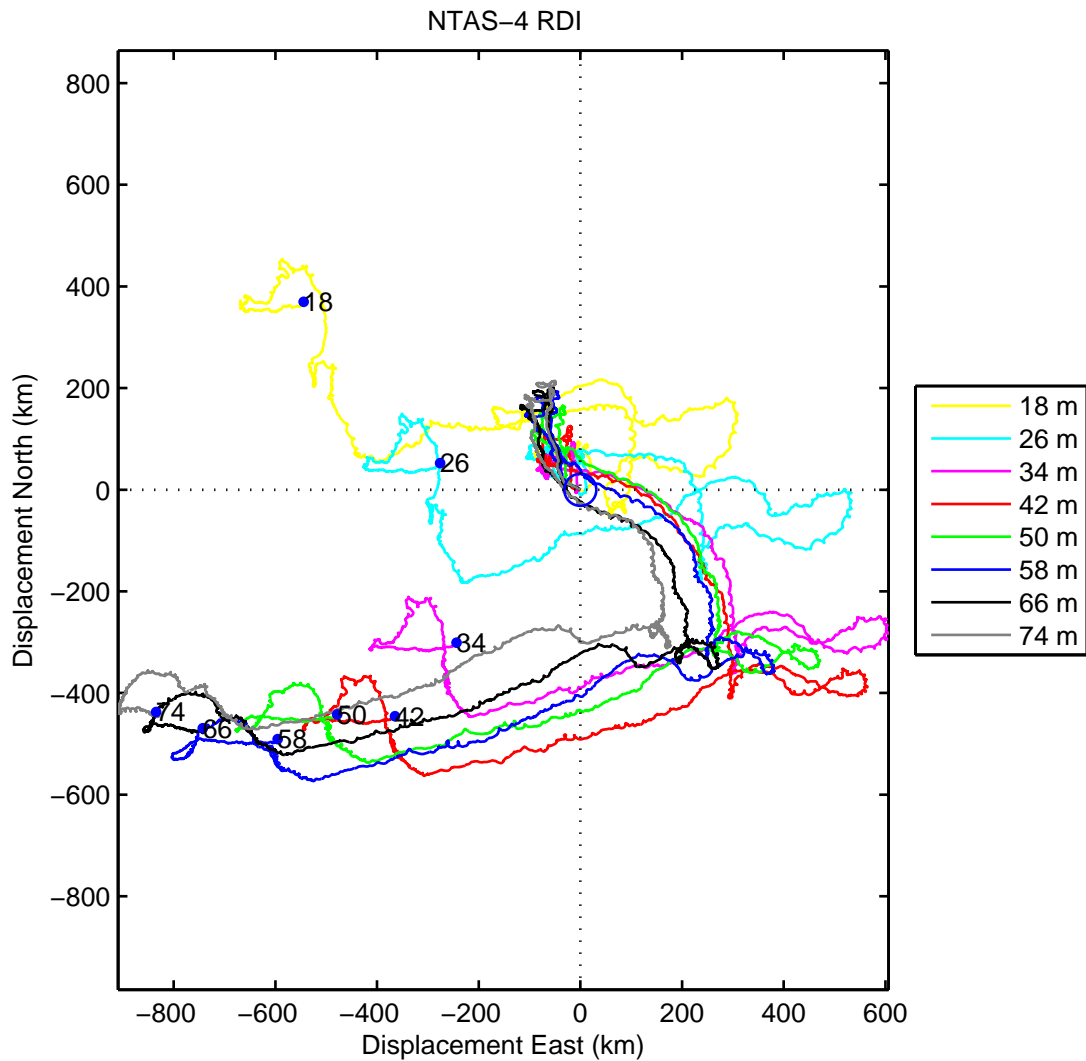


Figure 44: Superimposed progressive vector diagram of currents from the NTAS-4 RDI Workhorse. Vectors start at \circ at the origin (0,0) and end at the \bullet . Every second 4 m bin from 18 to 74 m is plotted as listed in the legend on the figure.

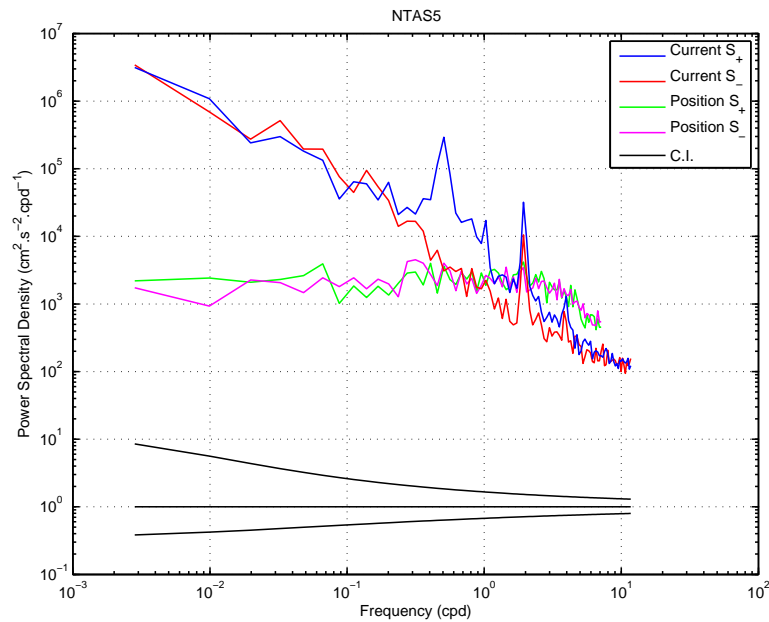


Figure 45: Showing the rotary spectra of velocities determined from the near-surface current meter (Aquadopp at 6 m) and the Argos buoy position from NTAS-5.

5.6 NTAS-5 Velocity Data

Rotary spectra for estimating the influence of the buoy motion on velocity data are shown in Figure 45.

5.6.1 Aquadopp

The time series of the speeds measured with the Aquadopp current meter on NTAS-5 is shown in Figure 46. The current velocities are shown integrated in a progressive vector diagram in Figure 47. The spectrum is shown in Figure 48. The spectral peaks are tabulated in Table 19.

5.6.2 RDI Workhorse ADCP

A time series of the current speed data from the RDI workhorse ADCP is shown in Figure 49. The spectra for all RDI Workhorse ADCP bins are shown as a waterfall plot in Figure 50. Tables of the spectral peaks obtained from the RDI Workhorse bins are shown in Tables 20 and 21. Only the deepest (78 m) and shallowest (14 m) bins are tabulated. Progressive vector diagrams for all bins of the Workhorse data are shown in Figure 51.

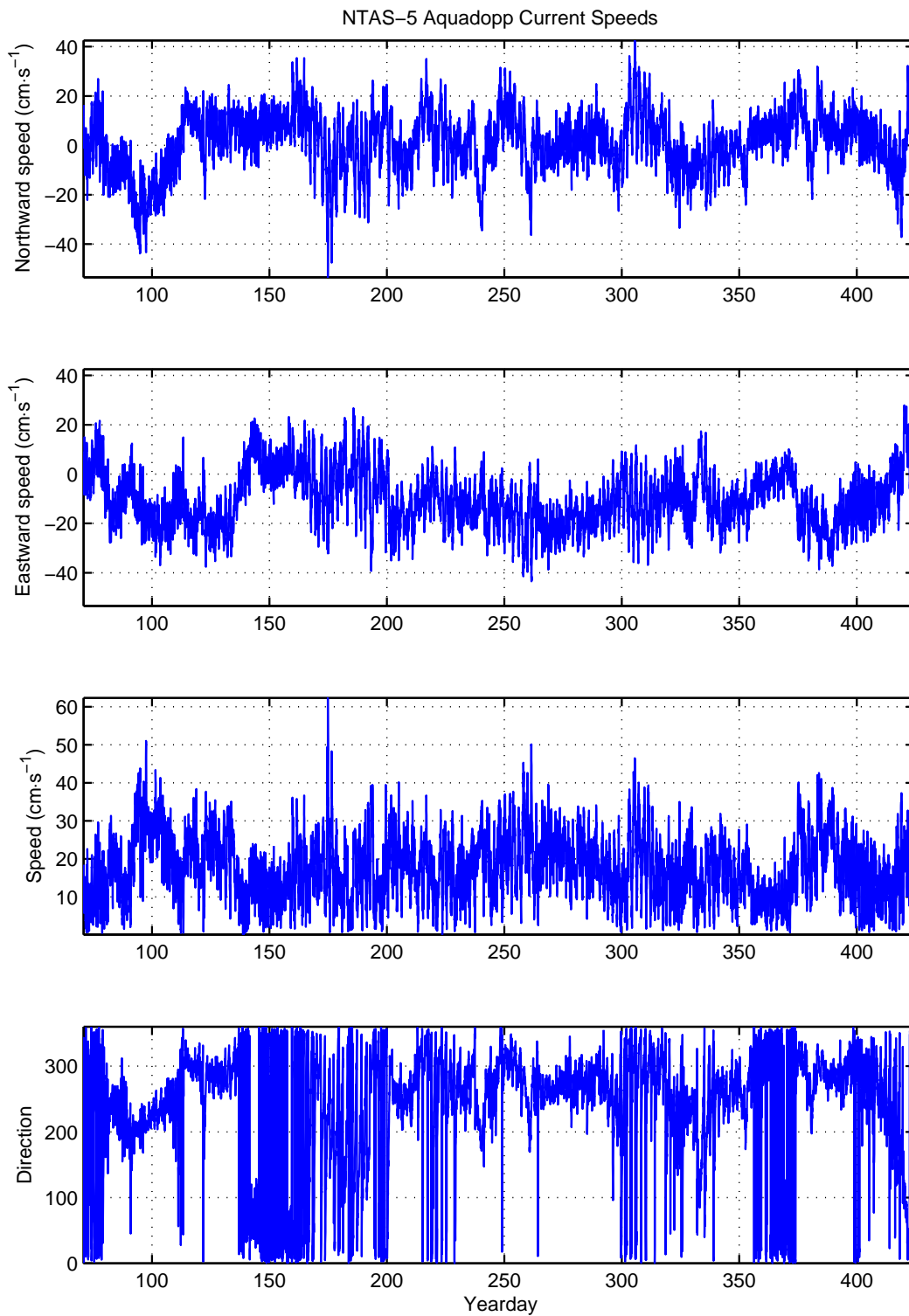


Figure 46: Unfiltered currents from NTAS-5 Aquadopp. (a) Northward current speeds. (b) Eastward current speeds. (c) Magnitude. (d) Direction.

Table 19: Spectral peak heights for NTAS-5 Aquadopp. Peaks are ordered relative to the baseline.

| Top 15 Peak Frequencies (NTAS-5 Aquadopp 6 m) | | | |
|---|----------|------------|---|
| f (cpd) | T (day) | T (hr) | PeakHgt ($\text{cm}^2 \cdot \text{s}^{-2}$) |
| 1.93359 | 0.51717 | 12.41212 | 51.162 |
| 0.51562 | 1.93939 | 46.54545 | 147.272 |
| 1.00781 | 0.99225 | 23.81395 | 41.579 |
| 0.01172 | 85.33333 | 2048.00000 | 13573.005 |
| 3.91406 | 0.25549 | 6.13174 | 2.851 |
| 3.83203 | 0.26096 | 6.26300 | 2.804 |
| 11.01562 | 0.09078 | 2.17872 | 0.667 |
| 11.98828 | 0.08341 | 2.00196 | 0.555 |
| 2.44922 | 0.40829 | 9.79904 | 4.279 |
| 0.80859 | 1.23671 | 29.68116 | 17.792 |
| 11.69531 | 0.08550 | 2.05210 | 0.488 |
| 11.25000 | 0.08889 | 2.13333 | 0.509 |
| 0.70312 | 1.42222 | 34.13333 | 20.063 |
| 10.33594 | 0.09675 | 2.32200 | 0.541 |
| 10.20703 | 0.09797 | 2.35132 | 0.538 |

Table 20: Spectral peak heights for NTAS-5 RDI Workhorse, 78 m bin. Peaks are ordered relative to the baseline.

| Top 15 Peak Frequencies (NTAS-5 Workhorse 78 m) | | | |
|---|----------|------------|---|
| f (cpd) | T (day) | T (hr) | PeakHgt ($\text{cm}^2 \cdot \text{s}^{-2}$) |
| 0.01172 | 85.33333 | 2048.00000 | 7226.505 |
| 1.93359 | 0.51717 | 12.41212 | 49.958 |
| 0.50391 | 1.98450 | 47.62791 | 85.313 |
| 2.00391 | 0.49903 | 11.97661 | 15.321 |
| 0.59766 | 1.67320 | 40.15686 | 38.851 |
| 1.40625 | 0.71111 | 17.06667 | 16.824 |
| 2.43750 | 0.41026 | 9.84615 | 9.249 |
| 2.51953 | 0.39690 | 9.52558 | 6.212 |
| 3.84375 | 0.26016 | 6.24390 | 3.607 |
| 1.82812 | 0.54701 | 13.12821 | 6.680 |
| 10.62891 | 0.09408 | 2.25799 | 1.344 |
| 5.66016 | 0.17667 | 4.24017 | 2.214 |
| 11.84766 | 0.08440 | 2.02572 | 1.120 |
| 8.73047 | 0.11454 | 2.74899 | 1.460 |
| 3.31641 | 0.30153 | 7.23675 | 3.372 |

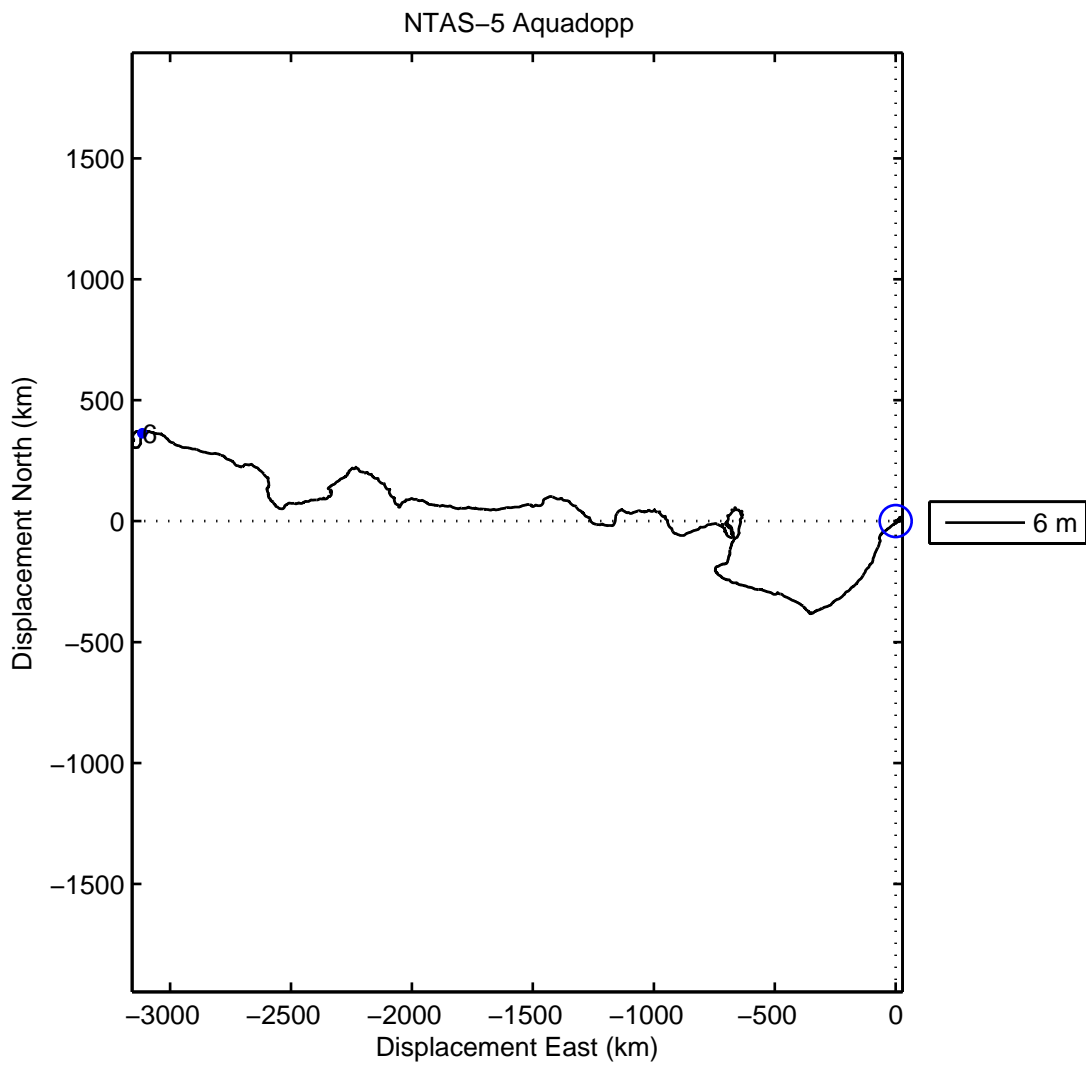


Figure 47: Progressive vector diagram of currents from the NTAS-5 Aquadopp.

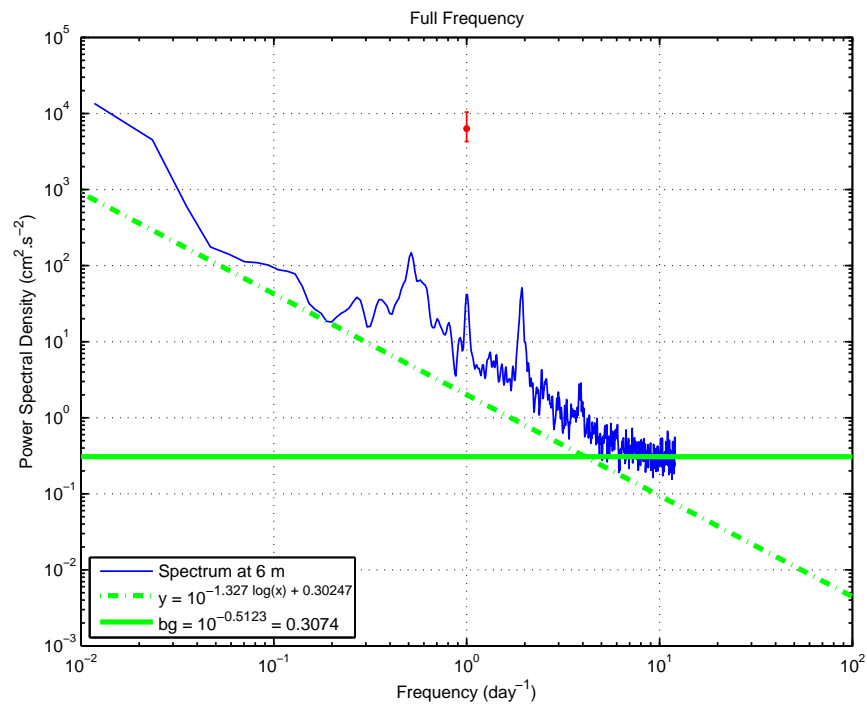


Figure 48: Spectrum of NTAS-5 Aquadopp current speed. Symbol at top center indicates confidence interval for the spectrum. Dashed line has the slope of the least-squares regression line passing through the data, but has been shifted down to pass through the minimum spectral density. The solid line indicates the level of instrumental noise, determined from the leveling off of the tail of the high frequency spectrum.

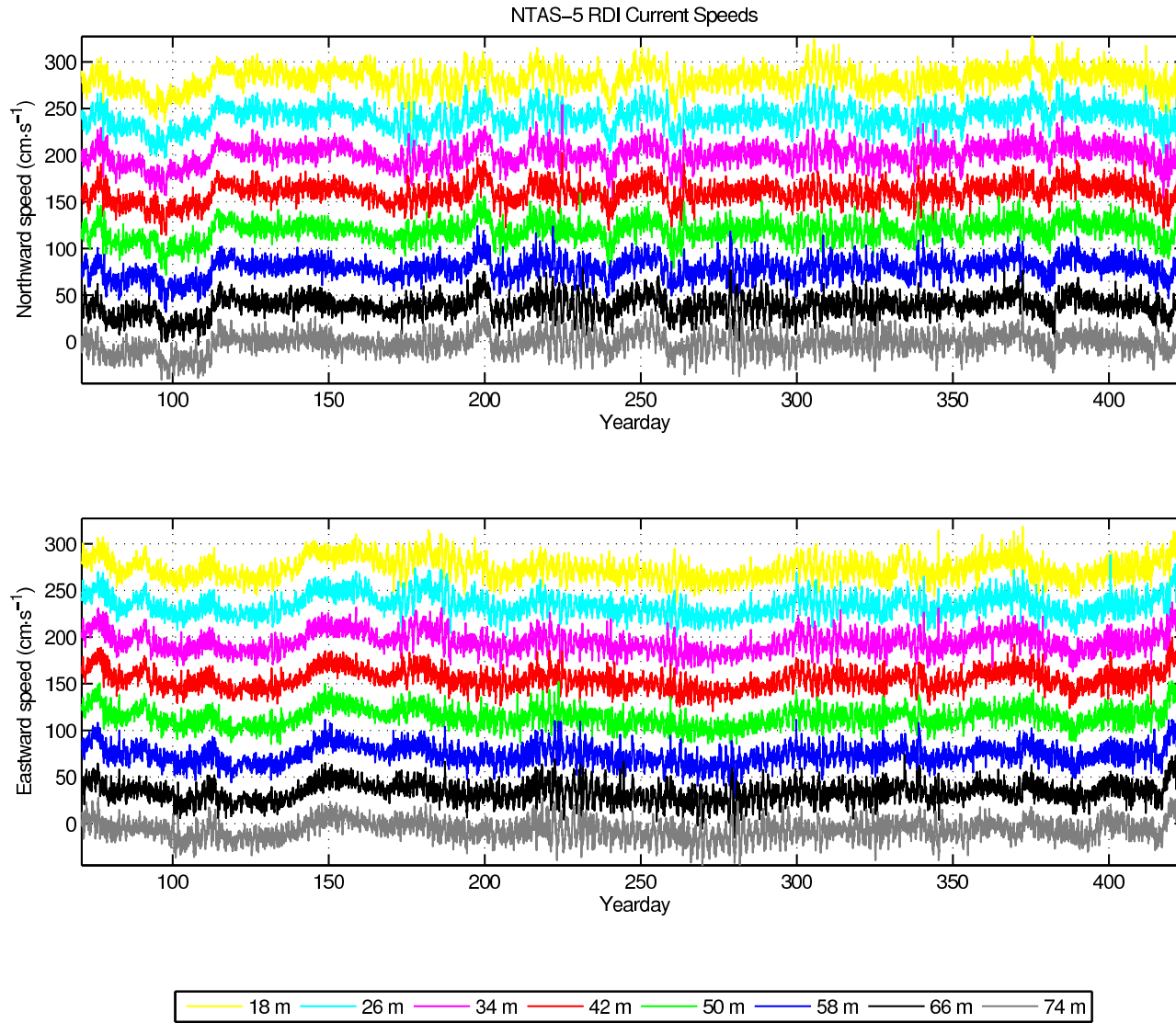


Figure 49: (a) Waterfall plots of the current speed time series from the NTAS-5 RDI Workhouse. Northerly (top) and easterly (bottom) current speeds for the ADCP bins. Series are offset by $40 \text{ cm}\cdot\text{s}^{-1}$. In each plot the axis values are correct for the lowest series. Each subsequent series is offset upwards. In each plot the series are from the [74, 66, 58, 50, 42, 34, 26, 18] m bins (every second data bin reading upwards from the lowest trace in each case).

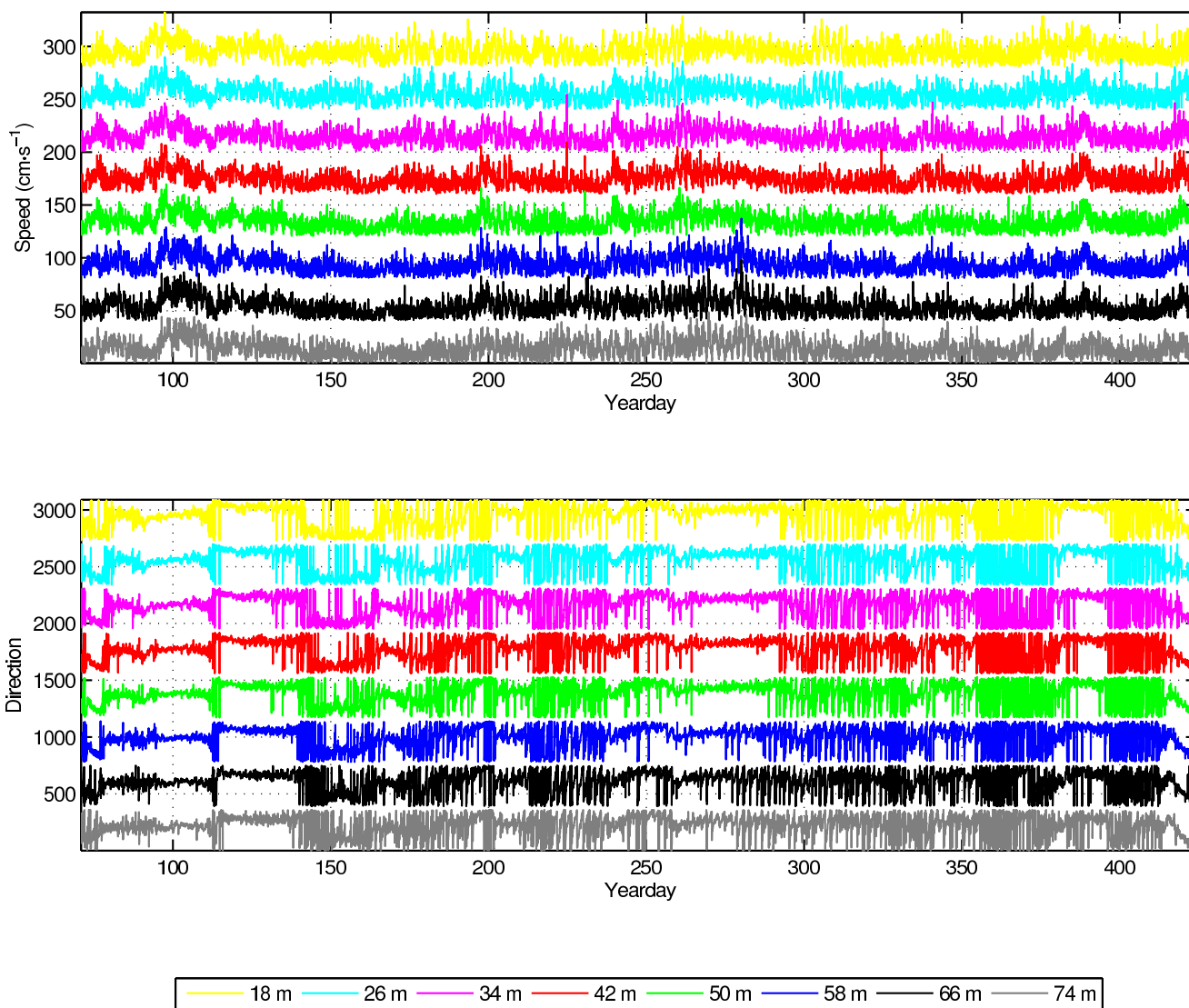


Figure 49: (b) Waterfall plots of the currents time series from the NTAS-5 RDI Workhorse. Current magnitude (top) and direction (bottom). The magnitude is offset by $40 \text{ cm}\cdot\text{s}^{-1}$. Each direction plot is offset by 390 degrees from the one below. In each plot the axis values are correct for the lowest series. Each subsequent series is offset upwards. In each plot the series are from the [74, 66, 58, 50, 42, 34, 26, 18] m bins (every second data bin reading from the lowest trace in each case).

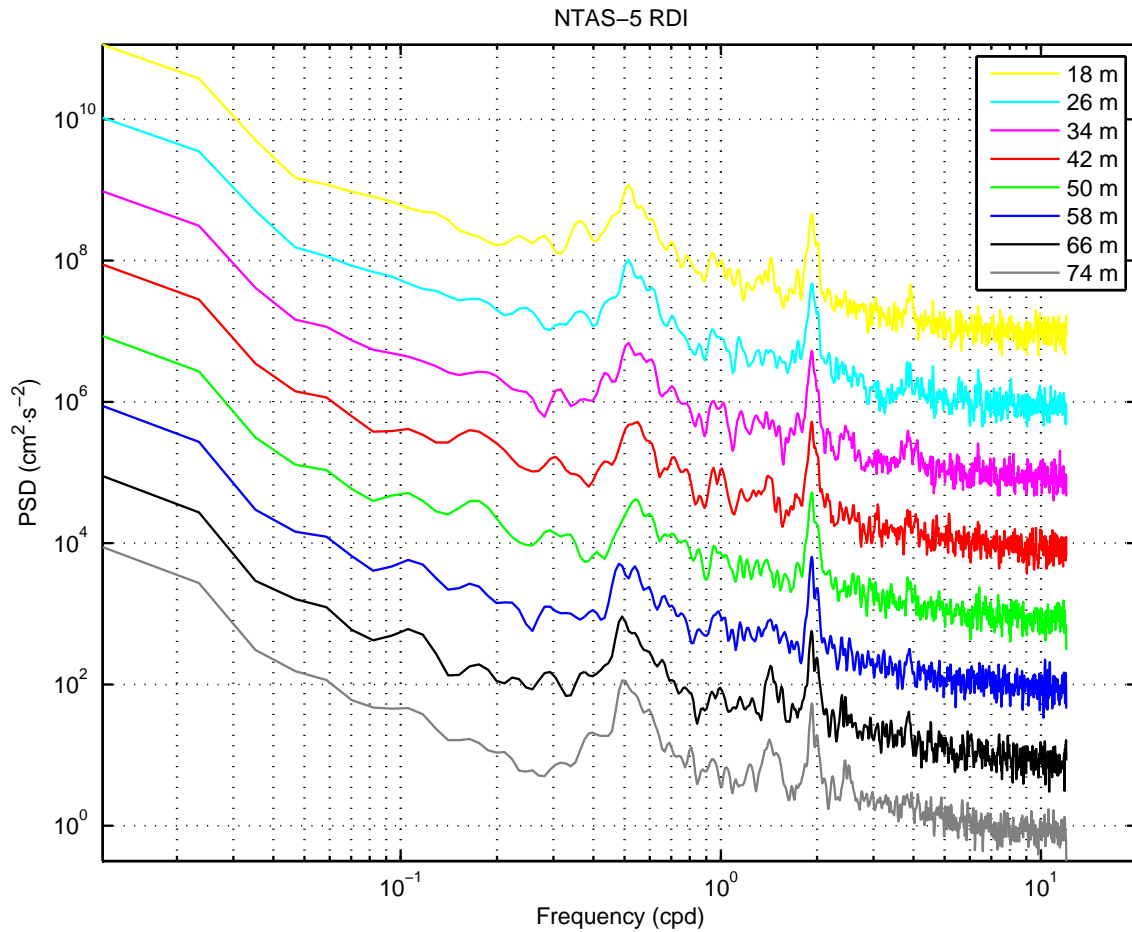


Figure 50: NTAS-5 RDI Workhorse spectra from 18 to 74 meters (every second 4 m bin is plotted from bottom (74 m) to top (18 m), each spectrum offset upwards by $10\times$ the previous spectrum).

Table 21: Spectral peak heights for NTAS-5 RDI Workhorse, 14 m bin. Peaks are ordered relative to the baseline.

| Top 15 Peak Frequencies (NTAS-5 Workhorse 14 m) | | | |
|---|----------|------------|---|
| f (cpd) | T (day) | T (hr) | PeakHgt (cm ² .s ⁻²) |
| 0.01172 | 85.33333 | 2048.00000 | 12132.681 |
| 1.93359 | 0.51717 | 12.41212 | 42.187 |
| 0.51562 | 1.93939 | 46.54545 | 116.825 |
| 2.00391 | 0.49903 | 11.97661 | 17.622 |
| 10.30078 | 0.09708 | 2.32992 | 2.420 |
| 0.99609 | 1.00392 | 24.09412 | 16.988 |
| 9.60937 | 0.10407 | 2.49756 | 2.248 |
| 0.36328 | 2.75269 | 66.06452 | 35.420 |
| 11.58984 | 0.08628 | 2.07078 | 1.844 |
| 11.98828 | 0.08341 | 2.00196 | 1.781 |
| 11.84766 | 0.08440 | 2.02572 | 1.778 |
| 9.97266 | 0.10027 | 2.40658 | 1.903 |
| 10.98047 | 0.09107 | 2.18570 | 1.752 |
| 9.73828 | 0.10269 | 2.46450 | 1.853 |
| 0.93750 | 1.06667 | 25.60000 | 13.346 |

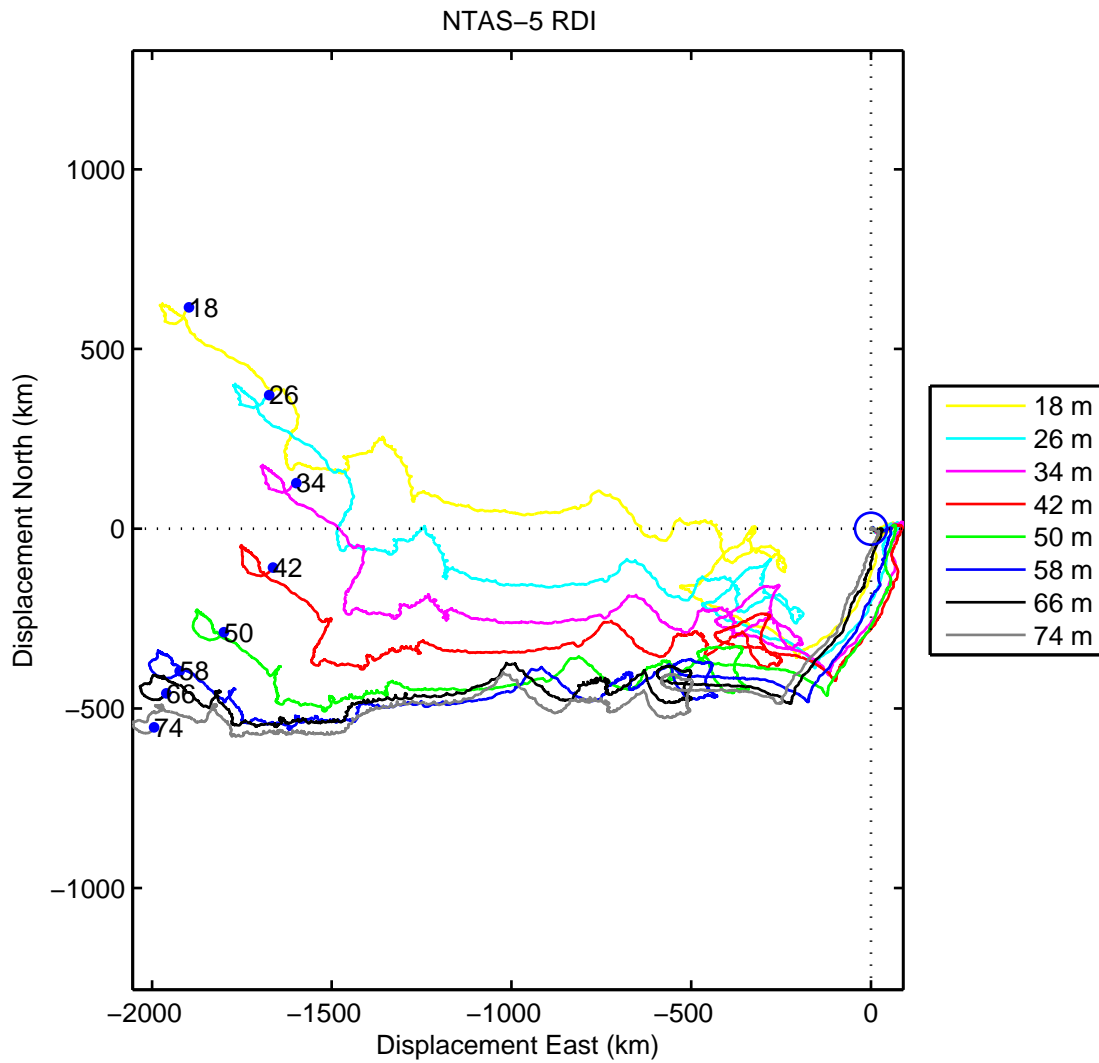


Figure 51: Superimposed progressive vector diagram of currents from the NTAS-5 RDI Workhorse. Vectors start at \circ at the origin (0,0) and end at the \bullet . Every second 4 m bin is plotted from 18 to 74 m, as indicated in the legend on the figure.

6 Comparisons of Data

After quality assessment and removal of worst offending outliers (e.g., the entire record of the Aquadopp current meter on NTAS-3 was removed), the velocity data collected were distributed as shown in Figure 52.

Where multiple current meter data are available, these are plotted together so that a comparison is made between the data sets.

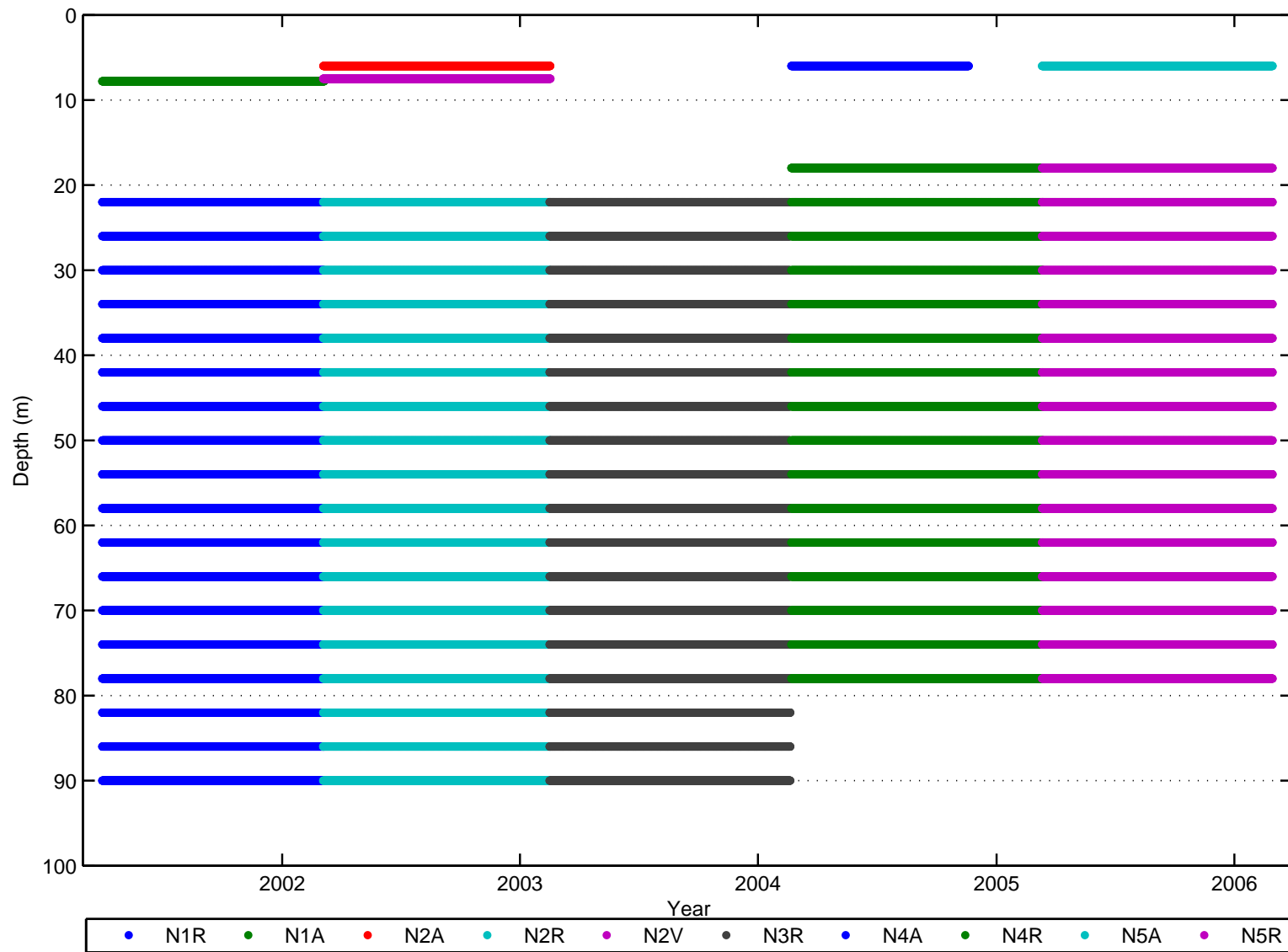


Figure 52: Data return for NTAS-1 to -5 current meters. Labels in the legend are in the form NTAS number and current meter type, e.g., N1A refers to the NTAS-1 Aquadopp. Type designators are A—Aquadopp, R—RDI Workhorse, and V—vector measuring current meter. Labels in the time axis refer to 00:00Z on January 1 of the year indicated.

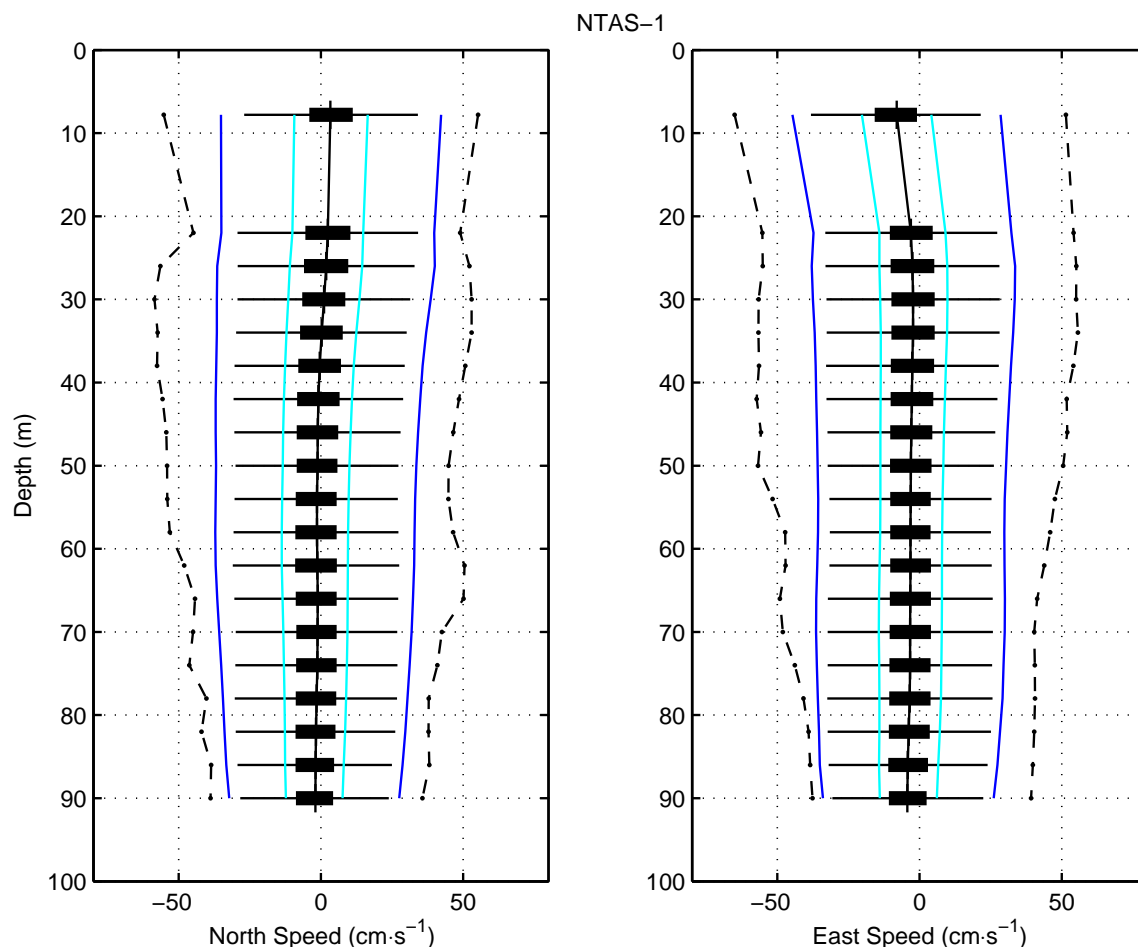


Figure 53: Vertical profile of all velocity data on NTAS-1. The data are shown as horizontal box-and-whisker plots. A + identifies the median value; a thick line covers the interquartile range; a thin line extends between the outlier limits; and the dots indicate the maximum and minimum values. Cyan and blue lines indicate one and three standard deviations from the mean respectively. (a) Northerly current speeds. (b) Easterly current speeds.

6.1 Intra-Deployment Comparisons

6.1.1 Comparison of Current Meters on NTAS-1

Vertical profiles of velocity from the NTAS-1 current meters are shown in Figure 53. Progressive vectors of all velocity data on NTAS-1 are shown in Figure 54. The spectrum for the Aquadopp and a selection of the spectra from the RDI NarrowBand depth bins appear in Figure 55.

6.1.2 Comparison of Current Meters on NTAS-2

Vertical profiles of velocity from the NTAS-2 current meters are shown in Figure 56. Progressive vectors of these velocity data are shown in Figure 57. Spectra for the Aquadopp and VMCM current meters and a selection of the spectra from the RDI Workhorse depth bins are shown in

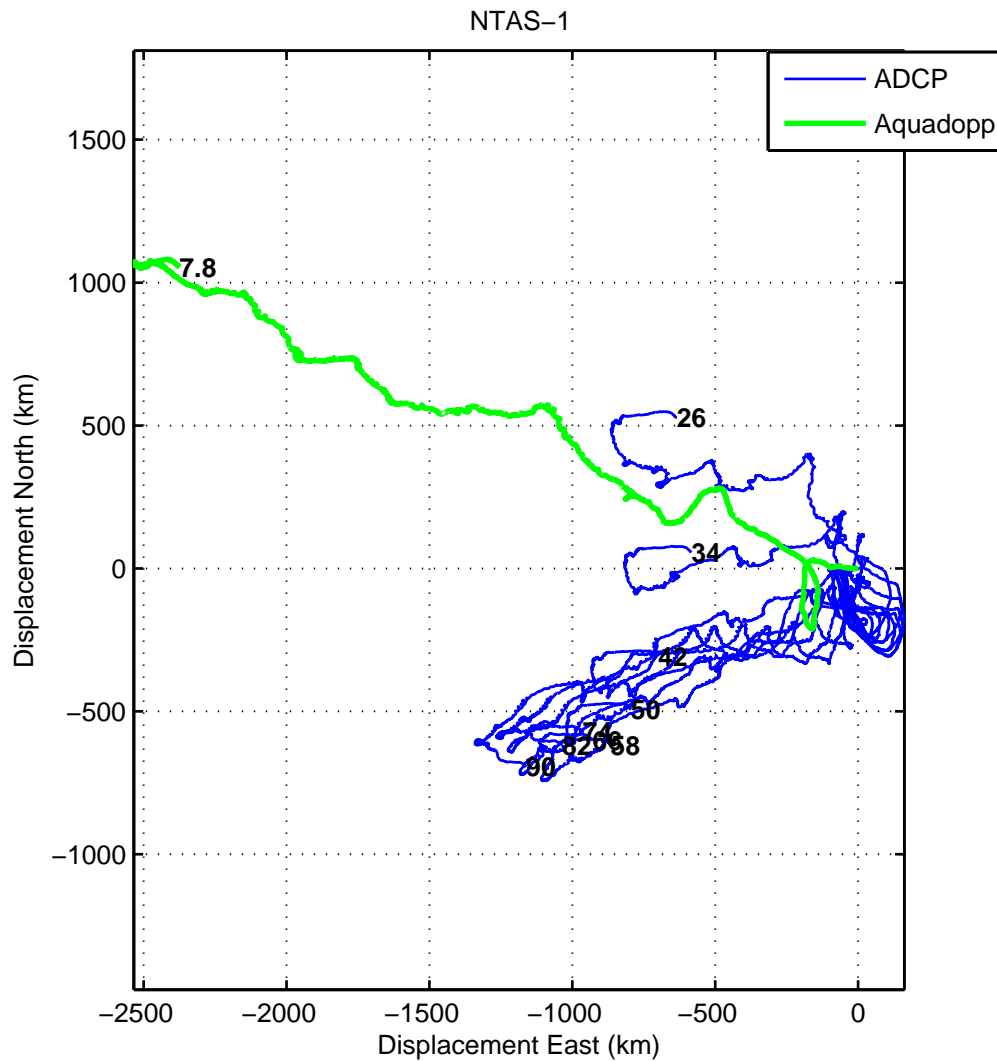


Figure 54: Progressive vectors of all velocity data on NTAS-1. The RDI data are plotted in blue, and the Aquadopp is plotted in a thicker line. The final point of each series is labelled with the nominal depth of the sensor or bin.

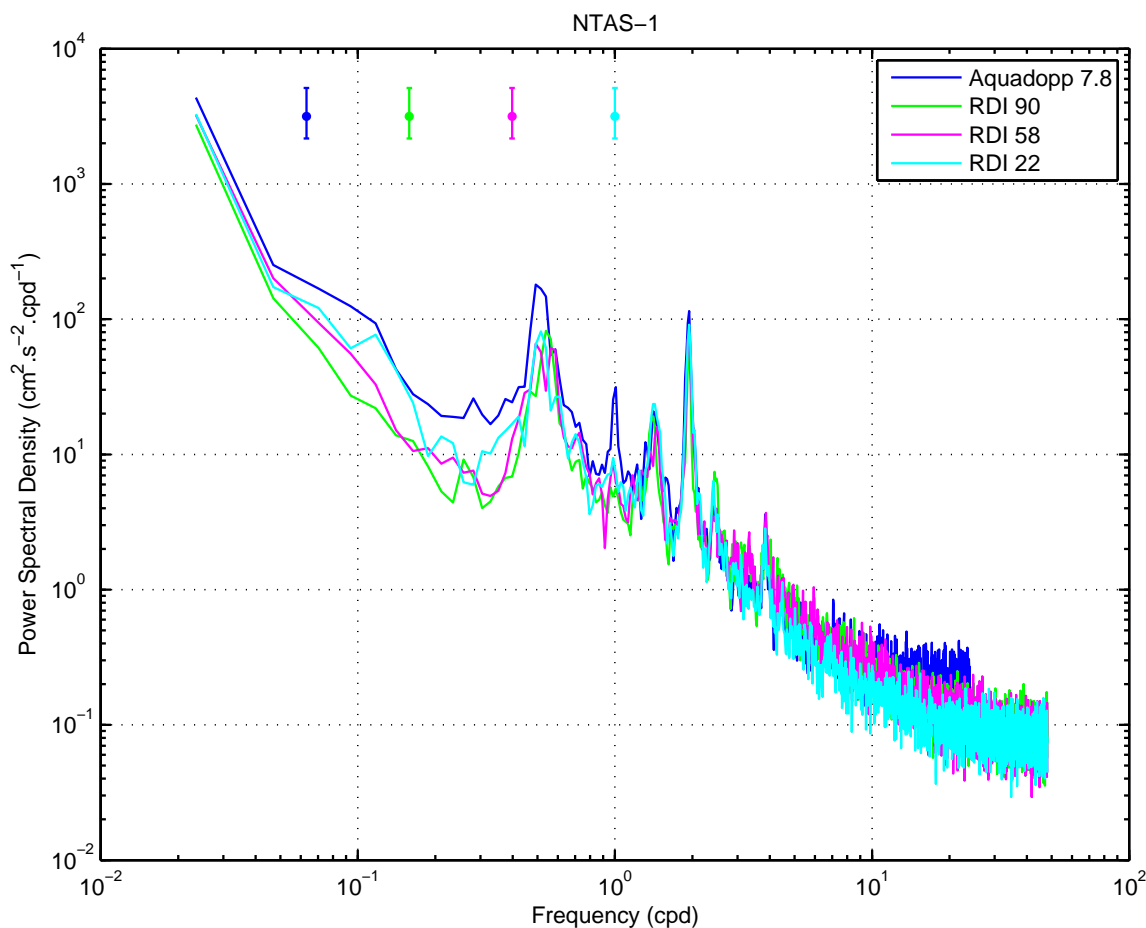


Figure 55: Spectra for the NTAS-1 current meters: Aquadopp and a selection of the RDI spectra (deepest bin, middle bin, and shallowest bin).

Figure 58.

6.1.3 Comparison of Current Meters on NTAS-3

Vertical profiles of velocity from the NTAS-3 current meters are shown in Figure 59. Data from the Aquadopp at 6 m depth indicated that the sensor failed and are omitted.

Progressive vectors of the velocity data on NTAS-3 are shown in Figure 60.

Spectra for the Aquadopp and a selection of the spectra from the RDI Workhorse depth bins are shown in Figure 61.

6.1.4 Comparison of Current Meters on NTAS-4

Vertical profiles of velocity from the NTAS-4 current meters are shown in Figure 62. Progressive vectors of all velocity data on NTAS-4 are shown in Figure 63. The spectrum for the Aquadopp and a selection of the spectra from the RDI WorkHorse depth bins appear in Figure 64.

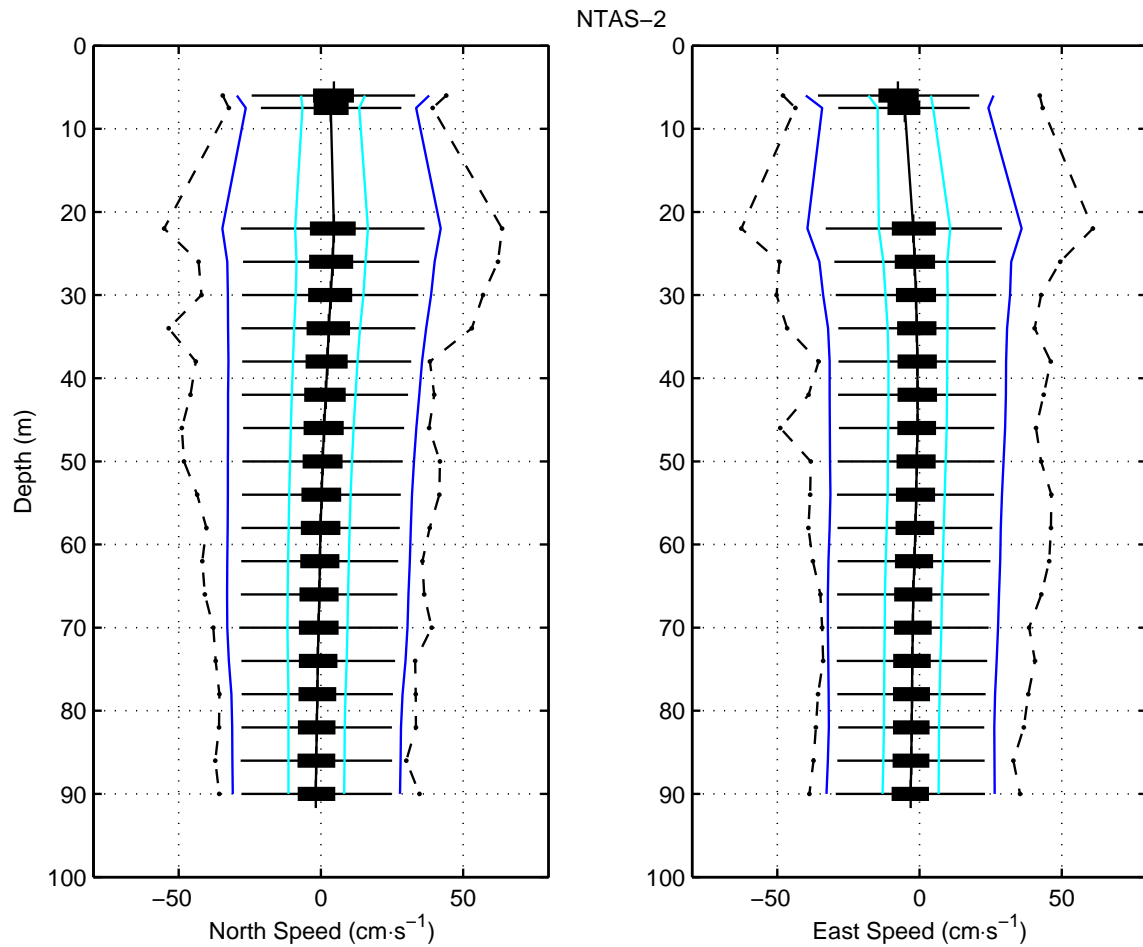


Figure 56: Vertical profile of all velocity data on NTAS-2. The data are shown as horizontal box-and-whisker plots. A + and the solid line identifies the median value; a thick line denotes the interquartile range; a thin line extends between the outlier limits at each depth; and the dashed line between dots indicates the maximum and minimum values. Cyan and blue lines indicate one and three standard deviations from the mean respectively. (a) Northerly current speeds. (b) Easterly current speeds.

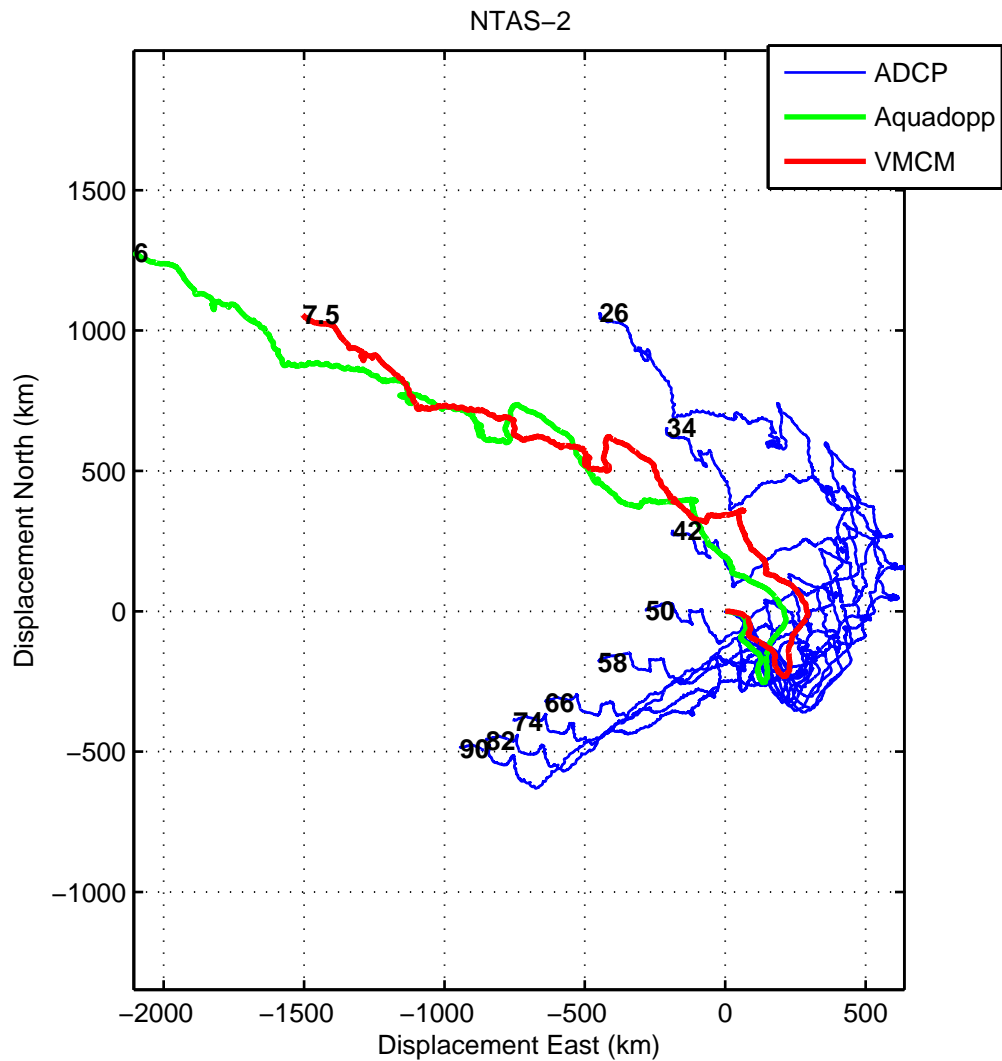


Figure 57: Progressive vectors of all velocity data on NTAS-2. The RDI data are plotted in blue, and the VMCM and Aquadopp are plotted in a thicker line. The final point of each series is labelled with the nominal depth of the sensor or bin.

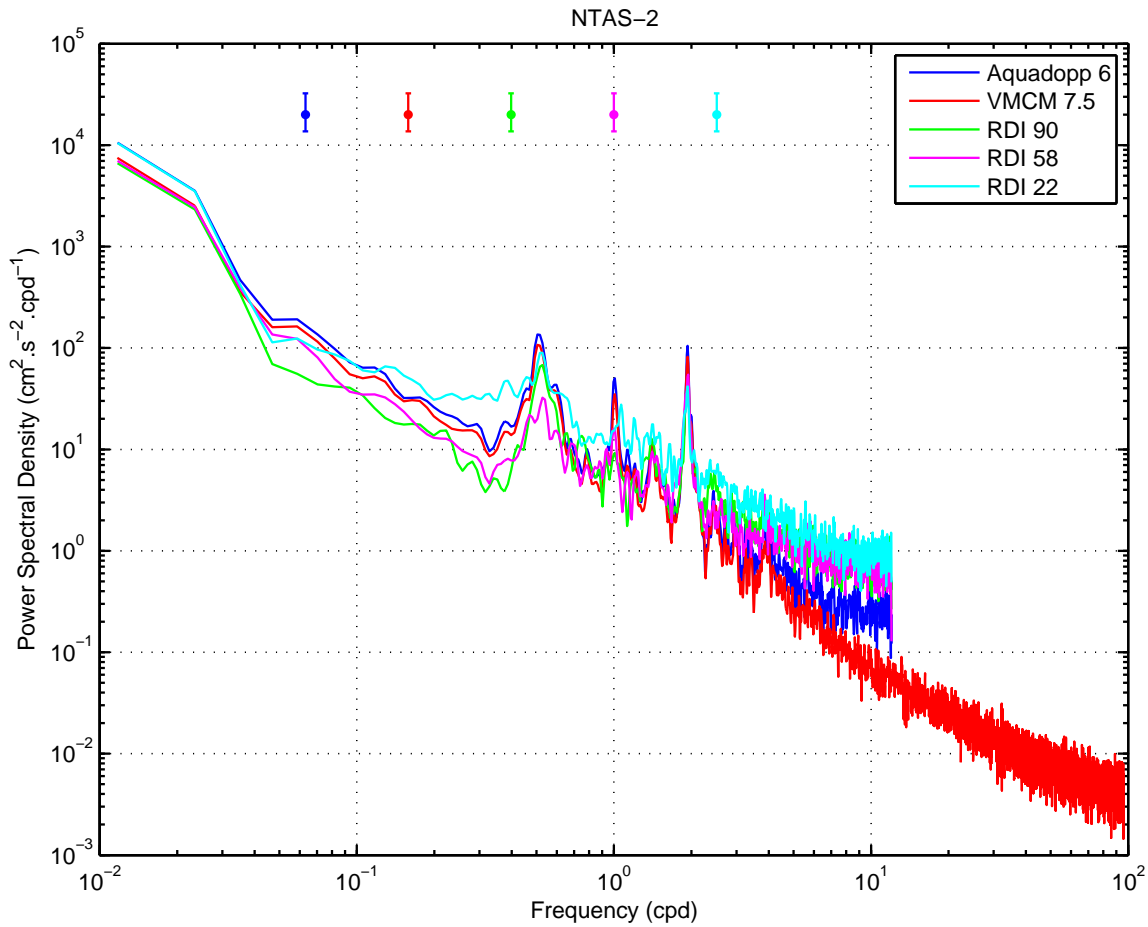


Figure 58: Spectra for the NTAS-2 current meters: VMCM, Aquadopp and a selection of the RDI spectra (deepest bin, middle bin, and shallowest bin).

6.1.5 Comparison of Current Meters on NTAS-5

Vertical profiles of velocity from the NTAS-5 current meters are shown in Figure 65. Progressive vectors of all velocity data on NTAS-5 are shown in Figure 66. The spectrum for the Aquadopp and a selection of the spectra from the RDI WorkHorse depth bins appear in Figure 67.

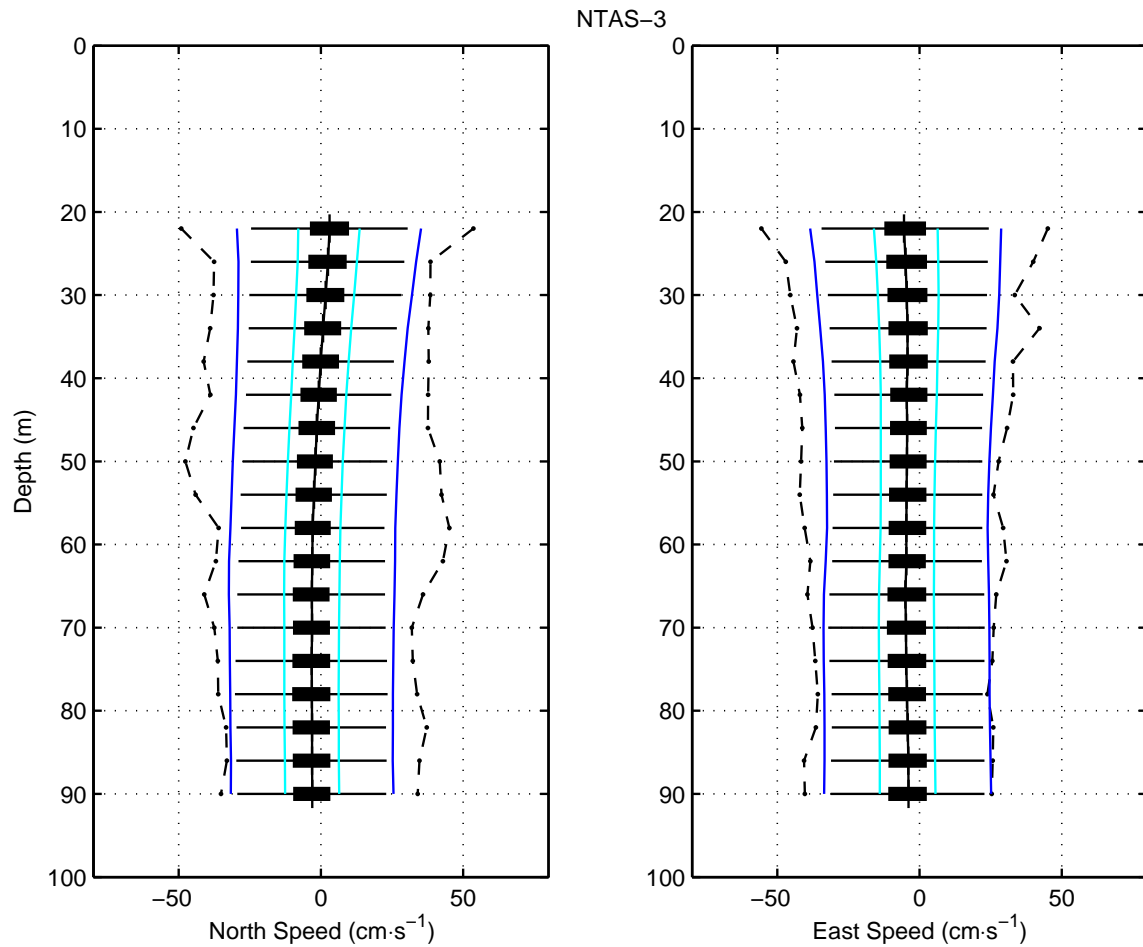


Figure 59: Vertical profile of RDI velocity data on NTAS-3. Aquadopp data were considered bad and are omitted (see Section 5.4.1). The data are shown as horizontal box-and-whisker plots. A + and the solid line identifies the median value; a thick line denotes the interquartile range; a thin line extends between the outlier limits at each depth; and the dashed line between dots indicates the maximum and minimum values. Cyan and blue lines indicate one and three standard deviations from the mean respectively. (a) Northerly current speeds. (b) Easterly current speeds.

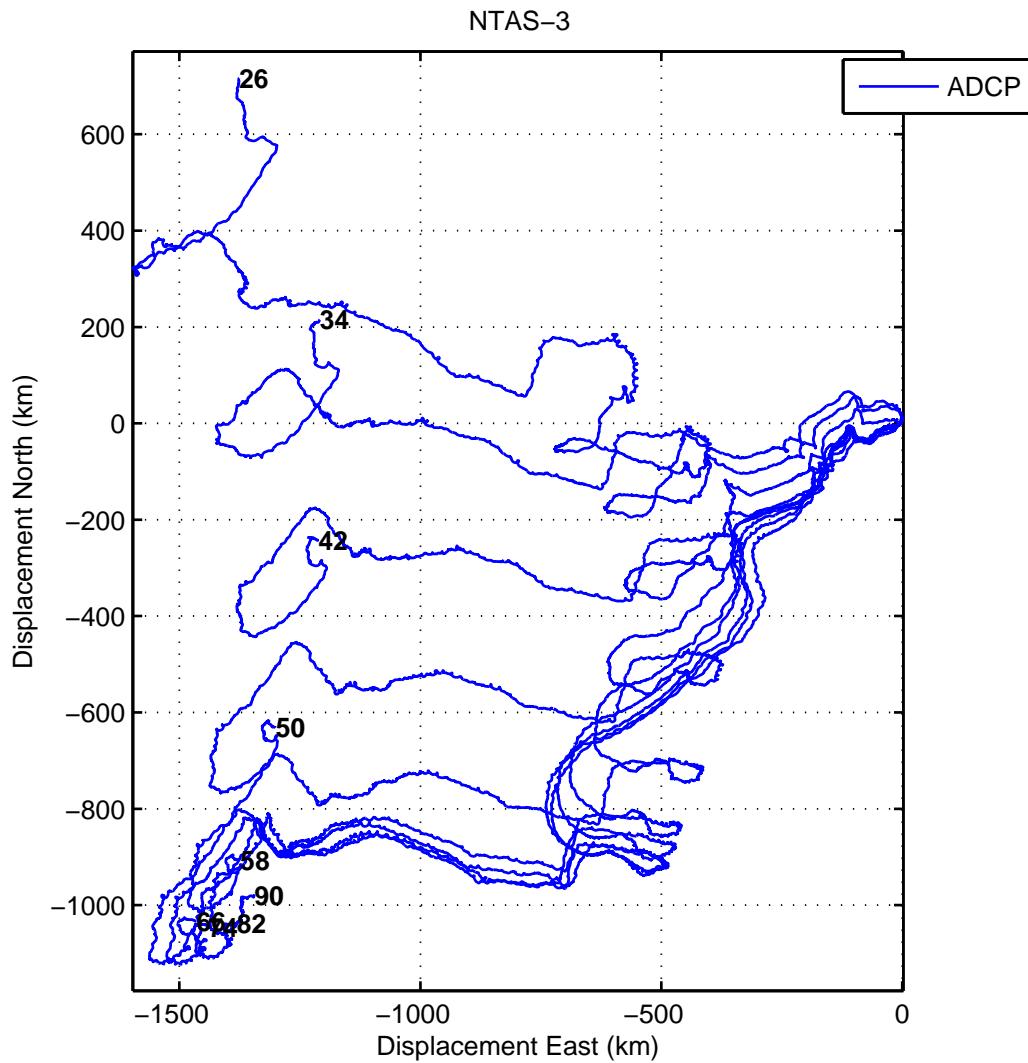


Figure 60: Progressive vectors of all velocity data on NTAS-3. The RDI bin data are plotted. The final point of each series is labelled with the nominal depth of the sensor or bin.

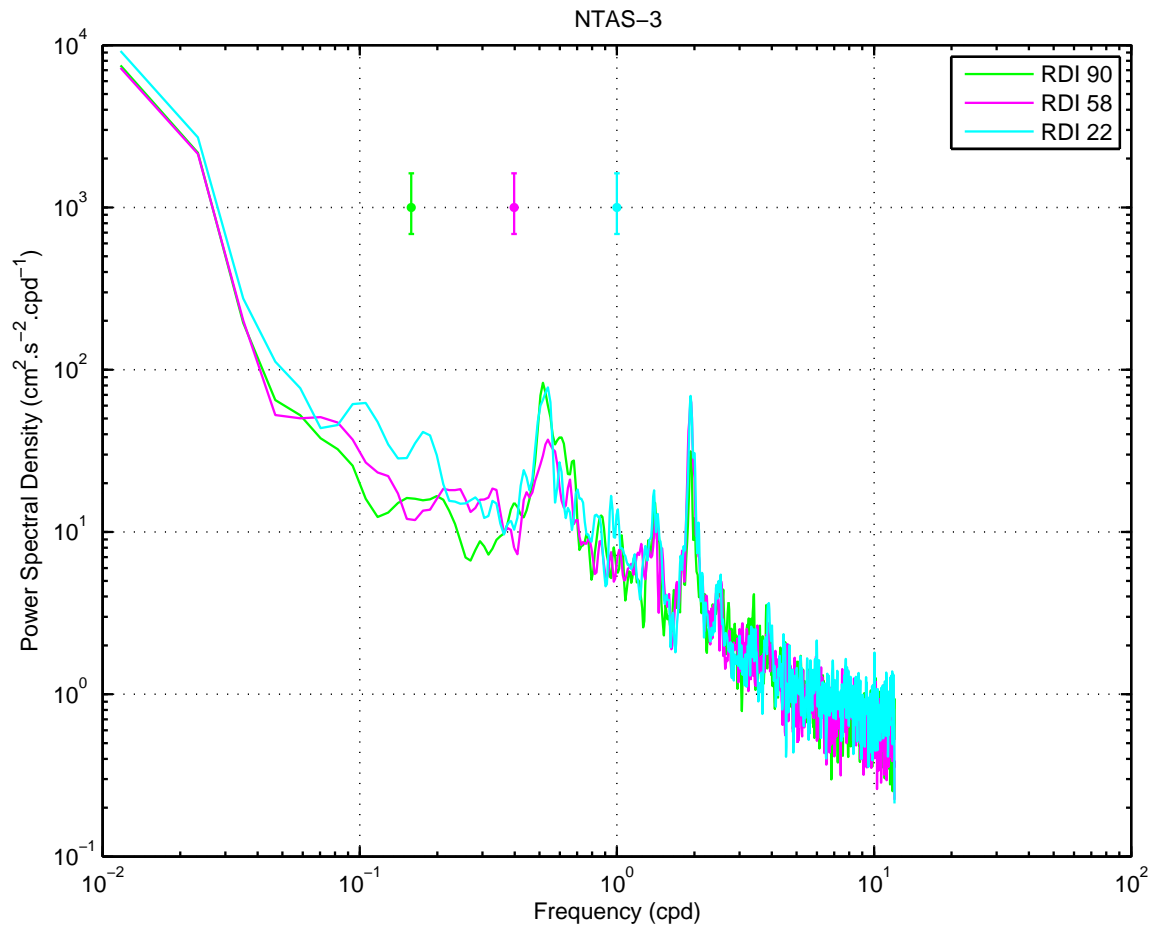


Figure 61: Spectra for the NTAS-3 velocities from the RDI WorkHorse ADCP. Aquadopp data (6 m) were bad and are omitted from the figure.

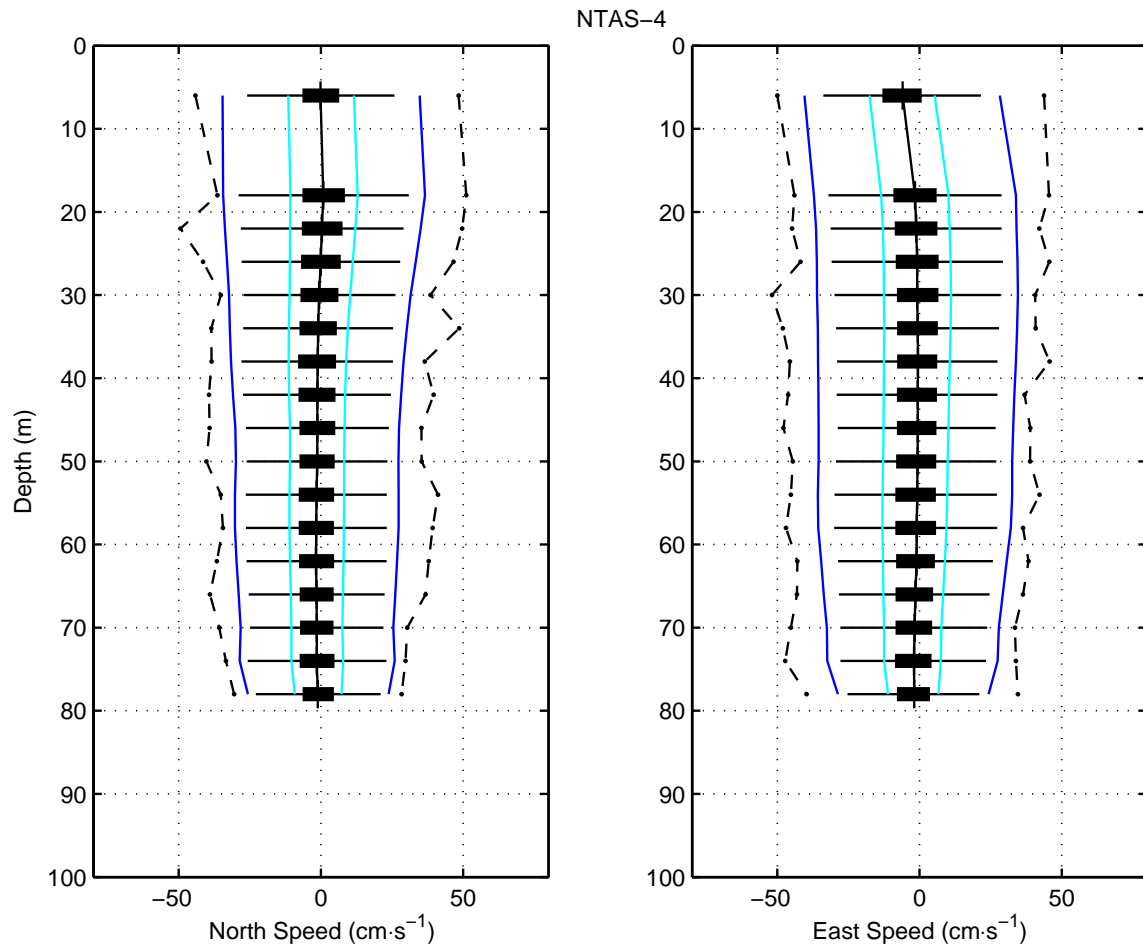


Figure 62: Vertical profile of all velocity data on NTAS-4. The data are shown as horizontal box-and-whisker plots. A + and the solid line identifies the median value; a thick line denotes the interquartile range; a thin line extends between the outlier limits at each depth; and the dashed line between dots indicates the maximum and minimum values. Cyan and blue lines indicate one and three standard deviations from the mean respectively. (a) Northerly current speeds. (b) Easterly current speeds.

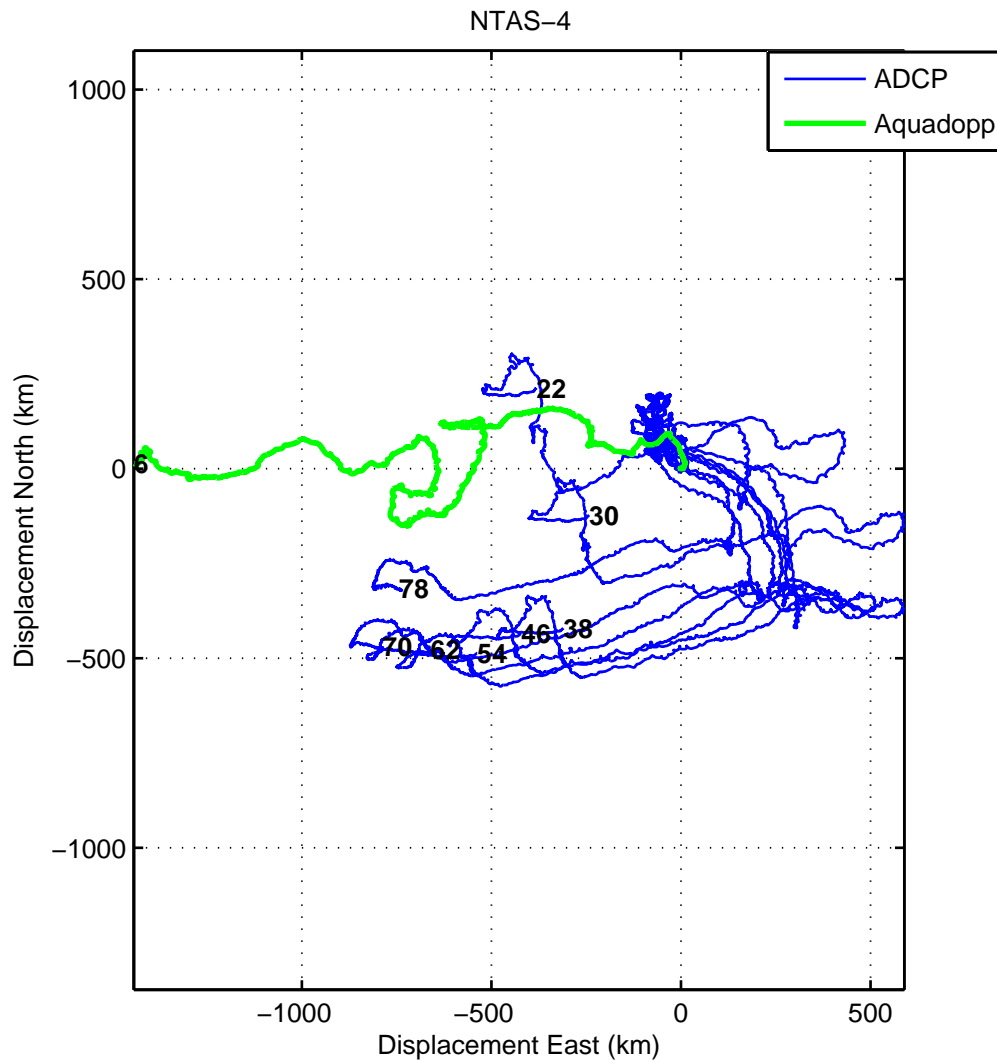


Figure 63: Progressive vectors of all velocity data on NTAS-4. The RDI data are plotted in blue, and the VMCM and Aquadopp are plotted in a thicker line. The final point of each series is labelled with the nominal depth of the sensor or bin.

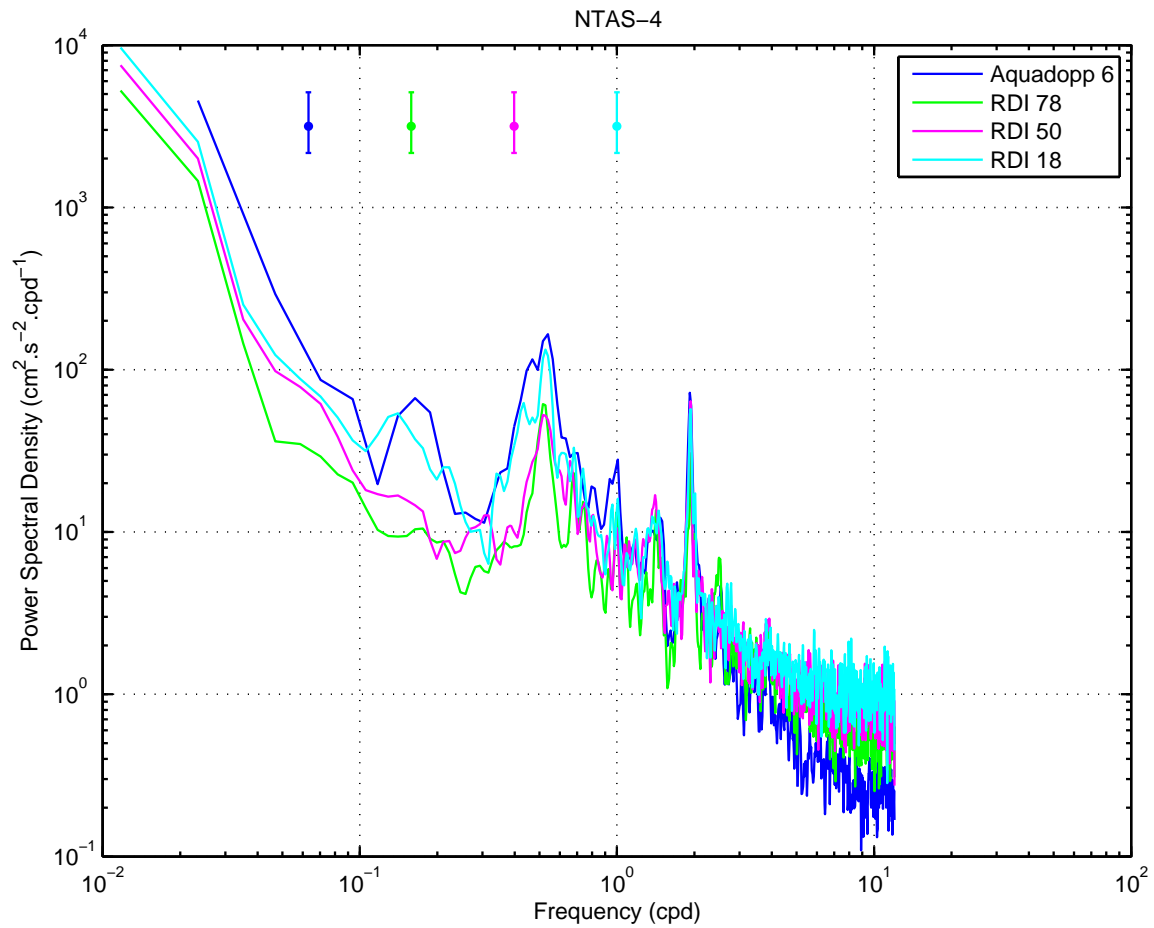


Figure 64: Spectra for the NTAS-4 velocities from the Aquadopp and RDI Workhorse current meters. The legend indicates the instrument and the nominal depth of the sensor.

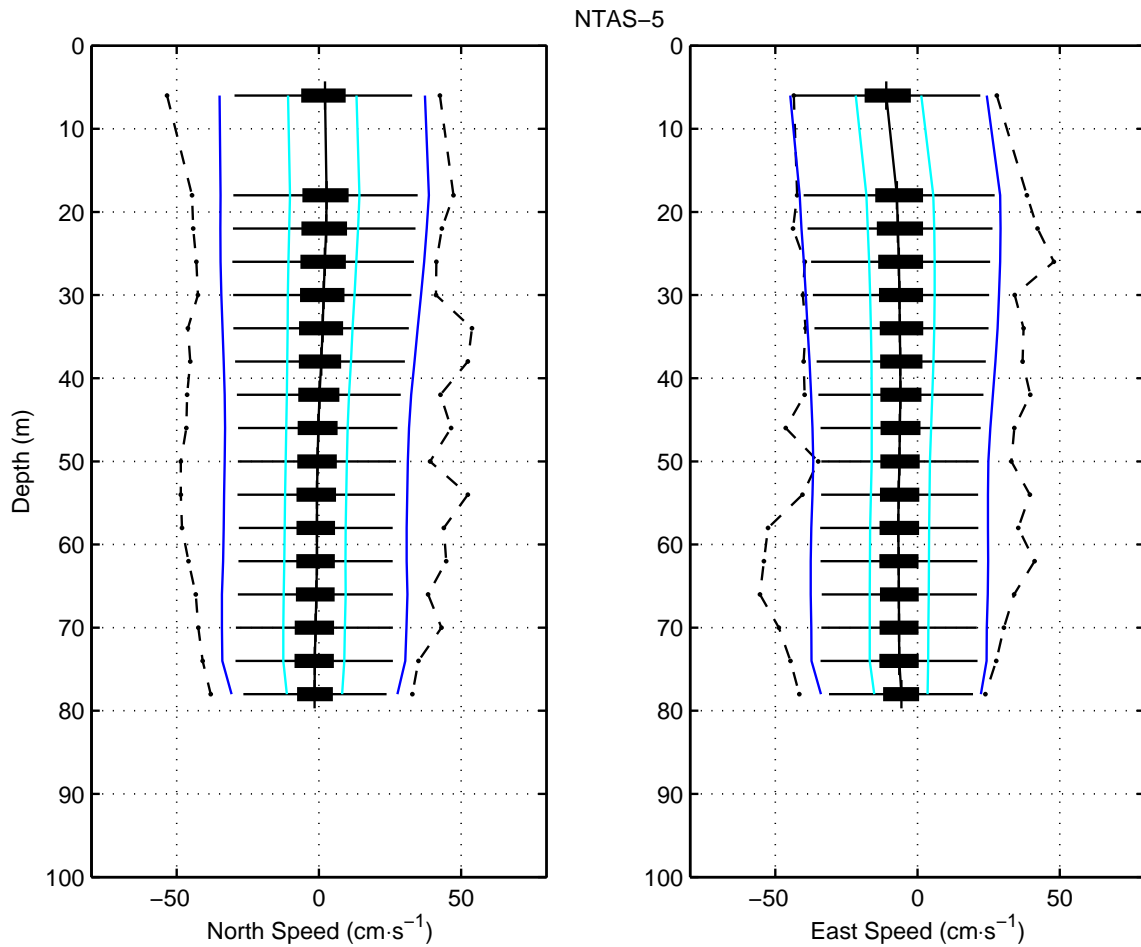


Figure 65: Vertical profile of all velocity data on NTAS-5. The data are shown as horizontal box-and-whisker plots. A + and the solid line identifies the median value; a thick line denotes the interquartile range; a thin line extends between the outlier limits at each depth; and the dashed line between dots indicates the maximum and minimum values. Cyan and blue lines indicate one and three standard deviations from the mean respectively. (a) Northerly current speeds. (b) Easterly current speeds.

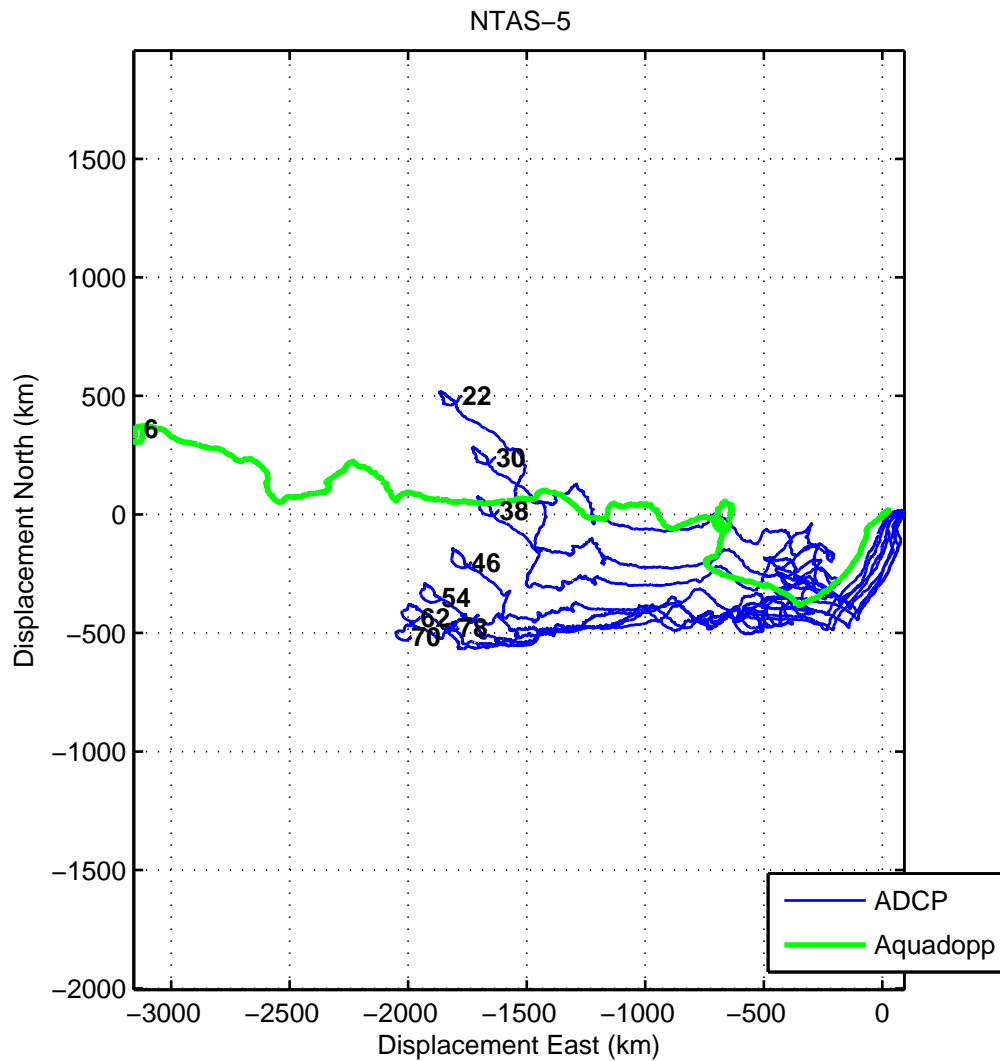


Figure 66: Progressive vectors of all velocity data on NTAS-5. The RDI bin data are plotted in blue, and the Aquadopp data are plotted in a thicker line. The final point of each series is labelled with the nominal depth of the sensor or bin.

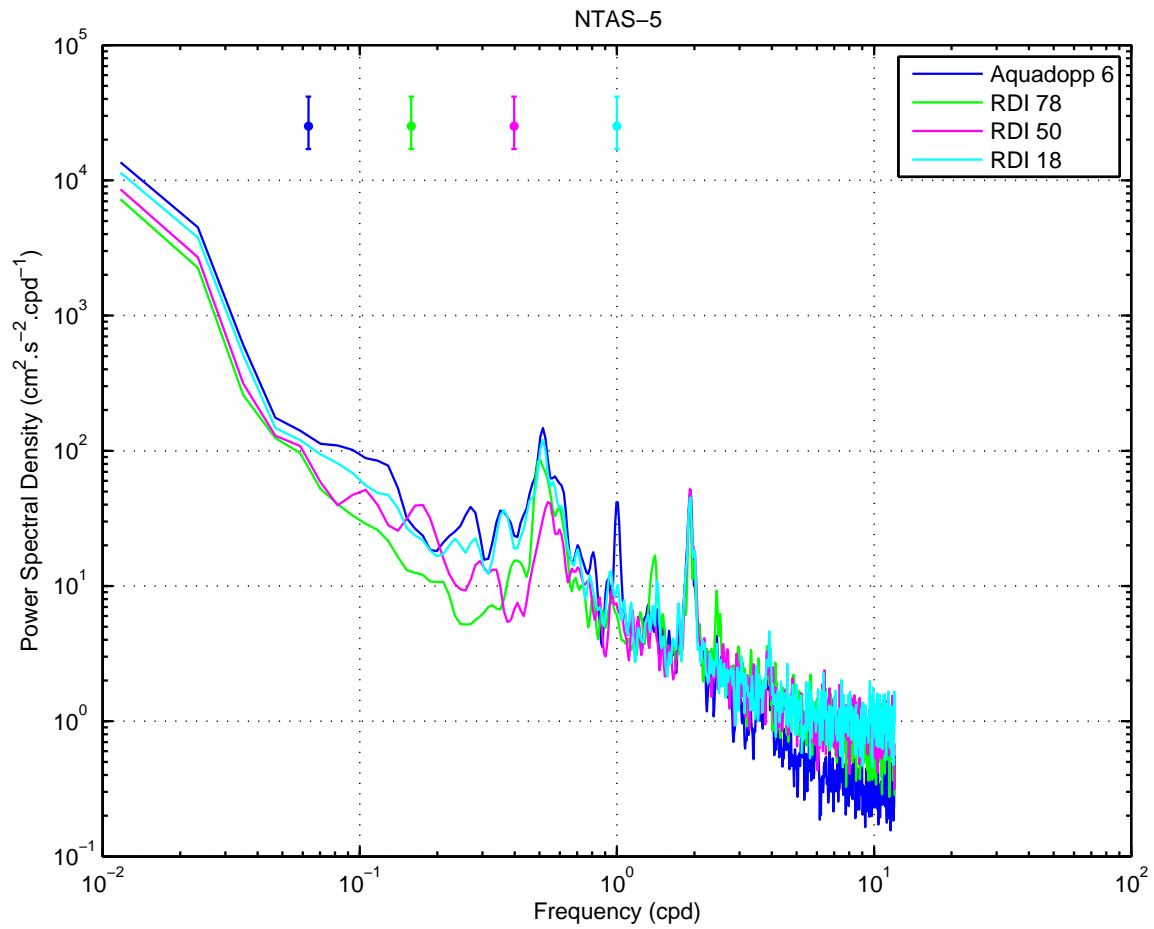


Figure 67: Spectra for the NTAS-5 current meters: the Aquadopp spectrum and a selection of the RDI spectra (deepest bin, middle bin, and shallowest bin) are shown. The legend indicates the instrument and the nominal depth of the sensor.

6.2 Inter-Deployment Comparisons

The complete five year record from NTAS-1 to -5 was examined (Figs. 68 and 69). Of particular interest appear to be the passage of mesoscale vortices

- near the beginning of NTAS-1 deployment (2001);
- during the turnaround of NTAS-1 and -2 (2002); and
- near the beginning of the NTAS-5 record (2005).

Vertical location and variability (Fig. 70) were determined for the common depth bins of the available RDI ADCP data.

Spectra from the long time series were constructed to demonstrate lower frequency signals, unresolved in the one-year deployments (Figs. 71, 72 and 73). The rotary spectrum of the shallowest common RDI ADCP depth bin is shown in Figure 74.

Due to gaps in the near-surface and maximum depth time series (see Fig. 52), progressive vector figures could not be created. Instead only a subset of the RDI ADCP bins (depths 22, 46, and 78 m) were used (Fig. 75).

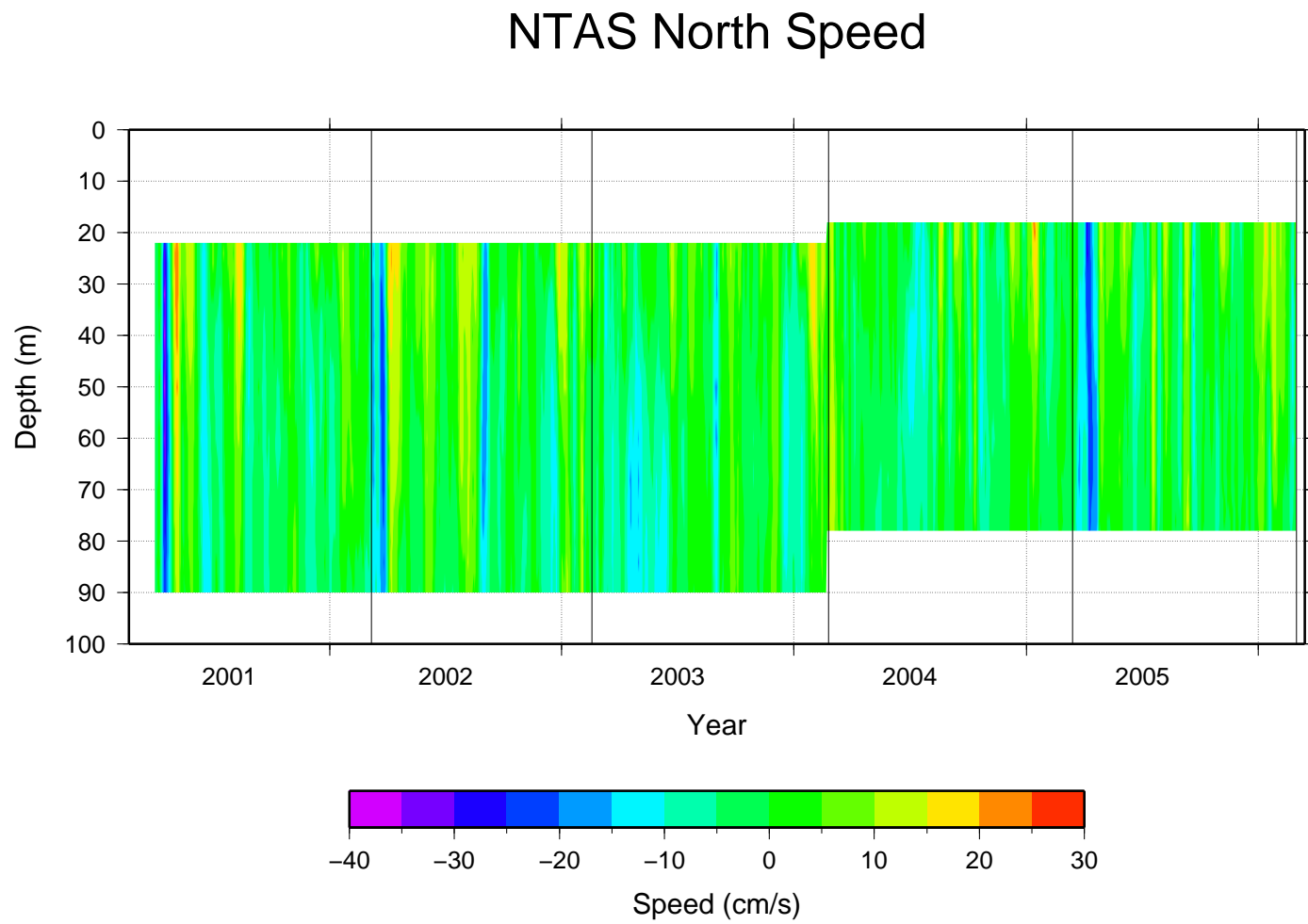


Figure 68: Northward current speeds from the RDI ADCPs on NTAS-1 to -5. Vertical lines indicate deployment turnaround times.

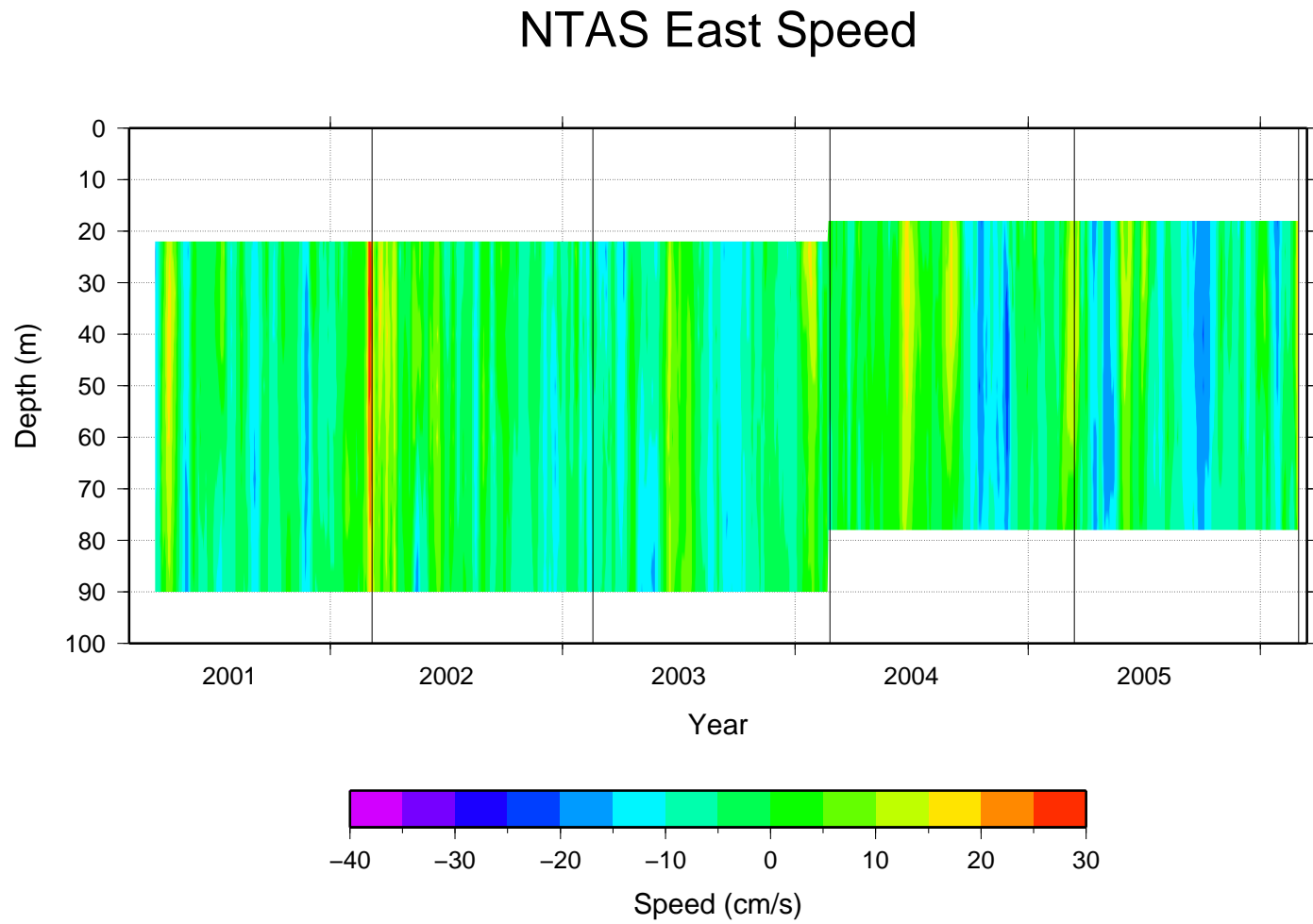


Figure 69: Eastward current speeds from the RDI ADCPs on NTAS-1 to -5. Vertical lines indicate deployment turnaround times.

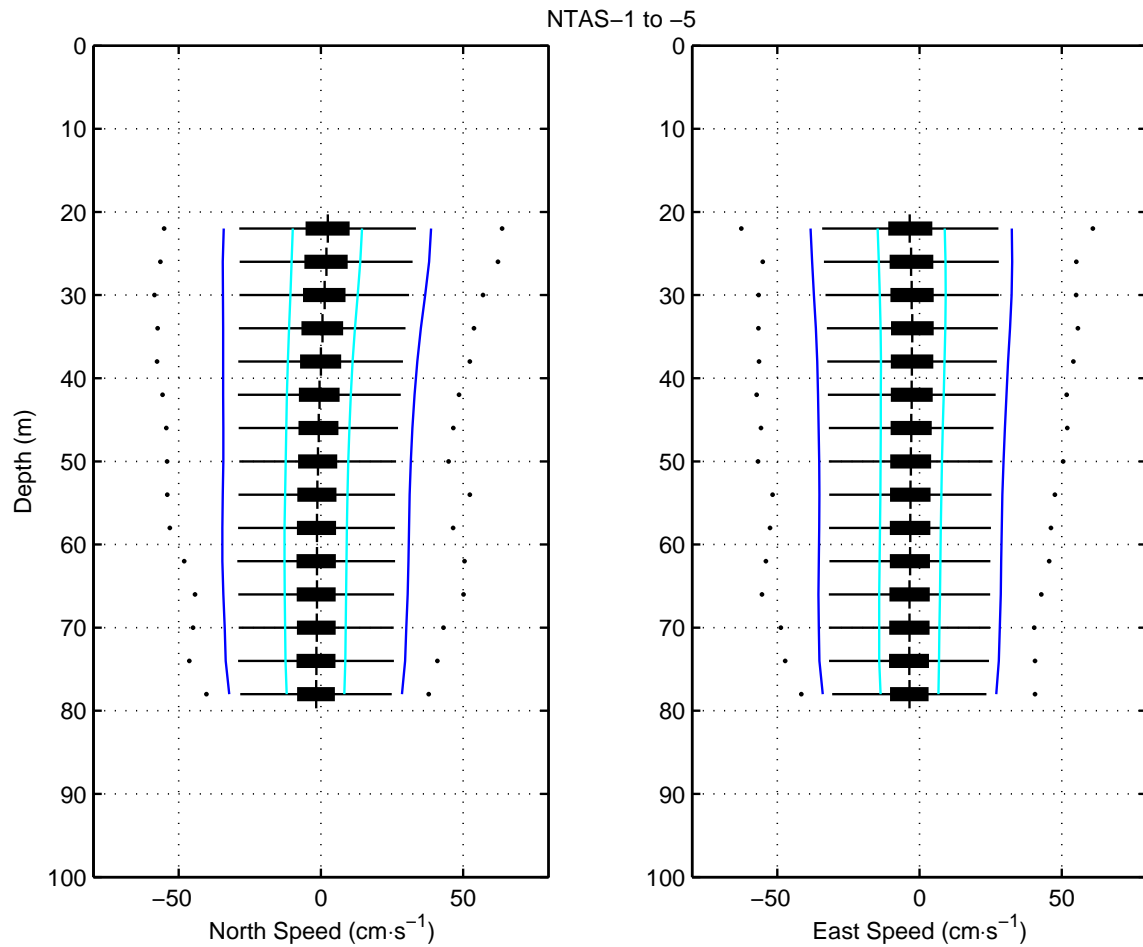


Figure 70: Vertical profile of all velocity data on NTAS-1 to -5 deployments. The data are shown as horizontal box-and-whisker plots. A + and the solid line identifies the median value; a thick line (box) denotes the interquartile range; a thin line (whiskers) extends between the outlier limits at each depth; and the dashed line between dots indicates the extreme (maximum and minimum) values. Cyan and blue lines indicate one and three standard deviations from the mean respectively. (a) Northerly current speeds. (b) Easterly current speeds.

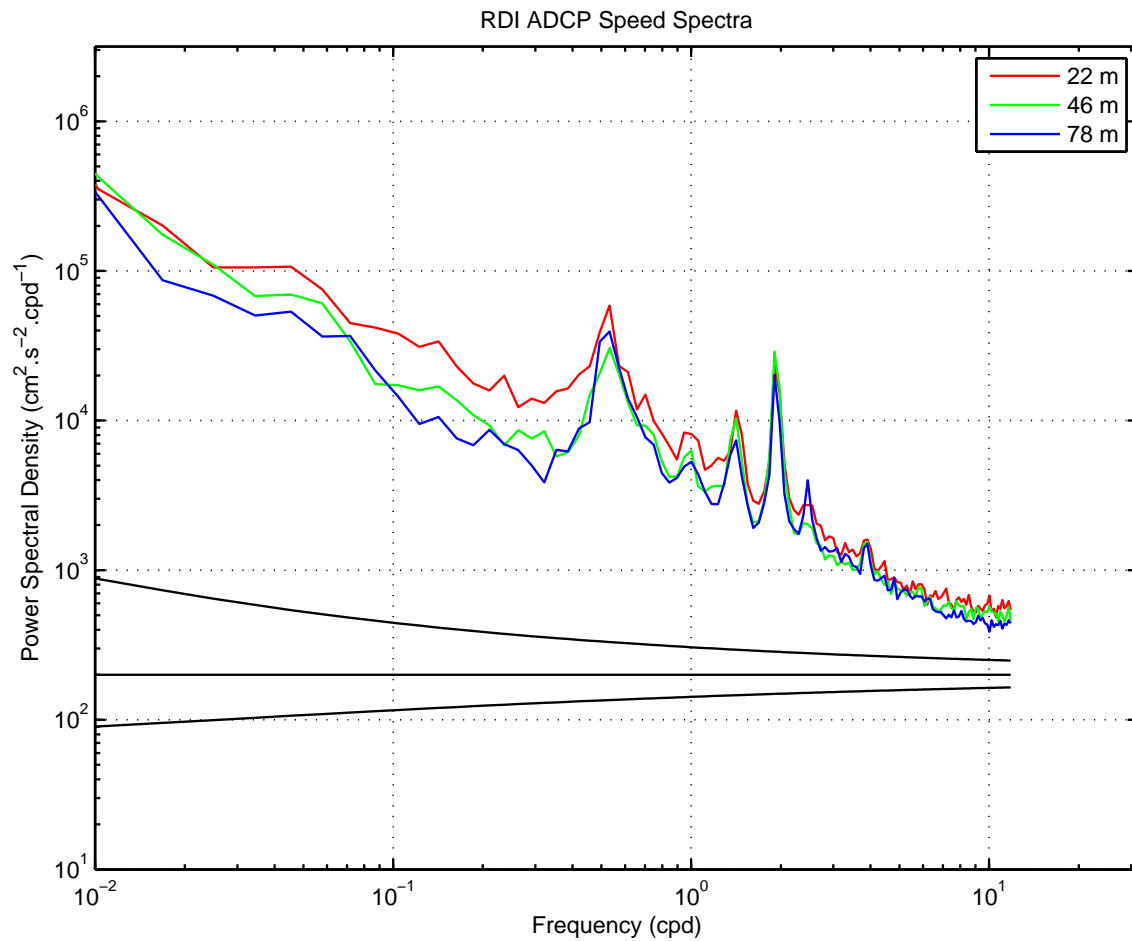


Figure 71: Current magnitude spectra on NTAS-1 to -5. Spectra are shown from the shallowest, mid-depth, and deepest common bins of the RDI ADCP.

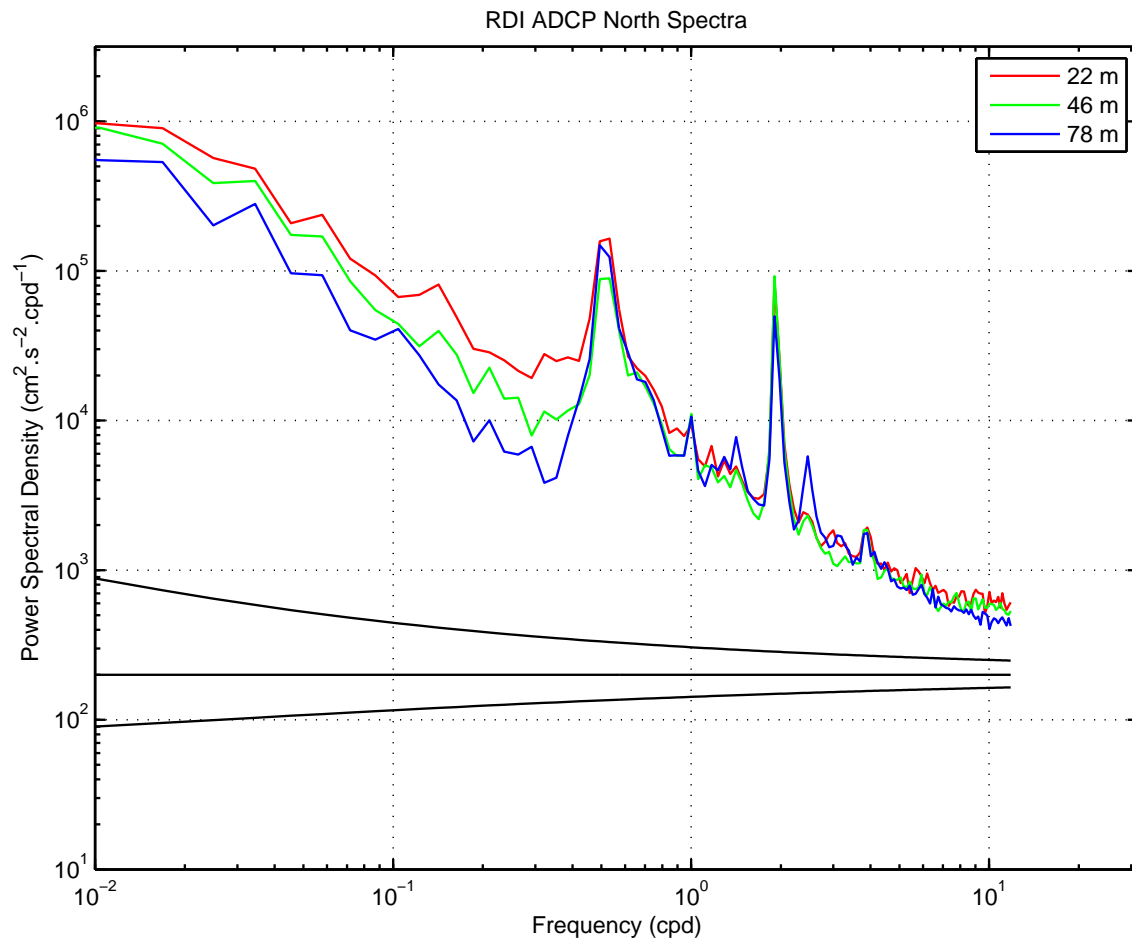


Figure 72: Northward current speed spectra on NTAS-1 to -5. Spectra are shown from the shallowest, mid-depth, and deepest common bins of the RDI ADCP.

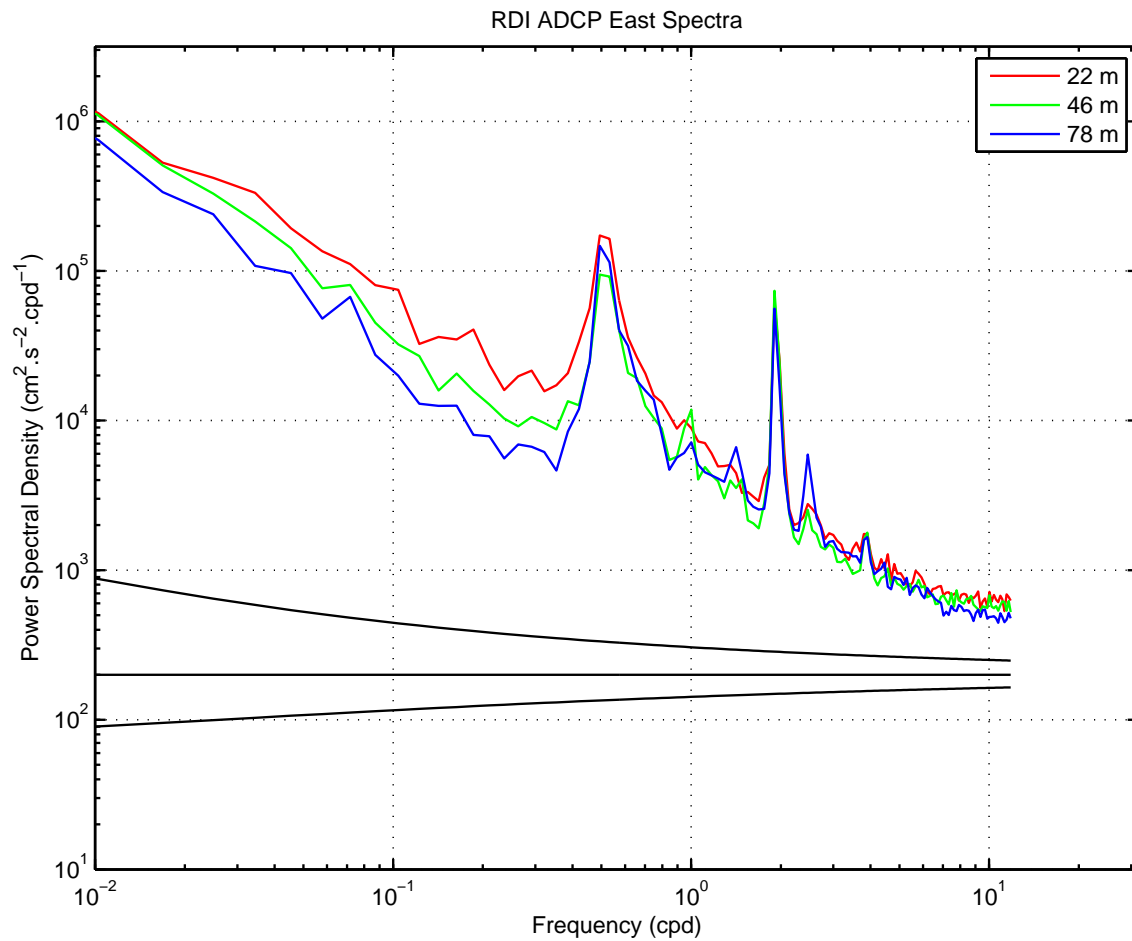


Figure 73: Eastward current speed spectra on NTAS-1 to -5. Spectra are shown from the shallowest, mid-depth, and deepest common bins of the RDI ADCP.

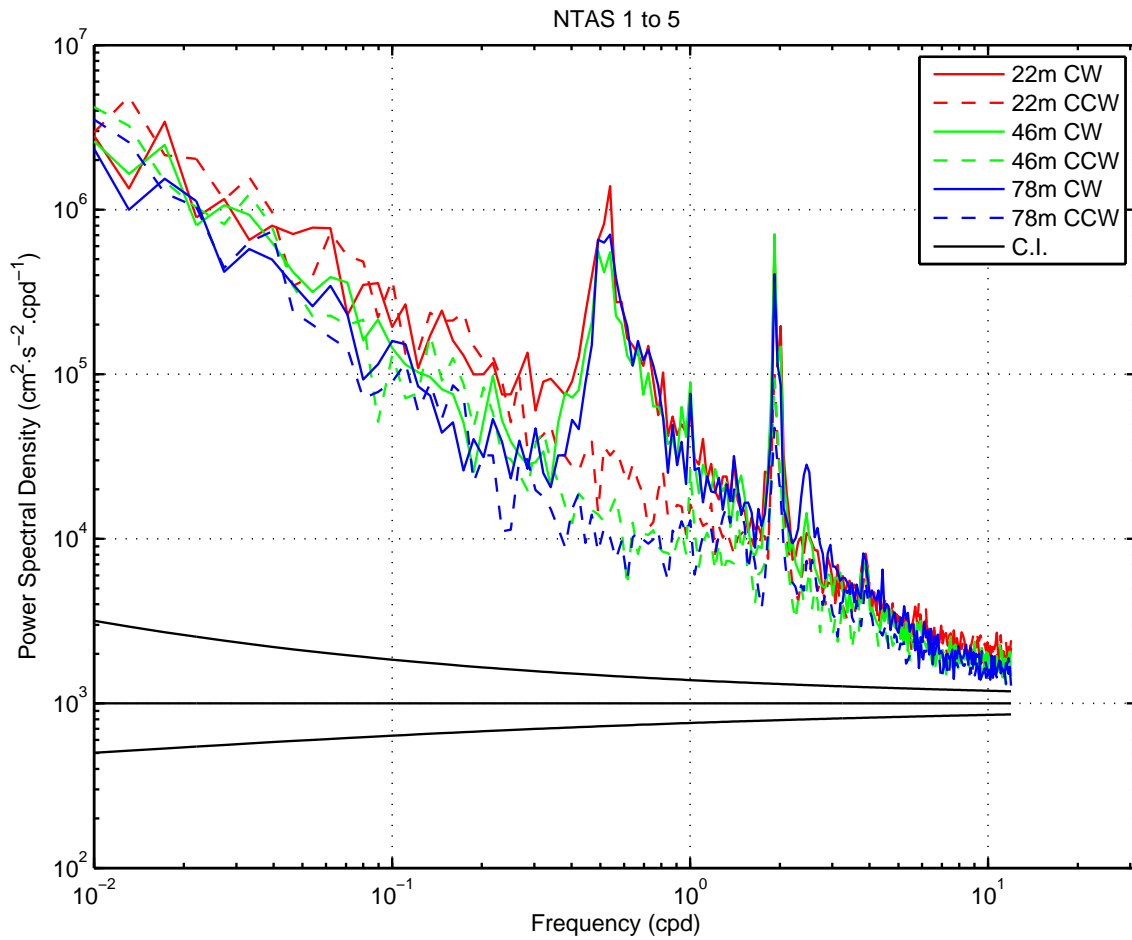


Figure 74: Showing the rotary spectra of velocities determined from representative RDI ADCP depth bins for the long time series of all NTAS-1 to -5 deployments. Spectra for the common near-surface (22 m), middle (46 m), and deepest (78 m) bins are shown. Clockwise (CW) spectra are shown with solid lines; counter-clockwise (CCW) spectra are shown with dashed lines. The frequency dependent confidence interval (C.I.) is shown below the spectra.

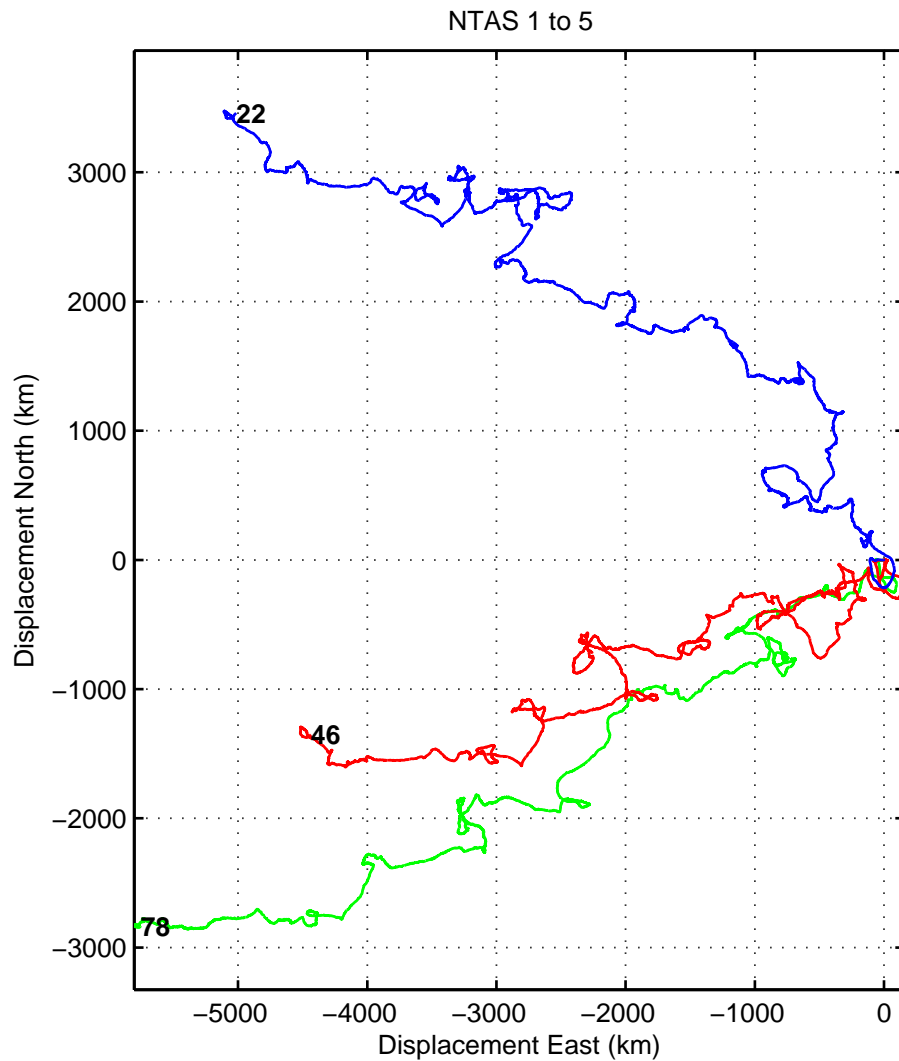


Figure 75: Progressive vectors of three depth bins (near-surface—blue, middle—red, and deepest—green) from the RDI bin data on all NTAS 1 to 5 deployments. The final point of each series is labelled with the nominal depth of the sensor or bin.

Acknowledgements

Generic Mapping Tools [Wessel and Smith, 1998] (version 4.5.5) was used in preparation of the report.

References

- Amante, C., and B. W. Eakins (2008), ETOPO1 1 Arc-Minute Global Relief Model: Procedures, Data Sources and Analysis, *Tech. rep.*, National Geophysical Data Center, NESDIS, NOAA, U.S. Department of Commerce, Boulder, CO, URL: <http://www.ngdc.noaa.gov/mgg/global/global.html>.
- Berens, P. (2009), CircStat: A MATLAB Toolbox for Circular Statistics, *J. Stat. Software*, 31(10), 1–21.
- Galbraith, N., and G. Allsup (2005), Buoy Telemetry, *Technical note*, Woods Hole Oceanographic Institution, Woods Hole, MA.
- Hosom, D. S., R. A. Weller, R. E. Payne, and K. E. Prada (1995), The IMET (Improved Meteorology) ship and buoy systems, *J. Atmos. Oceanic Tech.*, 12(3), 527–540, doi:10.1175/1520-0426(1995)012<0527:TIMSAB>2.0.CO;2.
- Plueddemann, A. J., N. R. Galbraith, W. M. Ostrom, G. H. Tupper, R. E. Handy, and J. M. Dunn (2001), The Northwest Tropical Atlantic Station (NTAS): NTAS-1 Mooring Deployment Cruise Report, *Tech. Rep. WHOI-2001-07*, Woods Hole Oceanographic Institution, Woods Hole, MA.
- Plueddemann, A. J., W. M. Ostrom, N. R. Galbraith, P. R. Bouchard, G. H. Tupper, J. M. Dunn, and M. A. Walsh (2002), The Northwest Tropical Atlantic Station (NTAS): NTAS-2 Mooring Turnaround Cruise Report, *Tech. Rep. WHOI-2002-07*, Woods Hole Oceanographic Institution, Woods Hole, MA.
- Plueddemann, A. J., W. M. Ostrom, N. R. Galbraith, J. C. Smith, J. R. Ryder, J. J. Holley, and M. A. Walsh (2003), The Northwest Tropical Atlantic Station (NTAS): NTAS-3 Mooring Turnaround Cruise Report, *Tech. Rep. WHOI-2003-04*, Woods Hole Oceanographic Institution, Woods Hole, MA.
- Plueddemann, A. J., W. M. Ostrom, N. R. Galbraith, P. R. Bouchard, B. P. Hogue, B. R. Wasnewski, and M. A. Walsh (2006), The Northwest Tropical Atlantic Station (NTAS): NTAS-4 Mooring Turnaround Cruise Report, *Tech. Rep. WHOI-2006-09*, Woods Hole Oceanographic Institution, Woods Hole, MA.
- Plueddemann, A. J., et al. (2012), The Northwest Tropical Atlantic Station (NTAS): NTAS-5 Mooring Turnaround Cruise Report, manuscript in prep.
- The Mathworks (2008), *Signal Processing Toolbox User's Guide (Matlab Release 2008b)*, 1040 pp., The Mathworks, Natick, MA.

Wessel, P., and W. H. F. Smith (1998), New, improved version of Generic Mapping Tools released, *Eos Trans. AGU*, 79(47), 579.

Wilcoxon, F. (1945), Individual comparisons by ranking methods, *Biometrics Bulletin*, 1(6), 80–83.

Appendices

A NTAS Velocity Statistics

Table A1: Gross statistical description of the various NTAS velocity time series. The first column provides the deployment number, the instrument depth and the instrument type. The second column provides reference for the following columns which show the mean, standard deviation and range (minimum and maximum values) of the northerly and easterly current components (North and East, in $\text{cm}\cdot\text{s}^{-1}$), the magnitude (Spd, in $\text{cm}\cdot\text{s}^{-1}$) and direction (Dir, in degrees clockwise from North). The means and standard deviations of directions were calculated using the Circular Statistics Toolbox for Matlab [Berens, 2009], assuming a von Mises distribution for the directional data.

| | | Mean | Std Deviation | Range | |
|--------------------------------|--------|-------|---------------|-------|-------|
| NTAS-1 (7.8 m) Aquadopp | North: | 3.6 | 12.9 | -55.3 | 55.3 |
| | East: | -8.1 | 12.2 | -65.0 | 51.5 |
| | Spd: | 17.2 | 9.8 | 0.1 | 65.3 |
| | Dir: | 291.4 | 59.7 | 0.0 | 360.0 |
| NTAS-1 (22 m) NarrowBand | North: | 2.4 | 12.5 | -44.8 | 49.0 |
| | East: | -2.5 | 11.6 | -55.3 | 54.1 |
| | Spd: | 15.3 | 8.3 | 0.0 | 56.0 |
| | Dir: | 306.2 | 71.9 | 0.0 | 360.0 |
| NTAS-1 (26 m) NarrowBand | North: | 1.8 | 12.7 | -56.5 | 52.3 |
| | East: | -2.2 | 11.9 | -55.1 | 55.1 |
| | Spd: | 15.4 | 8.8 | 0.0 | 56.7 |
| | Dir: | 304.8 | 73.7 | 0.0 | 360.0 |
| NTAS-1 (30 m) NarrowBand | North: | 1.0 | 12.5 | -58.5 | 53.0 |
| | East: | -2.0 | 11.8 | -56.6 | 55.1 |
| | Spd: | 15.1 | 8.6 | 0.2 | 58.8 |
| | Dir: | 295.1 | 74.9 | 0.0 | 360.0 |
| NTAS-1 (34 m) NarrowBand | North: | 0.2 | 12.3 | -57.4 | 53.0 |
| | East: | -2.0 | 11.6 | -56.7 | 55.7 |
| | Spd: | 14.8 | 8.4 | 0.0 | 57.4 |
| | Dir: | 277.8 | 75.3 | 0.0 | 360.0 |
| NTAS-1 (38 m) NarrowBand | North: | -0.5 | 12.1 | -57.6 | 50.8 |
| | East: | -2.2 | 11.4 | -56.4 | 54.1 |
| | Spd: | 14.6 | 8.3 | 0.0 | 57.8 |
| | Dir: | 262.6 | 74.8 | 0.0 | 360.0 |
| NTAS-1 (42 m) NarrowBand | North: | -1.0 | 12.0 | -55.7 | 48.6 |
| | East: | -2.4 | 11.3 | -57.3 | 51.7 |
| | Spd: | 14.5 | 8.2 | 0.0 | 57.3 |
| | Dir: | 254.9 | 73.9 | 0.0 | 360.0 |
| NTAS-1 (46 m) NarrowBand | North: | -1.4 | 11.9 | -54.4 | 46.6 |
| | East: | -2.6 | 11.2 | -55.8 | 51.9 |
| | Spd: | 14.4 | 8.2 | 0.0 | 55.8 |
| | Dir: | 251.7 | 73.1 | 0.0 | 360.0 |

continued...

Table A1: (continued)

| | | Mean | Std Deviation | Range | |
|--------------------------------|--------|-------|---------------|-------|-------|
| NTAS-1 (50 m) NarrowBand | North: | -1.7 | 11.7 | -54.1 | 44.9 |
| | East: | -2.7 | 11.1 | -56.8 | 50.5 |
| | Spd: | 14.3 | 8.1 | 0.0 | 57.3 |
| | Dir: | 249.8 | 72.6 | 0.0 | 360.0 |
| NTAS-1 (54 m) NarrowBand | North: | -1.9 | 11.7 | -54.0 | 44.8 |
| | East: | -2.8 | 10.9 | -51.7 | 47.6 |
| | Spd: | 14.2 | 8.1 | 0.0 | 55.1 |
| | Dir: | 248.2 | 72.1 | 0.0 | 360.0 |
| NTAS-1 (58 m) NarrowBand | North: | -2.1 | 11.7 | -53.2 | 46.5 |
| | East: | -2.9 | 10.9 | -47.2 | 45.9 |
| | Spd: | 14.2 | 8.1 | 0.0 | 54.6 |
| | Dir: | 247.2 | 72.1 | 0.0 | 360.0 |
| NTAS-1 (62 m) NarrowBand | North: | -2.1 | 11.6 | -48.1 | 50.5 |
| | East: | -3.1 | 11.0 | -47.1 | 43.8 |
| | Spd: | 14.3 | 8.1 | 0.0 | 51.1 |
| | Dir: | 249.1 | 72.3 | 0.0 | 360.0 |
| NTAS-1 (66 m) NarrowBand | North: | -2.0 | 11.5 | -44.2 | 50.1 |
| | East: | -3.2 | 11.1 | -49.1 | 41.4 |
| | Spd: | 14.2 | 8.1 | 0.0 | 50.6 |
| | Dir: | 251.8 | 72.3 | 0.0 | 360.0 |
| NTAS-1 (70 m) NarrowBand | North: | -2.0 | 11.3 | -45.0 | 42.5 |
| | East: | -3.2 | 11.1 | -48.1 | 40.3 |
| | Spd: | 14.2 | 7.9 | 0.0 | 48.1 |
| | Dir: | 252.2 | 72.1 | 0.0 | 360.0 |
| NTAS-1 (74 m) NarrowBand | North: | -1.9 | 11.1 | -46.3 | 41.0 |
| | East: | -3.3 | 10.9 | -43.9 | 40.5 |
| | Spd: | 14.1 | 7.7 | 0.0 | 46.5 |
| | Dir: | 249.8 | 72.0 | 0.0 | 360.0 |
| NTAS-1 (78 m) NarrowBand | North: | -2.0 | 10.8 | -40.3 | 37.9 |
| | East: | -3.3 | 10.8 | -40.8 | 40.6 |
| | Spd: | 13.9 | 7.4 | 0.0 | 41.9 |
| | Dir: | 246.2 | 71.5 | 0.0 | 360.0 |
| NTAS-1 (82 m) NarrowBand | North: | -2.1 | 10.6 | -42.0 | 37.9 |
| | East: | -3.5 | 10.6 | -39.0 | 40.3 |
| | Spd: | 13.8 | 7.2 | 0.0 | 46.8 |
| | Dir: | 244.5 | 70.4 | 0.0 | 360.0 |
| NTAS-1 (86 m) NarrowBand | North: | -2.3 | 10.3 | -38.6 | 38.1 |
| | East: | -3.9 | 10.4 | -38.5 | 39.9 |
| | Spd: | 13.6 | 7.0 | 0.0 | 42.3 |
| | Dir: | 245.0 | 68.8 | 0.0 | 360.0 |
| NTAS-1 (90 m) NarrowBand | North: | -2.4 | 10.0 | -38.8 | 35.7 |
| | East: | -3.9 | 10.0 | -37.6 | 39.2 |
| | Spd: | 13.2 | 6.8 | 0.0 | 40.6 |
| | Dir: | 244.9 | 67.8 | 0.0 | 360.0 |

continued...

Table A1: (continued)

| | | Mean | Std Deviation | Range | |
|-------------------------------|--------|-------|---------------|-------|-------|
| NTAS-2 (6 m) Aquadopp | North: | 4.3 | 11.3 | -34.5 | 44.0 |
| | East: | -7.0 | 11.0 | -48.0 | 42.3 |
| | Spd: | 15.8 | 8.1 | 0.3 | 49.9 |
| | Dir: | 299.5 | 59.2 | 0.0 | 360.0 |
| NTAS-2 (7.5 m) VMCM | North: | 3.5 | 10.0 | -32.3 | 39.3 |
| | East: | -5.0 | 9.7 | -43.6 | 43.3 |
| | Spd: | 13.2 | 7.5 | 0.1 | 44.3 |
| | Dir: | 300.4 | 61.2 | 0.0 | 360.0 |
| NTAS-2 (22 m) Workhorse | North: | 3.8 | 12.8 | -55.1 | 63.7 |
| | East: | -1.8 | 12.6 | -62.7 | 60.9 |
| | Spd: | 16.0 | 9.1 | 0.0 | 69.6 |
| | Dir: | 332.4 | 70.9 | 0.0 | 359.9 |
| NTAS-2 (26 m) Workhorse | North: | 3.5 | 12.1 | -43.0 | 62.3 |
| | East: | -1.5 | 11.2 | -49.2 | 49.5 |
| | Spd: | 14.8 | 8.3 | 0.1 | 73.2 |
| | Dir: | 335.5 | 70.8 | 0.0 | 360.0 |
| NTAS-2 (30 m) Workhorse | North: | 3.0 | 11.9 | -42.0 | 57.0 |
| | East: | -1.0 | 10.9 | -50.3 | 42.8 |
| | Spd: | 14.5 | 7.9 | 0.1 | 65.7 |
| | Dir: | 337.9 | 72.3 | 0.0 | 360.0 |
| NTAS-2 (34 m) Workhorse | North: | 2.2 | 11.6 | -53.6 | 53.1 |
| | East: | -0.7 | 10.5 | -46.6 | 40.5 |
| | Spd: | 13.9 | 7.5 | 0.1 | 62.8 |
| | Dir: | 339.8 | 73.9 | 0.1 | 359.9 |
| NTAS-2 (38 m) Workhorse | North: | 1.5 | 11.3 | -44.0 | 38.3 |
| | East: | -0.6 | 10.3 | -35.5 | 46.1 |
| | Spd: | 13.6 | 7.3 | 0.1 | 46.3 |
| | Dir: | 339.1 | 74.9 | 0.0 | 360.0 |
| NTAS-2 (42 m) Workhorse | North: | 1.0 | 11.2 | -45.8 | 39.9 |
| | East: | -0.6 | 10.3 | -39.0 | 43.6 |
| | Spd: | 13.4 | 7.3 | 0.2 | 47.9 |
| | Dir: | 334.1 | 76.1 | 0.0 | 360.0 |
| NTAS-2 (46 m) Workhorse | North: | 0.5 | 11.0 | -48.9 | 38.0 |
| | East: | -0.7 | 10.3 | -49.0 | 41.0 |
| | Spd: | 13.2 | 7.3 | 0.1 | 54.3 |
| | Dir: | 323.0 | 77.1 | 0.1 | 360.0 |
| NTAS-2 (50 m) Workhorse | North: | 0.0 | 10.9 | -48.2 | 41.9 |
| | East: | -0.9 | 10.2 | -38.3 | 42.8 |
| | Spd: | 13.1 | 7.2 | 0.1 | 48.2 |
| | Dir: | 302.4 | 77.6 | 0.0 | 360.0 |
| NTAS-2 (54 m) Workhorse | North: | -0.3 | 10.8 | -43.5 | 41.7 |
| | East: | -1.2 | 10.1 | -38.4 | 46.3 |
| | Spd: | 13.0 | 7.1 | 0.0 | 46.5 |
| | Dir: | 282.4 | 77.2 | 0.0 | 359.9 |

continued...

Table A1: (continued)

| | | Mean | Std Deviation | Range | |
|-------------------------------|--------|-------|---------------|-------|-------|
| NTAS-2 (58 m) Workhorse | North: | -0.6 | 10.7 | -40.3 | 38.3 |
| | East: | -1.5 | 10.0 | -39.1 | 46.2 |
| | Spd: | 13.0 | 7.1 | 0.2 | 46.2 |
| | Dir: | 268.8 | 76.5 | 0.1 | 360.0 |
| NTAS-2 (62 m) Workhorse | North: | -0.8 | 10.7 | -41.7 | 35.7 |
| | East: | -1.8 | 10.1 | -37.5 | 45.6 |
| | Spd: | 13.0 | 7.2 | 0.0 | 46.9 |
| | Dir: | 262.7 | 75.5 | 0.0 | 359.9 |
| NTAS-2 (66 m) Workhorse | North: | -1.1 | 10.6 | -40.8 | 36.3 |
| | East: | -2.1 | 10.0 | -34.9 | 42.8 |
| | Spd: | 13.0 | 7.2 | 0.2 | 49.3 |
| | Dir: | 256.9 | 74.6 | 0.0 | 360.0 |
| NTAS-2 (70 m) Workhorse | North: | -1.2 | 10.6 | -37.8 | 39.0 |
| | East: | -2.3 | 10.0 | -34.2 | 38.5 |
| | Spd: | 13.0 | 7.0 | 0.1 | 44.9 |
| | Dir: | 252.2 | 74.0 | 0.0 | 359.9 |
| NTAS-2 (74 m) Workhorse | North: | -1.3 | 10.3 | -37.0 | 33.1 |
| | East: | -2.5 | 9.9 | -33.9 | 40.6 |
| | Spd: | 12.9 | 6.9 | 0.3 | 42.0 |
| | Dir: | 250.6 | 73.2 | 0.0 | 360.0 |
| NTAS-2 (78 m) Workhorse | North: | -1.4 | 10.0 | -35.7 | 33.3 |
| | East: | -2.7 | 9.8 | -35.7 | 38.2 |
| | Spd: | 12.6 | 6.8 | 0.1 | 40.5 |
| | Dir: | 248.5 | 72.5 | 0.1 | 360.0 |
| NTAS-2 (82 m) Workhorse | North: | -1.5 | 9.9 | -35.9 | 33.4 |
| | East: | -2.8 | 9.7 | -36.4 | 36.7 |
| | Spd: | 12.6 | 6.7 | 0.1 | 41.8 |
| | Dir: | 245.4 | 71.8 | 0.0 | 359.7 |
| NTAS-2 (86 m) Workhorse | North: | -1.6 | 9.9 | -37.2 | 30.0 |
| | East: | -2.9 | 9.8 | -37.3 | 33.0 |
| | Spd: | 12.6 | 6.6 | 0.2 | 38.8 |
| | Dir: | 243.8 | 71.5 | 0.0 | 359.8 |
| NTAS-2 (90 m) Workhorse | North: | -1.6 | 9.8 | -35.8 | 34.6 |
| | East: | -3.1 | 9.9 | -38.8 | 35.3 |
| | Spd: | 12.7 | 6.7 | 0.2 | 40.8 |
| | Dir: | 242.6 | 70.8 | 0.0 | 359.9 |
| NTAS-3 (6 m) Aquadopp | North: | -0.9 | 1.3 | -3.9 | 3.9 |
| | East: | -3.0 | 1.0 | -4.0 | 2.3 |
| | Spd: | 3.5 | 0.4 | 0.2 | 4.1 |
| | Dir: | 252.3 | 27.4 | 0.1 | 359.6 |
| NTAS-3 (22 m) Workhorse | North: | 2.8 | 10.8 | -49.1 | 53.6 |
| | East: | -4.9 | 11.2 | -55.6 | 45.1 |
| | Spd: | 14.6 | 7.8 | 0.2 | 71.2 |
| | Dir: | 298.4 | 65.4 | 0.0 | 360.0 |

continued. . .

Table A1: (continued)

| | | Mean | Std Deviation | Range | |
|-------------------------------|--------|-------|---------------|-------|-------|
| NTAS-3 (26 m) Workhorse | North: | 2.2 | 10.4 | -37.6 | 38.5 |
| | East: | -4.3 | 10.9 | -47.0 | 40.0 |
| | Spd: | 14.0 | 7.4 | 0.0 | 47.1 |
| | Dir: | 295.0 | 67.0 | 0.0 | 359.9 |
| NTAS-3 (30 m) Workhorse | North: | 1.5 | 10.2 | -37.8 | 38.5 |
| | East: | -4.0 | 10.7 | -45.5 | 33.5 |
| | Spd: | 13.6 | 7.2 | 0.1 | 53.2 |
| | Dir: | 287.7 | 68.5 | 0.0 | 360.0 |
| NTAS-3 (30 m) Workhorse | North: | 1.5 | 10.2 | -37.7 | 38.4 |
| | East: | -4.0 | 10.6 | -45.4 | 35.8 |
| | Spd: | 13.5 | 7.1 | 0.1 | 53.1 |
| | Dir: | 162.3 | 68.5 | 0.0 | 360.0 |
| NTAS-3 (34 m) Workhorse | North: | 0.7 | 10.0 | -38.9 | 37.8 |
| | East: | -3.8 | 10.4 | -43.1 | 42.2 |
| | Spd: | 13.2 | 7.0 | 0.1 | 52.4 |
| | Dir: | 277.0 | 69.6 | 0.1 | 360.0 |
| NTAS-3 (38 m) Workhorse | North: | -0.1 | 9.8 | -41.2 | 37.9 |
| | East: | -3.8 | 10.1 | -44.4 | 32.9 |
| | Spd: | 12.9 | 6.8 | 0.1 | 45.8 |
| | Dir: | 265.9 | 69.6 | 0.1 | 360.0 |
| NTAS-3 (42 m) Workhorse | North: | -0.8 | 9.7 | -38.9 | 37.7 |
| | East: | -3.8 | 9.9 | -42.0 | 32.9 |
| | Spd: | 12.7 | 6.6 | 0.1 | 45.3 |
| | Dir: | 257.2 | 69.4 | 0.0 | 360.0 |
| NTAS-3 (46 m) Workhorse | North: | -1.4 | 9.7 | -44.8 | 37.6 |
| | East: | -3.9 | 9.7 | -41.2 | 30.8 |
| | Spd: | 12.7 | 6.6 | 0.1 | 44.8 |
| | Dir: | 249.1 | 68.7 | 0.0 | 359.9 |
| NTAS-3 (50 m) Workhorse | North: | -2.0 | 9.7 | -47.7 | 41.8 |
| | East: | -4.1 | 9.6 | -41.7 | 27.8 |
| | Spd: | 12.7 | 6.6 | 0.3 | 47.9 |
| | Dir: | 242.6 | 67.8 | 0.2 | 359.9 |
| NTAS-3 (54 m) Workhorse | North: | -2.4 | 9.7 | -44.1 | 42.4 |
| | East: | -4.2 | 9.5 | -42.2 | 26.0 |
| | Spd: | 12.8 | 6.6 | 0.1 | 46.3 |
| | Dir: | 238.0 | 67.1 | 0.1 | 359.9 |
| NTAS-3 (58 m) Workhorse | North: | -2.8 | 9.7 | -36.0 | 45.2 |
| | East: | -4.3 | 9.4 | -40.4 | 29.4 |
| | Spd: | 12.9 | 6.6 | 0.0 | 47.8 |
| | Dir: | 235.1 | 66.4 | 0.0 | 359.9 |
| NTAS-3 (62 m) Workhorse | North: | -3.1 | 9.7 | -37.0 | 42.9 |
| | East: | -4.4 | 9.5 | -38.4 | 30.6 |
| | Spd: | 13.0 | 6.7 | 0.0 | 45.4 |
| | Dir: | 234.1 | 65.7 | 0.0 | 359.9 |

continued...

Table A1: (continued)

| | | Mean | Std Deviation | Range | |
|-------------------------------|--------|-------|---------------|-------|-------|
| NTAS-3 (66 m) Workhorse | North: | -3.2 | 9.7 | -41.0 | 35.9 |
| | East: | -4.6 | 9.7 | -39.4 | 26.9 |
| | Spd: | 13.2 | 6.6 | 0.1 | 43.5 |
| | Dir: | 233.7 | 65.1 | 0.2 | 360.0 |
| NTAS-3 (70 m) Workhorse | North: | -3.3 | 9.6 | -37.5 | 32.0 |
| | East: | -4.6 | 9.7 | -37.6 | 26.1 |
| | Spd: | 13.2 | 6.6 | 0.1 | 42.0 |
| | Dir: | 233.7 | 65.5 | 0.2 | 359.8 |
| NTAS-3 (74 m) Workhorse | North: | -3.3 | 9.6 | -36.2 | 32.3 |
| | East: | -4.5 | 9.7 | -36.7 | 25.6 |
| | Spd: | 13.2 | 6.6 | 0.1 | 38.3 |
| | Dir: | 233.6 | 65.9 | 0.1 | 359.9 |
| NTAS-3 (78 m) Workhorse | North: | -3.3 | 9.5 | -36.1 | 33.8 |
| | East: | -4.4 | 9.7 | -35.8 | 23.9 |
| | Spd: | 13.1 | 6.6 | 0.1 | 37.6 |
| | Dir: | 232.4 | 66.0 | 0.0 | 359.9 |
| NTAS-3 (82 m) Workhorse | North: | -3.3 | 9.5 | -33.4 | 37.2 |
| | East: | -4.3 | 9.7 | -36.5 | 25.9 |
| | Spd: | 13.0 | 6.7 | 0.2 | 38.4 |
| | Dir: | 231.9 | 66.5 | 0.0 | 359.9 |
| NTAS-3 (86 m) Workhorse | North: | -3.2 | 9.5 | -33.1 | 34.6 |
| | East: | -4.2 | 9.7 | -40.6 | 25.7 |
| | Spd: | 13.0 | 6.7 | 0.0 | 42.3 |
| | Dir: | 230.6 | 67.1 | 0.0 | 360.0 |
| NTAS-3 (90 m) Workhorse | North: | -3.1 | 9.5 | -35.1 | 34.1 |
| | East: | -4.2 | 9.8 | -40.3 | 25.4 |
| | Spd: | 13.0 | 6.7 | 0.1 | 42.9 |
| | Dir: | 230.9 | 67.1 | 0.2 | 360.0 |
| NTAS-4 (6 m) Aquadopp | North: | 0.1 | 11.6 | -44.1 | 48.5 |
| | East: | -6.1 | 11.5 | -50.0 | 43.8 |
| | Spd: | 14.8 | 9.1 | 0.0 | 55.8 |
| | Dir: | 269.6 | 65.2 | 0.0 | 359.8 |
| NTAS-4 (18 m) Workhorse | North: | 1.1 | 11.8 | -36.4 | 51.1 |
| | East: | -1.6 | 11.8 | -44.0 | 45.5 |
| | Spd: | 14.6 | 8.3 | 0.1 | 51.4 |
| | Dir: | 303.2 | 76.9 | 0.0 | 359.9 |
| NTAS-4 (22 m) Workhorse | North: | 0.6 | 11.5 | -49.4 | 49.7 |
| | East: | -1.1 | 11.7 | -44.8 | 42.2 |
| | Spd: | 14.3 | 8.2 | 0.1 | 55.6 |
| | Dir: | 295.5 | 78.3 | 0.1 | 360.0 |
| NTAS-4 (26 m) Workhorse | North: | 0.2 | 11.1 | -41.4 | 46.6 |
| | East: | -0.8 | 11.8 | -41.9 | 45.6 |
| | Spd: | 14.0 | 8.0 | 0.1 | 54.0 |
| | Dir: | 273.1 | 79.5 | 0.0 | 360.0 |

continued...

Table A1: (continued)

| | | Mean | Std Deviation | Range | |
|-------------------------------|--------|-------|---------------|-------|-------|
| NTAS-4 (30 m) Workhorse | North: | -0.4 | 10.6 | -35.2 | 38.5 |
| | East: | -0.7 | 11.8 | -51.9 | 40.7 |
| | Spd: | 13.8 | 7.9 | 0.1 | 53.0 |
| | Dir: | 235.7 | 79.2 | 0.1 | 360.0 |
| NTAS-4 (34 m) Workhorse | North: | -0.9 | 10.4 | -38.5 | 48.6 |
| | East: | -0.7 | 11.7 | -48.1 | 40.8 |
| | Spd: | 13.6 | 7.8 | 0.1 | 51.9 |
| | Dir: | 211.8 | 78.5 | 0.0 | 359.8 |
| NTAS-4 (38 m) Workhorse | North: | -1.3 | 10.1 | -38.5 | 36.5 |
| | East: | -0.9 | 11.6 | -45.6 | 45.7 |
| | Spd: | 13.4 | 7.7 | 0.1 | 49.1 |
| | Dir: | 206.4 | 77.9 | 0.0 | 359.9 |
| NTAS-4 (42 m) Workhorse | North: | -1.3 | 9.9 | -39.4 | 39.6 |
| | East: | -1.1 | 11.5 | -46.2 | 36.9 |
| | Spd: | 13.2 | 7.6 | 0.1 | 57.1 |
| | Dir: | 207.9 | 77.7 | 0.0 | 360.0 |
| NTAS-4 (46 m) Workhorse | North: | -1.3 | 9.6 | -39.2 | 35.4 |
| | East: | -1.3 | 11.4 | -47.8 | 39.0 |
| | Spd: | 13.0 | 7.5 | 0.1 | 51.9 |
| | Dir: | 211.8 | 77.6 | 0.0 | 360.0 |
| NTAS-4 (50 m) Workhorse | North: | -1.3 | 9.5 | -40.2 | 35.4 |
| | East: | -1.4 | 11.3 | -44.5 | 38.9 |
| | Spd: | 12.9 | 7.5 | 0.1 | 46.1 |
| | Dir: | 209.9 | 77.3 | 0.0 | 359.8 |
| NTAS-4 (54 m) Workhorse | North: | -1.5 | 9.6 | -35.2 | 41.2 |
| | East: | -1.6 | 11.4 | -45.2 | 42.2 |
| | Spd: | 13.0 | 7.5 | 0.2 | 46.3 |
| | Dir: | 208.8 | 76.5 | 0.0 | 360.0 |
| NTAS-4 (58 m) Workhorse | North: | -1.5 | 9.6 | -34.4 | 39.3 |
| | East: | -1.8 | 11.3 | -46.9 | 36.4 |
| | Spd: | 13.0 | 7.5 | 0.1 | 51.3 |
| | Dir: | 208.1 | 76.3 | 0.0 | 359.9 |
| NTAS-4 (62 m) Workhorse | North: | -1.4 | 9.4 | -36.6 | 37.9 |
| | East: | -2.0 | 10.9 | -43.0 | 38.3 |
| | Spd: | 12.6 | 7.4 | 0.1 | 47.6 |
| | Dir: | 213.5 | 75.8 | 0.2 | 360.0 |
| NTAS-4 (66 m) Workhorse | North: | -1.4 | 9.2 | -39.0 | 36.8 |
| | East: | -2.2 | 10.5 | -43.1 | 36.4 |
| | Spd: | 12.3 | 7.1 | 0.0 | 48.2 |
| | Dir: | 223.7 | 75.2 | 0.0 | 359.9 |
| NTAS-4 (70 m) Workhorse | North: | -1.4 | 8.9 | -35.7 | 30.4 |
| | East: | -2.4 | 10.1 | -45.3 | 33.5 |
| | Spd: | 12.0 | 6.8 | 0.1 | 45.5 |
| | Dir: | 229.9 | 74.5 | 0.0 | 360.0 |

continued...

Table A1: (continued)

| | | Mean | Std Deviation | Range | |
|-------------------------------|--------|-------|---------------|-------|-------|
| NTAS-4 (74 m) Workhorse | North: | -1.3 | 9.1 | -33.4 | 29.7 |
| | East: | -2.5 | 10.0 | -47.2 | 33.9 |
| | Spd: | 12.1 | 6.7 | 0.1 | 49.0 |
| | Dir: | 235.8 | 74.2 | 0.0 | 359.9 |
| NTAS-4 (78 m) Workhorse | North: | -0.9 | 8.2 | -30.5 | 28.4 |
| | East: | -2.2 | 8.8 | -39.7 | 34.6 |
| | Spd: | 10.8 | 5.9 | 0.0 | 40.3 |
| | Dir: | 241.6 | 74.3 | 0.0 | 360.0 |
| NTAS-5 (6 m) Aquadopp | North: | 1.2 | 12.0 | -53.4 | 42.5 |
| | East: | -10.2 | 11.5 | -43.5 | 27.9 |
| | Spd: | 17.6 | 8.5 | 0.1 | 62.3 |
| | Dir: | 280.7 | 56.4 | 0.1 | 360.0 |
| NTAS-5 (14 m) Workhorse | North: | 2.3 | 12.3 | -42.0 | 48.5 |
| | East: | -7.1 | 11.8 | -40.2 | 34.5 |
| | Spd: | 16.8 | 7.9 | 0.1 | 50.9 |
| | Dir: | 291.2 | 63.4 | 0.0 | 360.0 |
| NTAS-5 (18 m) Workhorse | North: | 2.0 | 12.2 | -44.6 | 47.3 |
| | East: | -6.2 | 11.7 | -42.3 | 38.5 |
| | Spd: | 16.3 | 7.9 | 0.3 | 52.4 |
| | Dir: | 290.8 | 65.3 | 0.0 | 359.9 |
| NTAS-5 (22 m) Workhorse | North: | 1.6 | 12.1 | -44.2 | 43.2 |
| | East: | -5.8 | 11.7 | -43.8 | 42.2 |
| | Spd: | 16.0 | 7.8 | 0.3 | 55.2 |
| | Dir: | 288.5 | 66.0 | 0.0 | 359.9 |
| NTAS-5 (26 m) Workhorse | North: | 1.2 | 11.9 | -43.1 | 41.3 |
| | East: | -5.5 | 11.5 | -39.7 | 48.0 |
| | Spd: | 15.7 | 7.7 | 0.2 | 50.0 |
| | Dir: | 285.8 | 66.7 | 0.0 | 360.0 |
| NTAS-5 (30 m) Workhorse | North: | 0.8 | 11.7 | -42.5 | 41.2 |
| | East: | -5.3 | 11.3 | -40.3 | 34.2 |
| | Spd: | 15.4 | 7.5 | 0.1 | 47.2 |
| | Dir: | 282.4 | 67.0 | 0.1 | 359.8 |
| NTAS-5 (34 m) Workhorse | North: | 0.4 | 11.4 | -46.1 | 53.8 |
| | East: | -5.2 | 11.1 | -39.4 | 37.3 |
| | Spd: | 15.1 | 7.4 | 0.1 | 54.5 |
| | Dir: | 279.6 | 67.2 | 0.0 | 360.0 |
| NTAS-5 (38 m) Workhorse | North: | 0.1 | 11.2 | -45.2 | 52.4 |
| | East: | -5.3 | 10.9 | -40.1 | 36.9 |
| | Spd: | 14.8 | 7.3 | 0.1 | 57.0 |
| | Dir: | 275.0 | 67.2 | 0.0 | 360.0 |
| NTAS-5 (42 m) Workhorse | North: | -0.4 | 10.9 | -46.3 | 42.8 |
| | East: | -5.4 | 10.6 | -39.7 | 39.6 |
| | Spd: | 14.4 | 7.4 | 0.2 | 49.5 |
| | Dir: | 270.1 | 66.6 | 0.0 | 360.0 |

continued...

Table A1: (continued)

| | | Mean | Std Deviation | Range | |
|-------------------------------|--------|-------|---------------|-------|-------|
| NTAS-5 (46 m) Workhorse | North: | -0.7 | 10.8 | -46.6 | 46.5 |
| | East: | -5.7 | 10.4 | -46.4 | 34.0 |
| | Spd: | 14.2 | 7.4 | 0.1 | 51.4 |
| | Dir: | 266.4 | 65.8 | 0.1 | 360.0 |
| NTAS-5 (50 m) Workhorse | North: | -0.9 | 10.7 | -48.5 | 39.1 |
| | East: | -5.9 | 10.3 | -35.0 | 33.0 |
| | Spd: | 14.2 | 7.4 | 0.1 | 49.6 |
| | Dir: | 263.3 | 65.3 | 0.0 | 359.7 |
| NTAS-5 (54 m) Workhorse | North: | -1.1 | 10.7 | -48.5 | 52.4 |
| | East: | -6.1 | 10.3 | -40.5 | 39.5 |
| | Spd: | 14.2 | 7.5 | 0.1 | 54.8 |
| | Dir: | 261.0 | 64.7 | 0.1 | 360.0 |
| NTAS-5 (58 m) Workhorse | North: | -1.3 | 10.7 | -48.2 | 44.0 |
| | East: | -6.3 | 10.4 | -52.6 | 35.4 |
| | Spd: | 14.3 | 7.7 | 0.1 | 57.2 |
| | Dir: | 260.3 | 64.3 | 0.0 | 360.0 |
| NTAS-5 (62 m) Workhorse | North: | -1.4 | 10.8 | -45.9 | 44.8 |
| | East: | -6.4 | 10.4 | -54.0 | 41.2 |
| | Spd: | 14.3 | 7.9 | 0.2 | 54.8 |
| | Dir: | 259.8 | 64.2 | 0.3 | 359.8 |
| NTAS-5 (66 m) Workhorse | North: | -1.5 | 10.9 | -43.3 | 38.4 |
| | East: | -6.4 | 10.4 | -55.4 | 33.9 |
| | Spd: | 14.4 | 7.9 | 0.0 | 58.3 |
| | Dir: | 258.5 | 64.3 | 0.0 | 359.9 |
| NTAS-5 (70 m) Workhorse | North: | -1.7 | 10.8 | -42.4 | 43.1 |
| | East: | -6.5 | 10.3 | -48.7 | 30.4 |
| | Spd: | 14.3 | 7.9 | 0.1 | 54.9 |
| | Dir: | 257.3 | 64.0 | 0.2 | 360.0 |
| NTAS-5 (74 m) Workhorse | North: | -1.8 | 10.7 | -40.9 | 35.0 |
| | East: | -6.5 | 10.3 | -44.7 | 27.7 |
| | Spd: | 14.3 | 7.9 | 0.3 | 48.6 |
| | Dir: | 255.3 | 64.0 | 0.0 | 360.0 |
| NTAS-5 (78 m) Workhorse | North: | -1.6 | 9.7 | -38.1 | 32.9 |
| | East: | -5.9 | 9.4 | -41.5 | 23.8 |
| | Spd: | 13.0 | 7.1 | 0.1 | 43.7 |
| | Dir: | 254.0 | 64.2 | 0.0 | 360.0 |

| | | | |
|---|--------------------------------------|--|-------------------------------------|
| REPORT DOCUMENTATION PAGE | 1. REPORT NO. WHOI-2012-05 | 2. | 3. Recipient's Accession No. |
| 4. Title and Subtitle Northwest Tropical Atlantic Station (NTAS): Velocity Data Report for Deployments 1 to 5 | | 5. Report Date September 2012 | |
| 7. Author(s) C. M. Duncombe Rae and A. J. Plueddemann | | 6. | |
| 9. Performing Organization Name and Address Woods Hole Oceanographic Institution Woods Hole, Massachusetts 02543 | | 8. Performing Organization Rept. No. | |
| 12. Sponsoring Organization Name and Address NOAA | | 10. Project/Task/Work Unit No. | |
| | | 11. Contract(C) or Grant(G) No. (C)NA09OAR4320129 (G) | |
| | | 13. Type of Report & Period Covered Technical Report | |
| | | 14. | |
| 15. Supplementary Notes This report should be cited as: Woods Hole Oceanographic Institution Tech Report, WHOI-2012-05. | | | |
| 16. Abstract (Limit: 200 words) This report presents velocity data from the Northwest Tropical Atlantic Station (NTAS) deployments 1 through 5, from March 30, 2001, to February 28, 2006. The NTAS project has maintained a series of moorings near 14°50'N, 51°00'W in the northwest tropical Atlantic for air-sea flux measurement. The moorings include a surface buoy outfitted with Air- Sea Interaction Meteorology (ASIMET) systems for determination of bulk air-sea fluxes and oceanographic sensors along the upper 120 m of the mooring line. This report describes and presents the velocity data recovered from current meters and Acoustic Doppler Current Profilers (ADCPs) during the first five years of the NTAS project. | | | |
| 17. Document Analysis a. Descriptors UOP - Upper Ocean Processes Group velocity profilers b. Identifiers/Open-Ended Terms c. COSATI Field/Group | | | |
| 18. Availability Statement Approved for public release; distribution unlimited. | | 19. Security Class (This Report) UNCLASSIFIED | 21. No. of Pages 113 |
| | | 20. Security Class (This Page) | 22. Price |